CORRELATING ANTISENSE RNA PERFORMANCE WITH THERMODYNAMIC CALCULATIONS

Imen Tanniche

A thesis presented to the faculty of the

Virginia Polytechnic Institute and State University

in partial fulfillment for the requirements for the degree of

Master of Science

in

Biological Systems Engineering

Ryan S. Senger, Chair

Mike Zhang

Foster Agblevor

Hafedh Belghith

December 5, 2012

Blacksburg, Virginia

Keywords: antisense RNA, fluorescent proteins, expression level, minimum free energy, down-regulation, complex stability.

CORRELATING ANTISENSE RNA PERFORMANCE WITH THERMODYNAMIC CALCULATIONS

Imen Tanniche

ABSTRACT

Antisense RNA (asRNA) strategies are identified as an effective and specific method for gene down-regulation at the post-transcriptional level. In this study, the major purpose is to find a corraltion between the expression level and minimum free energy to enable the design of specific asRNA fragments. The thermodynamics of asRNA and mRNA hybridization were computed based on the fluorescent protein reporter genes. Three different fluorescent proteins (i) green fluorescent protein (GFP), (ii) cyan fluorescent protein (CFP) and (iii) yellow fluorescent protein (YFP) were used as reporters. Each fluorescent protein was cloned into the common *pUC19* vector. The asRNA fragments were randomly amplified and the resulted antisense DNA fragments were inserted into the constructed plasmid under the control of an additional inducible *plac* promoter and terminator. The expression levels of fluorescent reporter protein were determined in real time by plate reader. Different results have been observed according to the fluorescent protein and the antisense fragment sequence. The CFP expression level was decreased by 50 to 78% compared to the control. However, with the GFP, the down-regulation did not exceed 30% for the different constructs used. For certain constructs, the effect was the opposite of expected and the expression level was increased. In addition, the YFP showed a weak signal compared to growth media, therefore the expression level was hard to be defined. Based on these results, a thermodynamic model to describe the relationship between the particular asRNA used and the observed expression level of the fluorescent reporter was developed. The minimum free energy and binding percentage of asRNA-mRNA complex were computed by NUPACK software. The expression level was

drawn as a function of the minimum free energy. The results showed a weak correlation, but linear trends were observed for low energy values and low expression levels the *CFP* gene. The linear aspect is not verified for higher energy values. These findings suggest that the lower the energy is, the more stable is the complex asRNA-mRNA and therefore more reduction of the expression is obtained. Meanwhile, the non-linearity involves that there are other parameters to be investigated to improve the mathematical correlation. This model is expected to offer the chance to "fine-tune" asRNA effectiveness and subsequently modulate gene expression and redirect metabolic pathways toward the desired component. In addition, the investigation of the localization of antisense binding indicates that there are some regions that favors the hybridization and promote hence the down-regulation mechanisms.

ACKNOWLEDGMENTS

This project was primarily supported by a grant from the US Department of State (#S-TS800-09-GR-204) entitled, Virginia Tech-National Engineering School of Sfax partnership: towards strengthening of higher education & research capacities for better serving the economic development priorities in Tunisia. The grant was administered by the US Embassy in Tunis, Tunisia. This project was also partially supported by a fund from Virginia Tech (#425997).

This work would not have been completed without help and support of many individuals. I would like to thank everyone who has helped me along the way.

I would like to thank particularly my advisors. First and foremost, I would like to express my deepest gratitude to **Dr. Ryan Senger** for providing me with the opportunity to conduct my master thesis in his laboratory. He offered me so much advice, patiently supervising me and guiding me to the right direction. I have leant a lot from him. It was an honor to work with him and his team. I am also very grateful to **Pr. Hafedh Belghith** for his scientific advice and knowledge, many insightful discussions and valuable suggestions.

I would like to gratefully acknowledge the supervision of **Yang Yue** who has been abundantly helpful and has assisted me in numerous ways.

My special thanks go to Virginia Tech committee members: **Dr. Chenming Zhang** and **Dr. Foster Agblevor** and ENIS committee members: **Pr. Radhia Gargouri** and **Dr. Maha Karra** who accepted to review and judge my work.

Special thanks go also to all professors who contributed to the master of Fuel Processing Engineering, especially **Pr. Kamel Halouani**, **Pr. Sami Sayedi, Pr. Ali Gargouri** and **Pr. Slim Choura** for their continuous help and guidance.

The members of the Metabolic Engineering and Systems Biology Laboratory have contributed immensely to my personal and professional time at Virginia Tech. The team has been a source of friendships as well as good advice and collaboration. I would like to thank specially **Hadi Nazem-Bokaee, Ben Freedman, Ahmad Athamneh, Theresah Korbieh, Advait Apte and Jiun Yen.** I also thank undergrad students: **Nick Mangili** and **Parker Lee** for their precious help.

I do thank all Biological Engineering System staff for their kindness and willingness to help. Special thanks go to **Susan Rosebrough.**

I am forever grateful to my friends for their constant support and encouragement throughout my research work and whose support motivated me in attaining my goal.

Finally, I take this opportunity to express the profound gratitude to my beloved family for their constant encouragement and support. Their prayers have enabled me to reach the present position in life.

Imen Tanniche

LIST OF ABBREVIATIONS

°C: Degree Celsius
µg: Micrograms
2'-MOE: 2'-O-methoxyethyl
2'O-Me: 2'-O-methyl
asRNA: Antisense RNA
Bp: Base pair
cDNA: Complementary DNA
CFP: Cyan Fluorescent Protein
cm: centimeter
DNA: Deoxyribonucleic acid
dsRNA: Double stranded RNA
***E. coli**: Escherichia coli*
EB: Elution Buffer from QIAGEN
FDA: Food and Drug Administration
GFP: Green Fluorescent Protein
h: hours
IPTG: Isopropylthio-β-galactoside
kb: kilo base
kcal: Kilo calorie
KCl: Potassium Chloride
L: Liter
LB: Luria Bertani
LNA: Locked nucleic acid
M: Molar
MFE: Minimum Free Energy
Mg^{2+}: Magnesium ion
$MgCl_2$: Magnesium Dichloride
$MgSO_4$: Magnesium Sulfate
Min: Minute
mL: Milliliter
mol: mole
mRNA: messenger RNA
Na^+: Sodium ion
NaCl: Sodium Chloride
ng: Nanogram
OD: Optical density
ON: Oligonucleotide
PCR: Polymerase Chain Reaction
PMO: Phosphoroamidate Morpholino oligomer
PNA: Peptide Nucleic Acid
pro: promoter
RBS: Ribosome Binding Site
RFU: Relative Fluorescence Unit
RNA: Ribonucleic Acid
rRNA: Ribosomal RNA
SD: Shine Dalgarno
siRNA: Small (Short) Interfering RNA
SOC: Super Optimal broth
term: terminator
T_m: Melting temperature
X-gal: 5-bromo-4-chloro-3-indolyl-β-D-galactopyranoside
YFP: Yellow Fluorescent Protein
ZsYFP: *Zoanthus sp* Yellow Fluorescent Protein

TABLE OF CONTENTS

LIST OF FIGURES

LIST OF TABLES

Chapter 1: INTRODUCTION

In recent years, antisense ribonucleic acid (asRNA) strategies have attracted more attention as a revolutionary tool for studying gene function and for discovering new and more specific treatments of diseases in humans, animals, and plants. An antisense RNA concept is an innovative strategy, which consists of an antisense nucleic acid strand that hybridizes with its complementary target mRNA (sense), resulting in its inactivation. The binding of asRNA to the target mRNA will exert repression of the translation process through different mechanisms. These interruptions are referred to as “knock-down” or “knock-out” depending whether the genetic message is partially or completely eliminated, respectively. This technique allows down-regulation of protein expression with ease of implementation and flexibility, which are not seen in gene deletion or knock-out technologies. Therefore, it can be applied in metabolic engineering to control the flow of specific metabolic pathways by controlling key enzymes production. The approach is to introduce into a host cell a recombinant expression vector that contains an asRNA open reading frame, which is controlled by a promoter of choice. Once the asRNA is transcribed, it pairs with a targeted mRNA molecule inhibiting particularly the synthesis of the target protein. The effectiveness of such process was proven in many biological systems. However, some asRNA fragments have been found in the literature to have more potential at down-regulation than others. Computational methods offer the tools to design these asRNA but thermodynamic models have not yet been investigated. In this study, the major aim was to find a correlation between the minimum free energy and expression level to enable the design of specific asRNA. The model is expected to predict the quantitative gene expression level (relative to an uninhibited control) given the primary sequence input of the asRNA. The thermodynamics of asRNA and mRNA hybridization were computed based on the fluorescent protein reporter genes. Three different fluorescent proteins (i) green fluorescent protein (GFP), (ii) cyan fluorescent protein

(CFP) and (iii) yellow fluorescent protein (YFP) were cloned separately into the common *pUC19* vector. The asRNA constructs were obtained from a combinatorial PCR design for the GFP and a separate design for CFP and YFP. The resulting antisense DNA fragments were inserted into the constructed plasmid under the control of an additional inducible *plac* promoter and terminator. The expression levels of fluorescent reporter protein were determined in real time by plate reader. A correlation to describe the relationship between the minimum free energy of a particular asRNA and the observed expression level of the fluorescent reporter was developed. The mathematical correlation is expected to offer the opportunity to "fine-tune" asRNA effectiveness and by consequence modulate gene expression. This has direct impacts in modern metabolic engineering strategies that look for knocking down gene expression or pathway usage by a determined amount, without resorting to a complete knockout. This may also result in the development of metabolic switches, where pathway usage can be knocked down by the "on/off" mechanism of an inducible promoter controlling an asRNA open reading frame. The ultimate purpose is to redirect metabolic pathways toward valuable chemical commodities and specific products. Such advances would enable the control of complex pathways and eliminate undesired products in favor of the target product depending on the purpose of the applications as for down-regulation of unwanted pathways to improve biofuel production.

This thesis is organized as follows. Chapter 2 contains a full literature review related to asRNA technologies, fluorescent proteins and thermodynamic calculations. Materials and methods are contained in Chapter 3. The results and a discussion are contained in Chapter 4. Finally, the conclusions and suggestions for future research are contained in Chapter 5.

Chapter 2: LITERATURE REVIEW

2.1. BACKGROUND: ANITSENSE RNA TECHNOLOGY

Regulation of protein expression can occur at three different levels. Regulation can occur at (i) the transcription of the gene, (ii) at the level of messenger RNA (mRNA) translation (post-transcription) which influences the amount of protein produced and (iii) after protein synthesis by post-translational modifications. Both mRNA and protein are subjected to modifications to control how much of gene product is present and expressed. In general, every step that is required to make an active gene product can be the focus of regulatory mechanism.

To study the mechanisms of post-transcriptional regulation, mRNA should be the major focus. There are three main types of anti-mRNA strategies so far identified. The first is based on catalytically active oligonucleotides, known as ribozymes, initially discovered by Thomas Cech (1981, 1982) and Sidney Altman in 1983. The second strategy involves RNA inference (Rocheleau et al., 1997; Fire et al., 1998), induced by small interfering RNA (siRNA) molecules (Fire et al., 1998; Agami, 2002). The third method utilizes single stranded antisense oligonucleotides. It is the most validated approach and was first discovered by Zamecnik and Stephenson (1970).

In the 1970's, a synthetic oligonucleotide complementary to the mRNA of *Rous sarcoma* virus was introduced into a cell-free system. The complementary construct inhibited the formation of new virus, and also prevented transformation of cells into sarcoma cells. Translation of the *Rous sarcoma* viral message was also greatly impaired. The findings presented in these initial experiments showed that these "antisense" oligonucleotides could inhibit gene expression in a sequence specific way (Zamecnik and Stephenson, 1978).

Antisense RNA (asRNA) control is now recognized as an efficient and specific means of regulating gene expression at the post-transcriptional level (Knee and Murphy, 1997). Naturally occurring asRNAs are small, diffusible, untranslated transcripts that pair to target

RNAs at specific regions of complementarity to control their biological function (Chan et al., 2006). Hybridization of asRNA to a target mRNA via Watson-Crick base pairing can result in specific inhibition of gene expression by various mechanisms, depending on the chemical make-up of the asRNA and location of hybridization. This asRNA-mRNA hybridization often results in reduced levels of translation of the target transcript (Crooke, 2004; Chan et al., 2006). All asRNAs whose structures are known contain one or more stem-loop secondary structures. Target RNAs frequently, but not always, have complementary stem-loop structures. The loops are important determinants for the specificity of antisense-target RNA pairing, and the stems often determine the metabolic stability of the asRNA.

Naturally occurring asRNA control has now been identified in a variety of biological systems, most commonly in accessory DNA elements (plasmids and phage). AsRNAs find several functions, notably in plasmid-replication control. In other cases, asRNAs function as secondary repressors of gene expression, particularly in phages and transposons; consequently, intermediate expression and long half-lives are observed. AsRNA strategies may be used to repress protein production by using inducible promoters to transcribe an asRNA encoded on a recombinant plasmid. Finally, asRNA approaches may be used to down-regulate the products of multiple genes by expressing multiple asRNAs from a single plasmid. In all cases studied so far, asRNAs exert negative control, although mechanisms for positive control are quite plausible (Wagner and Simons, 1994).

AsRNA strategies may have a number of advantages over gene inactivation for metabolic engineering. In addition to rapid implementation, asRNA strategies can avoid the pitfalls of lethal mutations since complete inhibition of protein production is not likely. AsRNA strategies may be used as an “inducible” repressor of protein production by using inducible promoters to transcribe asRNA. In addition, the use of growth stage-specific promoters could result in enzyme down-regulation during specific stages of fermentation so that more

advanced metabolic engineering objectives could be implemented. Finally, asRNAs may be used to down-regulate the products of multiple genes by expressing multiple asRNAs from a single plasmid. In contrast to efforts directed toward determining the mechanism of asRNA action or the reduction in the amount of a single gene product (Desai and Papoutsakis, 1999), asRNA strategies are of interest in this research to accommodate a metabolic engineering strategy called "flux balance analysis with flux ratios (FBrAtio)" developed by McAnulty et al. (2012). In this approach, metabolism must be re-routed by "knocking-down" target gene expression using asRNA. Knocking-down gene expression calls for reducing expression of a targeted enzyme by a specified amount (e.g., 75%). Gene knockout strategies cannot accommodate this strategy because they effectively reduce gene expression by 100% (or 0% if ineffective). AsRNA can be "fine-tuned" for effectiveness leading to targeted gene expression knock-downs.

2.1.1. Naturally occurring asRNAs (Endogenous asRNAs)

2.1.1.1. Prokaryotes and viruses

AsRNA was originally found to occur naturally in prokaryotic organisms (Itoh and Tomizawa, 1980; Tomizawa et al., 1981), where it has been shown to be involved in several biological activities (Wagner and Simons, 1994). These include plasmid replication (Itoh and Tomizawa, 1980), cell division (Bouche and Bouche, 1989), transposon control (Simons and Kleckner, 1983), plasmid conjugation (Lee et al., 1992), and bacteriophage development (Krinke and Wulff, 1987). In all cases, asRNAs down-regulate the expression of sense transcripts at the post-transcriptional level (Wagner and Simons, 1994). In most cases, the antisense and target RNAs are transcribed in opposite directions from the same loci and, thus, the RNAs are completely complementary. Those asRNAs are known as cis-acting antisense. Large amounts of cis-encoded antisense transcripts have been recently discovered in a variety of bacterial species including *Helicobacter pylori* (Sharma et al., 2010), *Escherichia coli*

(Mendoza-Vargas et al., 2009), *Vibrio cholerae* (Liu et al., 2009) and *Listeria monocytogenes* (Toledo-Arana et al., 2009). In some cases, however, the antisense and target genes are encoded at different loci and the complementarity is only partial. These are the trans-acting antisense. AsRNAs have been also identified as acting elements in viruses such as Epstein Barr virus, herpes virus (Prang et al., 1995), human papillomavirus (HPV) (Higgins et al., 1991), and polyoma virus (Liu et al., 1994).

2.1.1.2. Eukaryotes

Naturally occurring asRNA in eukaryotes are involved in different biological activities including pre-mRNA processing; this system allows introns to be spliced out of a message to obtain the proper amino acids sequence (Adams et al., 1996). Other activities work also through an antisense principle such as RNA editing, rRNA modification and developmental regulation (Wagner and Flärdh, 2002).

2.1.1.3. Double-stranded RNA

The presence of highly repetitive sequences within the genome provides the potential for transcripts from different strands to yield RNAs that might anneal. This explains the presence of double stranded RNA (dsRNA) in eukaryotic cells and mainly within the nuclei. The identification of factors which employ dsRNA as a substrate emphasizes the role of asRNA in the regulation of gene expression (Kumar and Carmichael, 1998). This may be important since short RNA duplexes are abundant in the nucleus due to the highly complex secondary structures of many different RNAs.

2.1.2. Synthetic asRNA

Inside the cell unmodified oligonucleotides (ON) are degraded rapidly by nucleases; thus chemical modifications have been implemented in attempt to increase the resistance of the

antisense oligonucleotides to enzymatic degradation. The nucleobase, the sugar and the phosphate backbone are the most common targets for these chemical modifications.

The development of chemically modified ON is a complex process, because, in addition to nuclease resistance, stable duplexes must be obtained. These modifications may affect the skeleton and/or sugars (Luyten et al., 1998; Herdewijn, 2000). The importance of hybridization has been demonstrated by the correlation of antisense activity observed *in vitro* and *in vivo*, with the hybridization affinity expressed as the melting temperature (Tm) (Altmann et al., 1996; Zellweger et al., 2001). Changes in sugars (Sproat et al., 1989; Kawasaki et al., 1993), changes in the orientation of the sugar (Gagnor et al., 1989; Morvan et al., 1991) and modifications in skeleton (Crooke, 2004) influence the ability of ON to activate RNase-H. Therefore, the antisense oligonucleotides can be grouped into two categories: (i) "cutters" which can activate RNase-H and (ii) "blockers" that do not activate RNase-H. These are discussed in detail in the following section (Chapter 2: Part 2.1.3).

2.1.2.1. First generation of chemically modified asRNA

ONs with a phosphorothioate skeleton are the first generation of antisense oligonucleotide (Figure.2.1). The oxygen atoms of the phosphodiester backbone are replaced by sulfur atoms (Eckstein, 2000). These ON confer greater resistance to nucleases than ON with phosphodiesters skeleton and promote RNase-H mediated cleavage of target mRNA. However, they have lower binding affinity for target mRNA due to a decrease in the melting temperature (Chan et al., 2006). Phosphorothioate modified asRNAs have also been reported to trigger unspecific effects by interactions with cell surface and intracellular proteins (Lavigne et al., 2002). Despite these disadvantages, phosphorothioate modification is the most widely performed chemical modification of asRNAs for loss of function studies *in vitro* and *in vivo* for gene target identification and validation.

2.1.2.2. Second generation of chemically modified asRNA

The second generation of antisense oligonucleotide consists mainly of 2'-O-methyl (2'O-Me) and 2'-O-methoxyethyl (2'-MOE) oligonucleotide (Crooke, 2004). These modifications replace the sugar in position 2' by 2'-alkyl at the ribose (Figure.2.1). The skeleton can be of type phosphodiester or phosphorothioate. These asRNAs offer greater resistance to nucleases and higher affinity for the target mRNA. However, they do not support RNase-H mediated cleavage of mRNA, which lower their effectiveness (Altmann et al., 1996). Nevertheless, this property allows the second generation of antisense to have applications in models of splicing correction or alternative exon skipping *in vitro* and *in vivo*. Some examples are the application of antisense-mediated exon skipping approach for Duchenne muscular dystrophy mutations (Aartsma-Rus et al., 2009) and the utilization of antisense oligonucleotides to modulate splice site in Hutchinson-Gilford progeria syndrome (HGPS), a rare pediatric progeroid syndrome (Fong et al., 2009).

2.1.2.3. Third generation of chemically modified asRNA

The third generation of antisense oligonucleotides involves more complex chemical modification of the furanose ring of the nucleotide. The most studied oligonucleotides include the peptide nucleic acid (PNA), locked nucleic acid (LNA) and phosphoroamidate morpholino oligomer (PMO) (Figure.2.1). These modified ONs do not activate RNase-H.

(i) Peptide Nucleic Acid (PNA)

The PNA forms stable complexes with their complementary DNA or RNA strands. This high affinity results from the neutrality and flexibility of its artificial skeleton. They have a high resistance to enzymatic degradation in biological environments (Egholm et al., 1993). PNA qualities make it a well-qualified candidate in antisense strategies. However, this ON has difficulties to diffuse into the cells spontaneously (Chiarantini et al., 2005) and requires a vector.

(ii) The Locked Nucleic Acids (LNA)

The locked nucleic acids were described for the first time in 1998 (Singh et al., 1998). The LNA have a strong affinity for RNA due to their constraint structure. LNA oligomers on both ends provide highly efficient mRNA cleavage, in addition to high ON potency, target accessibility and nuclease resistance (Kurreck et al., 2002). Among all members of the LNA molecular family, α-L-LNA has been shown to demonstrate the highest efficacy in mRNA knockdown in both *in vitro* and *in vivo* studies, making it one of the most promising LNA antisense agents (Petersen and Wengel, 2003; Simoes-Wust et al., 2004).

(iii) Phosphoroamidate Morpholino Oligomer (PMO)

PMO represents a non-charged antisense oligonucleotide agent in which the ribose sugar is replaced by a six-membered morpholino ring and the phosphodiester bond is substituted by a phosphoroamidate linkage (Amantana and Iversen, 2005). PMOs do not elicit RNase-H activity (Summerton, 1999). Instead, the mechanism by which they alter gene expression involves binding to the target RNA sequence and sterically blocking ribosomal assembly or intron-exon splice junction sites, leading to translational arrest or splice-altering effects (Ghosh et al., 2000; Sazani and Kole, 2003). The antisense activity of several PMOs in animal models have been reviewed, some of which are presently in various stages of human clinical trials (Crooke, 2001; Amantana et al., 2005).

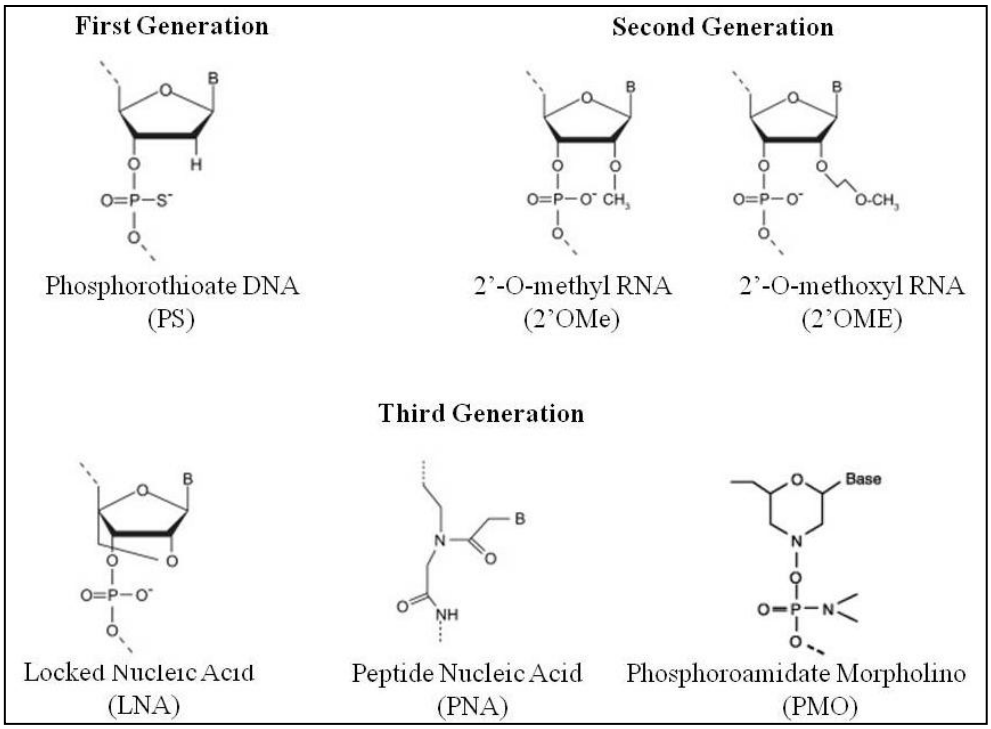

Figure.2.1. Chemical modifications of antisense oligonucleotides.

2.1.2.4. Naturally occurring antisense versus chemically modified antisense

Major differences between exogenous and endogenous asRNA strategies lie in: (i) delivery of the inhibitor; (ii) presumed mode of binding to the target RNA; (iii) details of the inhibitory reaction (Engdahl et al., 1997). Synthetic antisense are generally applied to the extracellular matrix and are taken up; whereas, asRNAs are most often transcribed intracellularly, after transient or stable introduction of an appropriate antisense gene (Nellen and Lichtenstein, 1993; Wagner, 1994).

Chemically designed antisense strands are designed to contain a low degree of secondary structure in order to permit efficient hybridization, while endogenous asRNAs are often larger and structurally more complex. Synthetic oligonuceotides approaches often rely on endogenous RNase-H activity to inactivate the target RNA. In contrast, endogenous asRNA-mediated silencing can occur by duplex-dependent blockage of a ribosome binding site (RBS) within an mRNA, duplex-dependent facilitated mRNA decay, asRNA-induced premature

termination of transcription and cleavage of the mRNA by an asRNA with ribozyme activity (Engdahl et al., 1997).

2.1.3. The antisense strategy

AsRNAs inhibit mRNA function in several ways, including modulation of splicing and inhibition of protein translation by disruption of ribosome assembly (Crooke, 2004). However, the most important mechanism seems to be the utilization of endogenous RNase-H enzymes by the antisense. RNase-H recognizes the mRNA-oligonucleotide duplex and cleaves the mRNA strand, leaving the antisense fragment intact (Kurreck, 2003; Shi and Hoekstra, 2004; Chan et al., 2006). The released fragment can then bind to other target RNA (Figure.2.2). Based on their strategy of action, two classes of antisense RNA can be distinguished: (i) RNase-H dependent oligonucleotides and (ii) steric-blocker oligonucleotides (Dias and Stein, 2002).

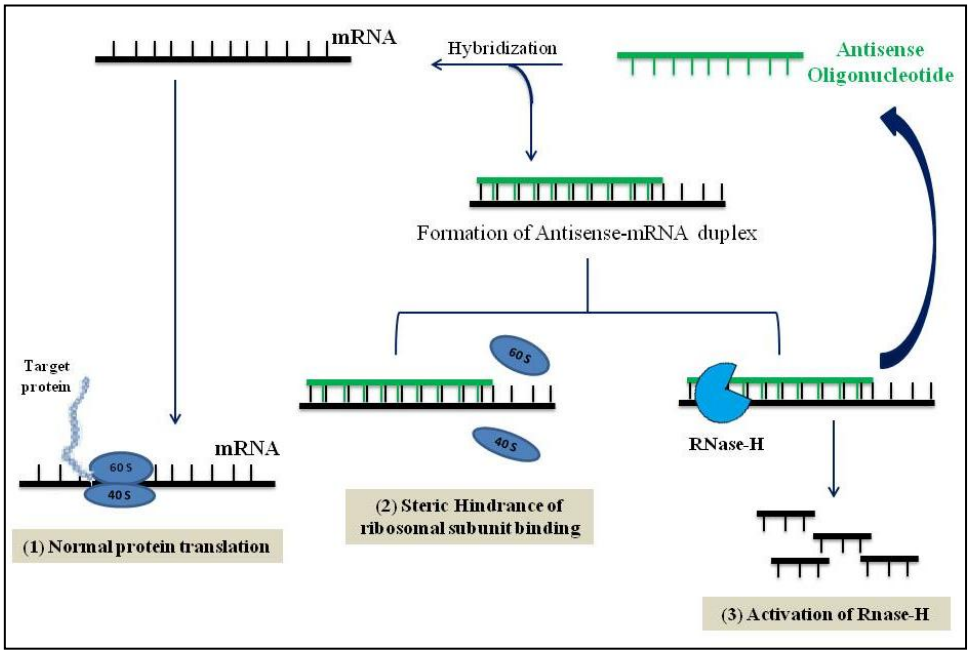

Figure.2.2. Antisense RNA different strategies.

2.1.3.1. RNase-H-dependent oligonucleotides

RNase-H is a ubiquitous enzyme that hydrolyzes the RNA strand of an RNA/DNA duplex. This enzyme will recognize selectively the hybrid and will degrade the mRNA at the site of complex formation (Seitz, 1999). The released antisense goes back to the catalytic cycle for further action (Figure.2.3). The oligonucleotides that activate RNase-H are potentially capable of destroying many RNA transcripts in their lifetime, which suggests that lower concentrations of these oligonucleotides may be sufficient to significantly inhibit gene expression (Zamecnik and Stephenson, 1978). The RNase-H-dependent oligonucleotides effectively reach 80-95% of the protein and target mRNA expression. This category of antisense inhibits protein expression when targeted to any region of mRNA (Dias and Stein, 2002). The importance of the RNase-H-dependent antisense has been investigated and demonstrated for several systems including wheat germ extract (Cazenave et al., 1993), rabbit reticulocyte lysate (Minshull and Hunt, 1986), and Myotonic Dystrophy type 1 (Lee et al., 2012; Wheeler et al., 2012). However, the mechanism of degradation of mRNA is not well elucidated.

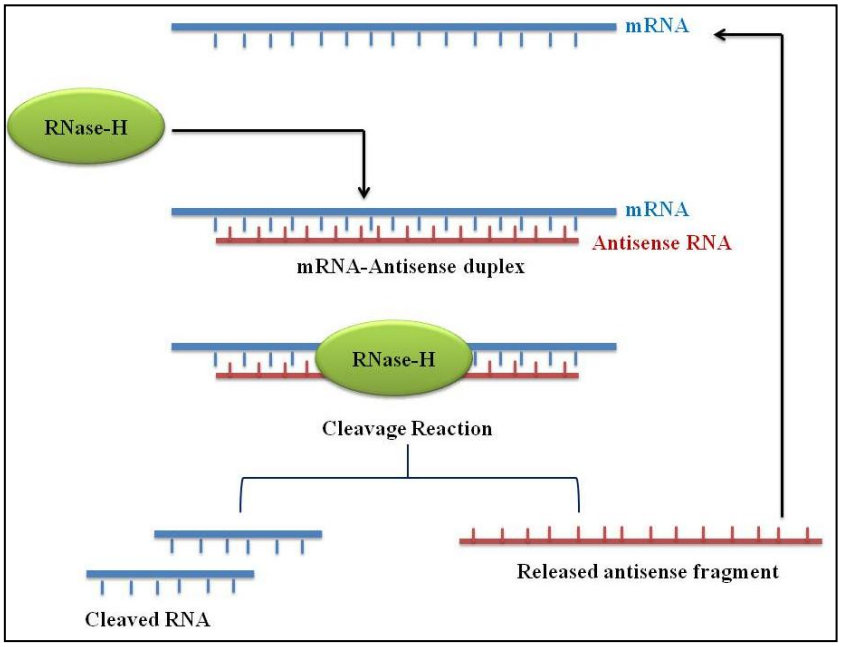

Figure.2.3. RNase-H dependent Antisense mechanism.

2.1.3.2. Steric-blocker oligonucleotides

Steric-blocker oligonucleotides, also called "second generation" oligonucleotides, have been reported to inhibit mRNA translation efficiently. In contrast to RNase-H-dependent oligonucleotides, the second generation oligonucleotides are efficient only when targeted to 5' or AUG initiation codon region (Larrouy et al., 1992; Dean et al., 1994). In this category, the down-regulation of protein expression can be attributed to the disruption of the ribosome subunits or by physically blocking the initiation or elongation steps of protein translation. It can also result from the interruption of polypeptide elongation (Nagel et al., 1993) (Figure.2.4).

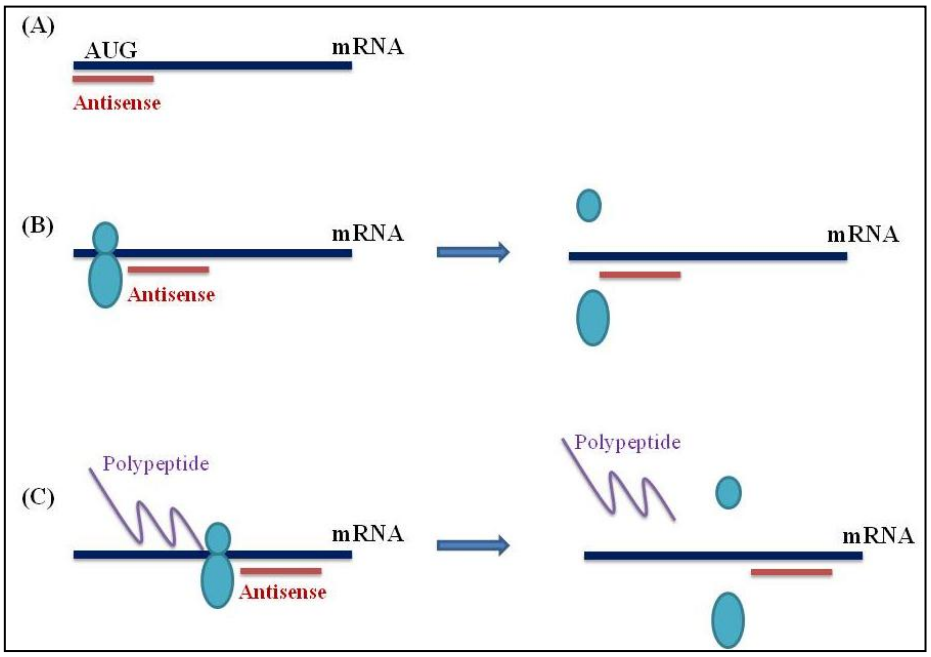

Figure.2.4. Steric-blocker antisense mechanism: Antisense oligonucleotides can interfere with (A) assembly of ribosomal subunits at the start codon, (B) disruption of ribosome subunits and (C) interruption of polypeptide elongation.

2.1.4. Pairing mechanism and kinetics

2.1.4.1. Pairing mechanism

Although the inhibition of target function is accomplished via different mechanisms (Wagner and Simons, 1994; Zeiler and Simons, 1997), it relies on the same parameter. In fact,

all mechanisms depend closely on rapid binding of asRNA to its target mRNA regardless of the pairing scheme. In all antisense control systems, the initial recognition element is described as loop structure (Franch et al., 1999). The bi-molecular interaction is comparable to anticodon-codon pairing. Three major pairing schemes were identified: (i) loop-loop (Figure.2.5 A), (ii) loop-linear (Figure.2.5 B) and (iii) linear-linear (Figure.2.5 C) (Craig et al., 1971; Bujalowski et al., 1986). Surprisingly, all these pairing schemes yield comparable second order binding rate constant, suggesting an upper limit of bi-molecular RNA interaction and non-preference in the recognition scheme.

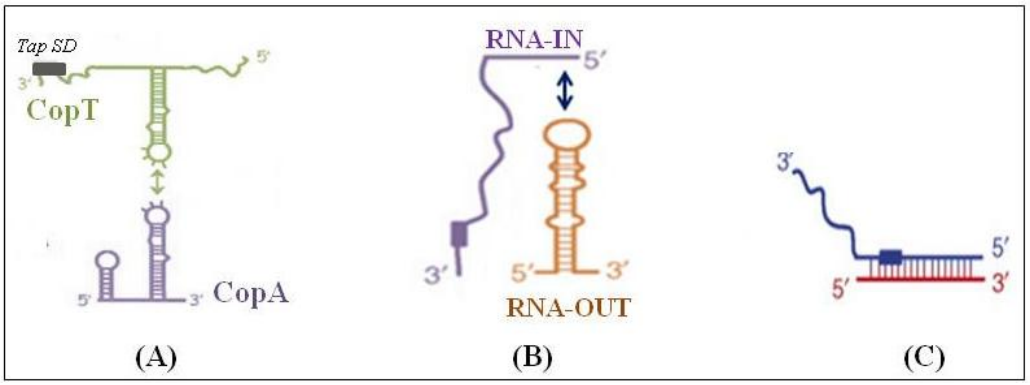

Figure.2.5. RNA pairing schemes: (A) Loop-loop pattern for CopA-CopT complex, (B) Loop-linear scheme for Tn10 RNA IN/RNA OUT interaction and (C) Linear-Linear scheme.

(i) Loop-Loop

The loop-loop pairing, also known as the "kissing complex", is the most used scheme in prokaryotes to initiate antisense-target binding. These systems were characterized by the RNAI/RNAII and CopA/CopT RNA pairs responsible for the replication control of the ColE1 and R1 plasmids, respectively (Tomizawa, 1984; Persson et al., 1988). Other antisense/target RNA pairs include the replication control units of plasmids pT181 (Novick et al., 1989).

(ii) Loop-Linear

Few asRNA systems use the loop-linear scheme as an initial recognition step. This is the case of the *hok/sok* post segregational killing system of plasmid R1 (Thisted et al., 1994),

RNA-IN/RNA-OUT of Tn10, controlling transposition frequency (Kittle et al., 1989). A comparison of the antisense target loops in the family of *hok* mRNAs shows the presence of an invariant sequence motif. In fact, this conserved motif has been identified in the majority of recognition loops of endogenous asRNA regulated gene systems (Franch et al., 1999).

2.1.4.2. Pairing kinetics

The binding rate is determined by the formation of an early intermediate, thus the kinetic scheme is approximated to Briggs-Haldane kinetics (Fersht, 1977). Binding kinetics of this kind appears ideal for the purpose of plasmid copy number control, because binding rates increase linearly with substrate concentration. This observation implies that proper regulation is possible over a wide range of plasmid copy numbers. Negative regulators that follow Michaelis-Menten kinetics would eventually reach plateau levels where binding rates and, therefore, inhibition, cannot be increased. Consequently, control would be lost at high copy numbers (Wagner and Simons, 1994).

2.1.5. Factors affecting asRNA efficiency

The design of an effective antisense remains largely an empirical process. In practice, many candidates are tested for their ability to down-regulate target gene expression, and then the most effective ones are selected (Milligan et al., 1993; Monia et al., 1996). Techniques such as gel-shift or oligonucleotide array assays are also used for the rapid screening of several candidates *in vitro* (Stull et al., 1996; Milner et al., 1997). Computational predictions have as well been applied to identify effective target sites on mRNA (Ding and Lawrence, 2001; Sipes and Freier, 2008). However, once inside the cell, several parameters intervene and can affect the efficiency and should be taken into consideration. These factors include (i) asRNA thermodynamic stability, (ii) antisense dose and position effects, (iii) target accessibility, (iv) RNA binding proteins and (v) cellular metabolism (Denhardt, 1992).

2.1.5.1. AsRNA stability

The stability of asRNA transcript is primarily affected by its sequence and it is partly determined by RNA-binding proteins (Pontius, 1993; Sczakiel, 1997). Antisense oligonucleotides are designed to be single stranded and are prone to adopt secondary and tertiary structure *in vivo* (Wyatt et al., 1994). Advances in research allow the prediction and pre-visualization of RNA secondary structure (Mathews, 2006; Wiese et al., 2008). For example, mfold and RnaPredict provide a computational efficient method for determining the lowest free energy structure and a set of diverse suboptimal structures. These computational methods improved the screening of potent asRNA fragments (Chan et al., 2006).

2.1.5.2. Antisense concentration

Generally, there is a correlation between intracellular dose of antisense and target gene inhibition. But, commonly, an excess of antisense over target RNA is more efficient at inhibiting protein synthesis (Harland and Weintraub, 1985; Melton, 1985). This surplus in antisense ratio is accomplished by using strong promoters for antisense genes.

2.1.5.3. Target accessibility

Target secondary structure and accessibility has been suggested by numerous studies based on computational modeling (Luo and Chang, 2004; Heale et al., 2005; Schubert et al., 2005). These studies were supported by compelling data based on experimental evaluation for target accessibility (Bohula et al., 2003; Overhoff et al., 2005; Westerhout et al., 2005).

The secondary and tertiary structures of mRNA have been proven to influence the hybridization efficiency and potency of antisense oligonucleotide *in vivo* (Vickers et al., 2000). In fact, RNA structure produces asymmetrical binding sites that result in very divergent affinity constants depending on the position of oligonucleotide in that structure. Consequently, the optimal length of oligonucleotide needed to achieve maximal affinity is affected (Crooke, 2000).

2.1.5.4. RNA binding proteins

RNA structure, annealing dynamics, and stability are dependent on RNA-binding proteins (Pontius, 1993; Sczakiel, 1997). Several proteins (RNA helicases, RNase III) bind to mRNA strand and may affect antisense efficiency (Fierro-Monti and Mathews, 2000).

On the other hand, many cellular proteins have been identified to facilitate the hybridization mechanism (Bertrand and Rossi., 1994). Examples of these proteins are (i) the ribonucleoprotein (RNP) A1 (Munroe and Dong, 1992), (ii) the tumour suppressor protein p53 (Wu et al., 1995; Nedbal et al., 1997), and (iii) the yeast initiation factor Tif III (Altmann et al., 1995).

2.1.5.5. Cellular metabolism

Several parameters influence asRNA based technology *in vivo*. Detailed studies by Chen et al., (1997) illustrate how these parameters can affect the antisense efficacy. In these experiments, an *E. coli* model system was used. They observed that when the rate of transcription is increased, the inhibition of target gene is absent. In contrast, when the translation is slowed, the target gene expression is decreased efficiently.

2.1.6. Applications of asRNA in metabolic engineering

Although the mechanism of asRNA action is not completely understood, asRNA strategies have been used to down-regulate levels of targeted gene products in prokaryotes (Engdahl et al., 1997; Kernodle et al., 1997). Antisense approaches have been successfully used to selectively reduce or eliminate the expression of mRNA targets and to study gene function (Patzel et al., 1999). Recently, more research efforts have been directed to the use of antisense techniques to engineer alterations in cellular pathways, including metabolic pathway regulation by altering crucial gene expression and metabolic fluxes. Generally, a particular product is of interest and its production requires the redirection of the cellular metabolism.

This can be done by gene over-expression and using pathway knockout, but with asRNA strategies only partial shut-down of the pathway is involved.

AsRNA strategies were employed to partially block biosynthesis of two major acetate pathway enzymes, phosphotransacetylase (PTA) and acetate kinase (ACK). This strategy was successful in limiting acetate accumulation and reducing its negative effects to increase the productivity of recombinant proteins in *E. coli* cells (Kim and Cha, 2003; Bakhtiari et al., 2010).

Some applications of asRNA technology in *Clostridium acetobutylicum* included the improvement of the production of commodity chemicals. In fact, asRNA fragments were designed with complementarities to two enzymes involved in the conversion of key products to undesirable chemicals. This method lowered their activities by 85 to 90% resulting in the augmentation of butanol (desired) and acetone (undesired) titers by +35 and -50%, respectively (Desai et al., 1999).

Another application combined both asRNA approaches and gene over-expression technologies to effectively alter the metabolism of wild-type *Clostridium acetobutylicum* (Figure.2.6). This application offered an opportunity to re-establish the acetone, butanol, and ethanol fermentation as an economically viable process. The study has shown that asRNA based down-regulation of CoA transferase (CoAT, the first enzyme in the acetone formation pathway) resulted in an increase on butanol to acetone selectivity with an overall reduction in butanol titers and yields (Tummala et al., 2003a). Further metabolic engineering enabled the re-establishment of butanol titer levels while maintaining low acetone production. This result was obtained by combining the *ctfB* (the second *CoAT* gene) asRNA with the over-expression of the alcohol-aldehyde dehydrogenase (*aad*, encoding the bi-functional aldehyde-alcohol dehydrogenase (AAD)). Significantly, this metabolically engineered strain produced the highest ethanol level ever in *C. acetobutylicum*. The high ethanol production was due to the

dual functionality of the AAD enzyme, which catalyzes both the formation of ethanol and butanol (Tummala et al., 2003b).

Other studies altered the pattern of *aad* expression by replacing the endogenous promoter with that of the phosphotransbutyrylase (*ptb*), which is responsible for butyrate formation. In addition, *CoAT* down-regulation was used to minimize acetone formation. This led to the production of high alcohol (butanol plus ethanol) titers, overall solvent titers of 30 g/L (compared to 20 g/L in wild type), and a higher alcohol/acetone ratio (Sillers et al., 2009).

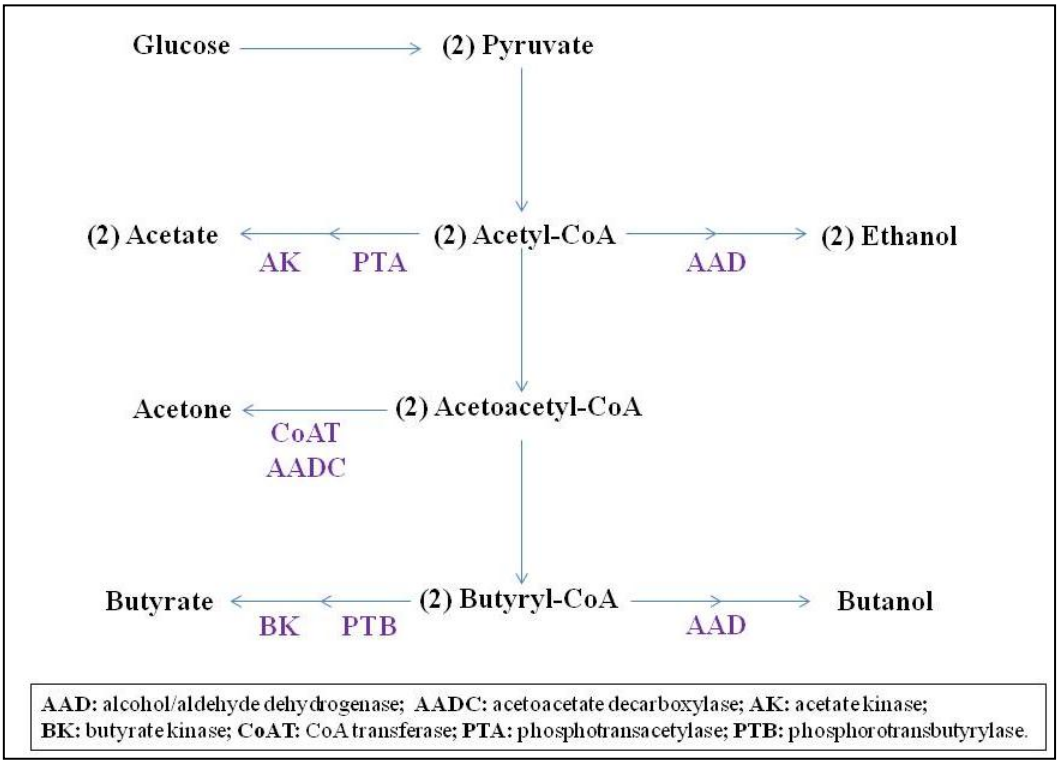

Figure.2.6. Metabolic pathways in *C. acetobutylicum* and associated fluxes.

The development of a butanol-tolerant clostridial mutant that is able to produce greater amounts of butanol in batch culture systems is of interest. Liyanage and his coworkers (2000) found that antisense inhibition of gene expression of glycerol dehydrogenase in *Clostridium beijerinckii* wild-type resulted in a 25% decrease in glycerol dehydrogenase activity with an increase in butanol tolerance.

Antisense strategies were also successfully used in the alteration of solvent productivity by controlling electron flow in an acetone/butanol-producing *Clostridium* species (Nakayama et al., 2008). In this study, a hydrogenase gene cluster (*hup CBA*) from *Clostridium saccharoperbutylacetonicum* strain N1-4 was cloned and down-regulated using asRNA method. As a result, hydrogen production in the antisense transformant increased 3.1-fold. Concurrently, the level of acetone increased 1.6-fold, and butanol production decreased to 75.6% compared to the control strain. This was the first report to demonstrate the correlation between hydrogen and butanol production at the molecular level (Figure.2.7) and the importance of hydrogenase in acetone and butanol production.

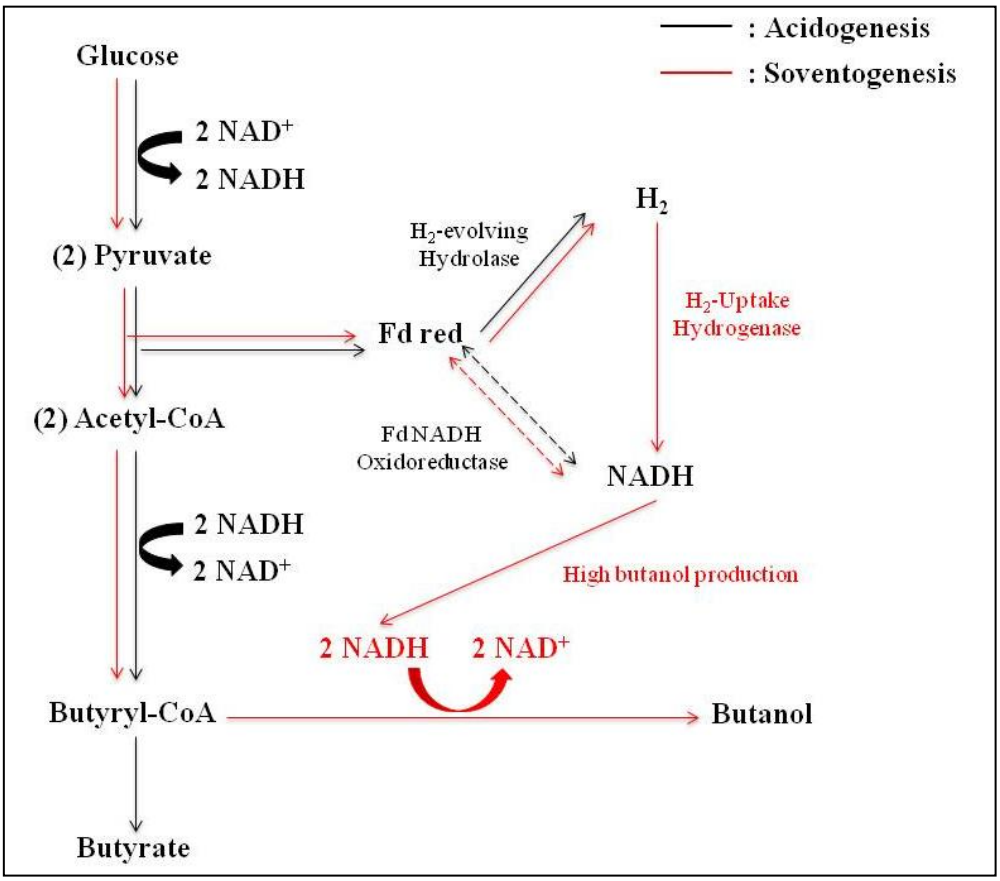

Figure.2.7. Possible functions of the hydrogen-uptake and hydrogen-evolving hydrogenases during solventogenesis of *C. saccharoperbutylacetonicum* strain N1-4.

2.2. FLUORESCENT PROTEINS AS REPORTERS

2.2.1. Generalities

Fluorescent proteins have become an essential tool in the production and analysis of transgenic organisms in basic and applied biology. These fluorescent proteins are obtained from reef coral (Matz et al., 1999). They confer a valuable, non-invasive approach for investigating biological systems in living cells and tissues. Reef coral fluorescent proteins are used as "reporters" that visualize, track and quantify several cellular mechanisms including protein synthesis and turnover *in vivo*. These fluorescent proteins exist in different colors ranging from green to cyan and red (among many others), and each fluorescent protein is characterized by its unique spectra. Thus, it can be combined with other proteins and used for simultaneous detection of multiple events in the same cell or mixed cell population. In addition, they do not require any additional substrates or cofactors for their fluorescence which makes them convenient to use in the laboratory.

2.2.2. Properties of reef coral fluorescent proteins

A large number of fluorescent proteins, their differently colored mutants and fusion proteins have been identified and isolated, resulting in a remarkable expansion of the color palette in recent years (Shaner et al., 2007). The table below summarizes some properties of the commonly used fluorescent proteins.

Table.2.1. Properties of some Fluorescent Proteins.

Cited form http://www.microscopyu.com/articles/livecellimaging/fpintro.htmL

Protein (Acronym)	*Excitation Maximum (nm)*	*Emission Maximum (nm)*	*Molar Extinction Coefficient*	*Quantum Yield*	*in vivo Structure*	*Relative Brightness (% of EGFP)*
Green Fluorescent Proteins						
GFP (wt)	395/475	509	21,000	0.77	Monomer	48
EGFP	484	507	56,000	0.60	Monomer	100
Emerald	487	509	57,500	0.68	Monomer	116
Superfolder GFP	485	510	83,300	0.65	Monomer	160
Azami Green	492	505	55,000	0.74	Monomer	121
Blue Fluorescent Proteins						
EBFP	383	445	29,000	0.31	Monomer	27
EBFP2	383	448	32,000	0.56	Monomer	53
Azurite	384	450	26,200	0.55	Monomer	43
mTagBFP	399	456	52,000	0.63	Monomer	98
Cyan Fluorescent Proteins						
ECFP	439	476	32,500	0.40	Monomer	39
mECFP	433	475	32,500	0.40	Monomer	39
Cerulean	433	475	43,000	0.62	Monomer	79
CyPet	435	477	35,000	0.51	Monomer	53
Yellow Fluorescent Proteins						
EYFP	514	527	83,400	0.61	Monomer	151
Topaz	514	527	94,500	0.60	Monomer	169
Venus	515	528	92,200	0.57	Monomer	156
mCitrine	516	529	77,000	0.76	Monomer	174
Orange Fluorescent Proteins						
Kusabira Orange	548	559	51,600	0.60	Monomer	92
Kusabira Orange2	551	565	63,800	0.62	Monomer	118
mOrange	548	562	71,000	0.69	Monomer	146
mOrange2	549	565	58,000	0.60	Monomer	104
Red Fluorescent Proteins						
mRuby	558	605	112,000	0.35	Monomer	117
mApple	568	592	75,000	0.49	Monomer	109
mStrawberry	574	596	90,000	0.29	Monomer	78
AsRed2	576	592	56,200	0.05	Tetramer	8
mCherry	587	610	72,000	0.22	Monomer	47

2.3. THERMODYNAMICS OF NUCLEOTIDE BOND FORMATION

2.3.1. RNA secondary structure

RNA folding is hierarchical (Tinoco and Bustamante, 1999). The first level of organization is the primary structure, which is the sequence of nucleotides. Intramolecular

base pairs can be formed between these nucleotides, folding the sequence onto itself; this is the secondary structure. Tertiary structure is the three-dimensional arrangement of atoms and the quaternary structure is the interaction with other molecules, which are often either proteins or other RNA strands (Mathews, 2006).

RNA folding is driven by secondary structural features. Therefore, the determination of RNA tertiary structure and function goes necessary through the elucidation of RNA secondary structure (Ding and Lawrence, 2003). Experimental determination of RNA structure remains difficult (Fürtig and al., 2003). Hence, research efforts have been directed to computational methods. Currently, there are three approaches for RNA secondary structure prediction. The first method is the comparative sequence analysis. This method infers base-pairs by determining canonical pairs that are common among multiple homologous sequences (Pace et al., 1999). Comparative analysis, however, requires multiple sequences, can be time-consuming, and requires significant insight. The second method consists of algorithms adding substructures to an initially unfolded sequence: pseudoknotted structures (Shapiro and Wu, 1997; Bindewald et al., 2010). The third and most popular prediction approach is the Minimum Free Energy (MFE) method with computer algorithm based on dynamic programming (Gardner and Giegerich, 2004).

2.3.2. NUPACK thermodynamic software

The NUPACK thermodynamic software package (http://www.nupack.org) arises among a multitude of free available software packages for RNA secondary structure prediction. The package currently enables thermodynamic analysis of dilute solutions of interacting nucleic acid strands and sequence design for systems involving one or more species of interacting strands (Zadeh et al., 2011).

The software allows the user to input the components and conditions of the solution: (i) temperature (or range of temperatures for melts), (ii) number of strand species, (iii) maximum complex size, (iv) strand sequences, and (v) strand concentrations (for calculations with maximum complex size greater than one). After compilation, the NUPACK software outputs (i) the melt profile plot, which describes the fraction of unpaired bases at equilibrium as a function of temperature. (ii) The ensemble pair fractions plot that depicts equilibrium base-pairing information for the dilute solution, taking into account the equilibrium concentration and base-pairing properties of each ordered complex, and (iii) the equilibrium concentration histogram which represents the equilibrium concentrations of the ordered complexes (Zadeh et al., 2011).

The basic features of the NUPACK software are: (i) calculation of the partition function and minimum free energy of secondary structure for un-pseudoknotted complexes of arbitrary numbers of interacting RNA or DNA strands. MFE is calculated using the nearest-neighbor empirical parameters for RNA in 1M Na^+ (Serra and Turner, 1995; Mathews et al., 1999) or for DNA in user-specified Na^+ and Mg^{2+} concentrations (SantaLucia, 1998; SantaLucia and Hicks, 2004; Koehler and Peyret, 2005). (ii) Calculation of the equilibrium concentrations for arbitrary species of complexes in a dilute solution (Dirks et al., 2007). (iii) Sequence design for one or more strands intended to adopt an un-pseudoknotted target secondary structure at equilibrium (Zadeh et al., 2011).

2.3.2.1. Minimum free energy

The stability of RNA secondary structure is quantified by the free energy change "ΔG". In fact, ΔG measures the difference in free energy between the folded and unfolded state of the RNA molecule. A folded RNA has negative free energy change, and the lower it is, the more stable the structure is (Layton and Bundschuh, 2005). The base pairs are usually favorable to stability and contribute a negative free energy change, while the loops are usually

destabilizing since they have positive energy values (Mohsen et al., 2010). ΔG represents the work done by a system at constant temperature and pressure when undergoing a reversible process. It is a function of enthalpy change "ΔH", entropy change "ΔS" and temperature T (in Kelvin), according to the Gibbs function (Gibbs, 1873):

$$\Delta G = \Delta H - T \cdot \Delta S$$

ΔH (kcal/mol) is the enthalpy change for RNA folding. The formation of RNA stems contributes the most to the enthalpy value through hydrogen bonding and stacking interactions. This reaction is qualified as exothermic; therefore, ΔH value is negative. ΔS (kcal/mol K) is the entropy change. It measures the change in the degree of disorder and represents also the quantity of dispersal of energy per temperature, or by the change in the number of microstates. While folding, RNA undergoes a number of structural transitions (microstates). The folding process limits the microstates of the loop nucleotides as compared to the unfolded strand. Hence, the loops contribute to the entropy more than to the enthalpy. (Tinoco and Bustamante, 1999).

There is significant evidence that RNA secondary structures usually adopt their MFE configuration in their natural environments (Tinoco and Bustamante, 1999). The most popular model for the predicting of MFE is the nearest-neighbor model (Tinoco et al., 1973). This model assumes that the stability of a given base pair depends on the identity of its adjacent base pair. Thermodynamic parameters for all possible double-helical nearest neighbors of Watson-Crick and G-U pairs have been determined (Freier et al., 1986a; He et al., 1991). Values for the free energy change at 37°C (ΔG°_{37}), enthalpy change (ΔH°), and entropy change (ΔS°) are predicted from the parameters for the three nearest-neighbor interactions and the initiation contribution (Hickey and Turner, 1985; Freier et al., 1986a; Freier et al., 1986b; Turner et al., 1988; He et al., 1991).The enthalpy and entropy changes are considered to be

temperature independent and allow prediction of the free energy of formation at any temperature:

$$\Delta G_T^\circ = \Delta H^\circ - T \cdot \Delta S^\circ$$

Where ΔG_T°, ΔH° and ΔS° are the standard change in free energy, the standard change in enthalpy and the standard change in entropy, respectively.

For a given sequence, the free energy of secondary structure "s" is estimated as the summation of the empirically determined free energies of the constituent loops (Tinoco et al., 1971; SantaLucia, 1998; Mathews et al., 1999).

$$\Delta G(s) = \sum_{loop \in s} \Delta G(loop)$$

For perfectly base-paired regions, the nearest neighbor model can predict within 10% the free energy change for duplex formation, ΔG_{37}° (Serra and Turner, 1995).

$$\Delta G_{37}^\circ = -R \cdot T \cdot lnK_{eq}$$

Where K_{eq} is the equilibrium constant for duplex formation at 37°C and R is the gas constant. This allows the calculation of the equilibrium constant for the reaction: $K_{eq} = e^{-\Delta G_T^\circ / RT}$.

2.3.2.2. Binding percentage

NUPACK calculates equilibrium concentration of ordered complexes as described in Dirks et al., 2007. For example, considering a dilute solution at equilibrium containing two strands A and B that can interact and form an ordered duplex AB. These relations are given:

$$\frac{x_{AB}}{x_A x_B} = \exp\left\{-\frac{\Delta G_{AB} - \Delta G_A - \Delta G_B}{kT}\right\}$$

$$= \frac{[AB]/\rho_{H_2O}}{\left([A]/\rho_{H_2O}\right)\left([B]/\rho_{H_2O}\right)}$$

$$= \frac{[AB]/\rho_{H_2O}}{[A][B]}$$

where for each ordered complex i, x_i is the mole fraction, $[i]$ is the concentration (e.g. in units of molar), ΔG_i is the free energy as reported by NUPACK, and ρ_{H2O} (≈ 55.14 mol/L at 37.0 °C) is the concentration of water.

Given the initial concentrations of the two strand species ($[A]_0$ and $[B]_0$), the concentration of AB is determined by finding the appropriate root of:

$$\frac{[AB]/\rho_{H_2O}}{([A]_0 - [AB])([B]_0 - [AB])} = \exp\left\{-\frac{\Delta G_{AB} - \Delta G_A - \Delta G_B}{kT}\right\}$$

The value of equilibrium concentrations are used as the binding percentage for the analysis of data.

2.4. REFRENCES

Aartsma-Rus, A., Fokkema, I., Verschuuren, J., Ginjaar, I., van Deutekom, J., van Ommen, G. J., & den Dunnen, J. T. (2009). Theoretic Applicability of Antisense-Mediated Exon Skipping for Duchenne Muscular Dystrophy Mutations. *Hum Mutat, 30*, 293-299.

Adams, M. D., Rudner, D. Z., & Rio, D. C. (1996). Biochemistry and regulation of pre-mRNA splicing. *Curr Opin Cell Biol, 8*, 331-339.

Agami, R. (2002). RNAi and related mechanisms and their potential use for therapy. *Curr Opin Chem Biol, 6*, 829-834.

Altmann, K. H., Fabbro, D., Dean, N. M., Geiger, T., Monia, B. P., Muller, M., & Nicklin, P. (1996). Second-generation antisense oligonucleotides: structure-activity relationships and the design of improved signal-transduction inhibitors. *Biochem Soc Trans, 24*, 630-637.

Altmann, M., Wittmer, B., Methot, N., Sonenberg, N.,& Trachsel, H. (1995). The Saccharomyces cerevisiae translation initiation factor Tif3 and its mammalian homologue, elF-4B, have RNA annealing activity. *EMBO J, 14*, 3820-3827.

Amantana, A., & Iversen, P. L. (2005). Pharmacokinetics and biodistribution of phosphorodiamidate morpholino antisense oligomers. *Curr Opin Pharmacol, 5*, 550-555.

Amantana, A., London, C. A.,Iversen, P. L., & Devi, G. R. (2004). X-linked inhibitor of apoptosis protein inhibition induces apoptosis and enhances chemotherapy sensitivity in human prostate cancer cells. *Mol Cancer Ther, 3*, 699-707.

Bakhtiari, N., Mirshahi, M., Babaeipour, V., & Maghsoudi, N. (2010). Inhibition of ackA and pta genes using two specific antisense RNAs reduced acetate accumulation in batch fermentation of E . coli BL21 (DE3). *Iran J Biotechnol, 8*, 243-251.

Bertrand, E., & Rossi, J. (1994). Facilitation of hammerhead ribozyme catalysis by the nucleocapsid protein of HIV-1 and the heterogeneous nuclear ribonucleoprotein A1. *EMBO J, 13*, 2904-2912.

Bindewald, E., Kluth, T., & Shapiro, B. A. (2010). CyloFold: secondary structure prediction including pseudoknots. *Nucleic Acids Res, 38*, W368-W372.

Bohula, E. A., Salisbury, A. J., Sohail, M., Playford, M. P., Riedemann, J., Southern, E. M., & Macaulay, V. M. (2003). The efficacy of small interfering RNAs targeted to the type 1 insulin-like growth factor receptor (IGF1R) is influenced by secondary structure in the IGF1R transcript. *J Mol Biol, 278*, 15991-15997.

Bouche, F., & Bouche, J. (1989). Genetic evidence that DicF, a second division inhibitor encoded by the Escherichia coli dicB operon, is probably RNA. *Mol Microbiol, 3*, 991-994.

Bujalowski, W., Jung, M., McLaughlin, L. W., & Pörschke, D. (1986). Codon-induced association of the isolated anticodon loop of tRNA phe. *Biochem, 25*, 6372-6378.

Cazenave, C., Frank, P., & Busen, W. (1993). Characterization of ribonuclease H activities present in two cell-free protein synthesizing systems, the wheat germ extract and the rabbit reticulocyte lysate. *Biochimie, 75*, 113-122.

Cech, T. R., Zaug, A. J., & Grabowski, P. J. (1981). In vitro splicing of the ribosomal RNA precursor of tetrahymena: Involvement of a guanosine nucleotide in the excision of the intervening sequence. *Cell, 27*, 487-496.

Chan, J. H., Shuhui, L., & Wong, W. S. (2006). Antisense oligonucleotides: from design to therapeutic application. *Clin Exp Pharmacol, 33*, 533-540.

Chen, H., Ferbeyre, G., & Cedergren, R. (1997). Efficient hammerhead ribozyme and antisense RNA targeting in a slow ribosome Escherichia coli mutant. *Nat Biotech, 15*, 432-435.

Chiarantini, L., Cerasi, A., Fraternale, A., Millo, E., Benatti, U., Sparnacci, K., Laus, L., Ballestri, M. & Tondelli, L. (2005). Comparison of novel delivery systems for antisense peptide nucleic acids. *J Control Release, 109*, 24-36.

Craig, M. E., Crothers, D. M., & Doty, P. (1971). Relaxation kinetics of dimer formation by self-complementary oligonucleotides. *J Mol Biol, 62*, 383-401.

Crooke, S. T. (2000). Progress in Antisense Technology: The End of the Beginning. *313*, 3-45.

Crooke,S. T. (2001). Antisense Drug Techcology- Principles, Strategies and Applications. In I. Book News (Ed.), (Vol. 25): Scitech Book News.

Crooke, S. T. (2004). Progress in antisense technology. *Annu Rev Med, 55*, 61-95.

Denhardt, D. (1992). Mechanism of action of antisense RNA. Sometime inhibition of transcription, processing, transport, or translation. *Ann NY Acad Sci, 660*, 70-76.

Desai, R. P., & Papoutsakis, E. T. (1999). Antisense RNA Strategies for Metabolic Engineering of Clostridium acetobutylicum. A*ppl Microbiol Biotechnol, 65*, 936-945.

Ding, Y., & Lawrence, C. E. (2001). Statistical prediction of single-stranded regions in RNA secondary structure and application to predicting effective antisense target sites and beyond. *Nucleic Acids Res, 29*, 1034-1046.

Ding, Y., & Lawrence, C. E. (2003). A statistical sampling algorithm for RNA secondary structure prediction. *Nucleic Acids Res, 31*, 7280-7301.

Dirks, R. M., Bois, J. S., Schaeffer, J. M., Winfree, E., & Pierce, N.A. (2007). Thermodynamic analysis of interacting nucleic acid strands. *SIAM Rev, 49*, 65-88.

Eckstein, F. (2000). Phosphorothioate oligodeoxynucleotides: what is their origin and what is unique about them? *Antisense Nucleic Acid Drug Dev, 10*, 117-121.

Egholm, M., Buchardt, O., Christensen, L., Behrens, C., Freier, S. M., Driver, D. A., Berg, R. H., Kim, S. K., Norden, B. & Nielsen, P. E. (1993). PNA hybridizes to complementary

oligonucleotides obeying the Watson-Crick hydrogen-bonding rules. *Nature, 365*, 566-568.

Engdahl, H. M., Hjalt, T. A. H., & Wagner, E. G. H. (1997). A two unit antisense RNA cassette test system for silencing of target genes. *Nucleic Acids Res, 25*, 3218-3227.

Fersht, A. (1977). Enzymes Structure and Mechanism (W. H. Freeman Ed.).

Fierro-Monti, I., & Mathews, M. (2000). Proteins binding to duplexed RNA: one motif, multiple functions. *Trends Biochem Sci, 25*, 241-246.

Fire, A., Xu, S., Montgomery, M. K., Kostas, S. A., Driver, S. E., & Mello, C. C. (1998). Potent and specific genetic interference by double-stranded RNA in Caenorhabditis elegans. *Nature, 391*, 806-811.

Fong, L. G.,Vickers,T. A., Farber,E. A., Choi, C., Yun, U. J., Hu, Y., Yang, S. H., Coffinier, C., Lee, R., Yin, L., Davies,B. S. J., Andres, D. A., Spielmann, H. P., Bennett, C. F. &Young, S. G. (2009). Activating the synthesis of progerin, the mutant prelamin A in Hutchinson-Gilford progeria syndrome, with antisense oligonucleotides. *Hum Mol Gen, 18*, 2462-2471.

Franch, T., Petersen, M., Wagner, E. G. H., Jacobsen, J. P., & Gerdes, K. (1999). Antisense RNA Regulation in Prokaryotes: Rapid RNA/RNA Interaction Facilitated by a General U-turn Loop Structure. *J Mol Biol, 294*, 1115-1125.

Freier, S. M., Kierzek, R., Jaeger, J. A., Sugimoto, N., Caruthers, M. H., Neilson, T. & Turner, D. H. (1986a). Improved free-energy parameters for predictions of RNA duplex stability. *Proc Natl Acad Sci, 83*, 9373-9377

Freier, S. M., Kierzek, R., Caruthers, M., Neilson, T., and Turner, D. (1986b). Free energy contributions of G.U and other terminal mismatches to helix stability. *Biochem, 25*, 3209–3213.

Fürtig, B., Richter, C., Wöhnert, J., & Schwalbe, H. (2003). NMR spectroscopy of RNA. *Chembiochem*, *4*, 936-962.

Gagnor, C., Rayner, B., Leonetti, J. P., Imbach, J. L., & Lebleu, B. (1989). Alpha-DNA.IX: Parallel annealing of alpha-anomeric oligodeoxyribonucleotides to natural mRNA is required for interference in RNase H mediated hydrolysis and reverse transcription. *Nucleic Acids Res*, *17*, 5107-5114.

Gardner, P. P., & Giegerich, R. (2004). A comprehensive comparison of comparative RNA structure prediction approaches. *BMC Bioinformatics*, *5*, 140.

Ghosh, C., Stein, D., Weller, D., & Iversen, P. (2000). Evaluation of antisense mechanisms of action. *Methods Enzymol*, *313*, 135-143.

Gibbs, J. W. (1873). A Method of Geometrical Representation of the Thermodynamic Properties of Substances by Means of Surfaces. *Transactions of the Connecticut Academy of Arts and Sciences*, *2*, 382-404.

Guerrier-Takada, C., Gardiner, K., Marsh, T., Pace, N., & Altman, S. (1983). The RNA moiety of ribonuclease P is the catalytic subunit of the enzyme. *Cell*, *35*, 849-857.

Harland, R., & Weintraub, H. (1985). Translation of mRNA injected into Xenopus oocytes is specifically inhibited by antisense RNA. *J. Cell Biol*, *101*, 1094-1099.

He, L., Kierzek, R., SantaLucia, J. Jr., Walter, A.E., & Turner, D.H. (1991). Nearest-neighbor parameters for G.cntdot.U mismatches: 5'GU3'/3'UG5' is destabilizing in the contexts CGUG/GUGC, UGUA/AUGU, and AGUU/UUGA but stabilizing in GGUC/CUGG. *Biochem*, *30*, 11124-11132.

Heale, B. S., Soifer, H. S., Bowers, C., & Rossi, J. J. (2005). siRNA target site secondary structure predictions using local stable substructures. *Nucleic Acids Res*, *33*, e30.

Herdewijn, P. (2000). Heterocyclic modifications of oligonucleotides and antisense technology. *Antisense Nucleic Acid Drug Dev*, *10*, 297-310.

Hickey, D. R., & Turner, D. H. (1985). Effects of terminal mismatches on RNA stability: thermodynamics of duplex formation for ACCGGGp, ACCGGAp, and ACCGGCp. *Biochem, 24*, 3987-3991.

Higgins, G., Uzelin, D., Phillips, G., & Burrell, C. (1991). Presence and distribution of human papillomavirus sense and antisense RNA transcripts in genital cancers. *J Gen Virol, 72*, 885-895.

Itoh, T., & Tomizawa, J. (1980). Formation of an RNA primer for initiation of replication of ColE1 DNA by ribonuclease H. *Proc Natl Acad Sci, 77*, 2450-2454.

Kawasaki, A. M., Casper, M. D., Freier, S. M., A., Lesnik E., Zounes, M. C., Cummins, L. L., Gonzalez, C. & Cook, P. D. (1993). Uniformly modified 2'-deoxy-2'-fluoro phosphorothioate oligonucleotides as nuclease-resistant antisense compounds with high affinity and specificity for RNA targets. *J Med Chem, 36*, 831-841.

Kernodle, D. S., Voladri, R. K., Menzies, B. E., Hager, C. C., & Edwards, K. M. (1997). Expression of an antisense hla fragment in Staphylococcus aureus reduces alpha-toxin production in vitro and attenuates lethal activity in a murine model. *Infect Immun, 65*, 179-184.

Kim, J. Y. H., & Cha, H. J. (2003). Down-Regulation of Acetate Pathway Through Antisense Strategy in *Escherichia coli*: Improved Foreign Protein Production. *Biotechnol Bioeng, 83*, 841-853.

Kittle, J. D., Simons, R. W., Lee, J., & Kleckner, N. (1989). Insertion sequence IS10 anti-sense pairing initiates by an interaction between the 50 end of the target RNA and a loop in the anti-sense RNA. *J Mol Biol, 210*, 561-572.

Koehler, R.T., & Peyret, N. (2005). Thermodynamic properties of DNA sequences: characteristic values for the human genome. *Bioinformatics, 21*, 3333-3339.

Krinke, L., & Wulff, D. (1987). OOP RNA, produced from multicopy plasmids, inhibits λ cII gene expression though an RNAse III-dependent mechanism. *Genes Devel, 1*, 1005-1013.

Kruger, K., Grabowski, P. J., Zaug, A. J., Sands, J., Gottschling, D. E., & Cech, T. R. (1982). Self-splicing RNA: Autoexcision and autocyclization of the ribosomal RNA intervening sequence of tetrahymena. *Cell, 31*(1), 147-157.

Kumar, M., & Carmichael, G. (1998). Antisense RNA: function and fate of duplex RNA in cells of higher eukaryotes. *Microbiol Mol Biol Rev, 62*, 1415-1434.

Kurreck, J. (2003). Antisense technologies: improvement through novel chemical modifications. *Eur J Biochem, 270*, 1628-1644.

Kurreck, J., Wyszko, E., Gillen, C., & Erdmann, V. A. (2002). Design of antisense oligonucleotides stabilized by locked nucleic acid. *Nucleic Acids Res, 30*, 1911-1918.

Larrouy, B., Blonski, C., Boiziau, C., Stuer, M., Moreau, S., Shire, D., & Toulme, J. J. (1992). RNase H-mediated inhibition of translation by antisense oligodeoxyribonucleotides: use of backbone modification to improve specificity. *Gene, 121*, 189-194.

Lavigne, C., Yelle, J., Sauve, G., & Thierry, A. R. (2002). Is antisense an appropriate nomenclature or design for oligodeoxynucleotides aimed at the inhibition of HIV-1 replication? *AAPS Pharm Sci, 4*, E9.

Layton, D. M., & Bundschuh, R. (2005). A statistical analysis of rna folding algorithms through thermodynamic parameter perturbation. *Nucleic Acids Res, 33*,. 519-524.

Lee, J. E., Bennett, C. F., & Cooper, T. A. (2012). RNase H-mediated degradation of toxic RNA in myotonic dystrophy type 1. *Proc Natl Acad Sci USA, 109*, 4221 - 4226.

Lee, S., Frost, L., & Paranchych, W. (1992). FinOP repression of the F plasmid involves extension of the half-life of FinP antisense RNA by FinO. *Mol Gen Genet, 235*, 131-139.

Liu, J. M., Livny, J., Lawrence, M. S., Kimball, M. D., Waldor, M. K., & Camilli, A. (2009). Experimental discovery of sRNAs in Vibrio cholerae by direct cloning, 5S/tRNA depletion and parallel sequencing. *Nucleic Acids Res, 37*, e46.

Liu, Z., Batt, D. B., & Carmichael, G. G. (1994). Targeted nuclear antisense RNA mimics natural antisense-induced degradation of polyoma virus early RNA. *Proc Natl Acad Sci USA, 91*, 4258-4262.

Liyanage, H., Young, M., & Kashket, E. R. (2000). Butanol tolerance of *Clostridium beijerinckii* NCIMB 8052 associated with down-regulation of gldA by antisense RNA. *J Mol Microbiol Biotechnol, 2*, 87-93.

Luo, K.Q., & Chang, D.C. (2004). The gene-silencing efficiency of siRNA is strongly dependent on the local structure of mRNA at the targeted region. *Biochem Biophys Res, 318*, 303-310.

Luyten, G. P., van der Spek, C. W., Brand, I., Sintnicolaas, K., de Waard-Siebinga, I., Jager, M. J., de Jong, P. T., Schrier, P.T., & Luider, T. M. (1998). Expression of MAGE, gp100 and tyrosinase genes in uveal melanoma cell lines. *Melanoma Res, 8*, 11-16.

Mathews, D. H. (2006). Revolutions in RNA Secondary Structure Prediction. *J Mol Biol, 359*, 526-532.

Mathews, D. H., Sabina, J., Zuker, M., & Turner, D.H. (1999). Expanded sequence dependence of thermodynamic parameters improves prediction of RNA secondary structure. *J Mol Biol, 288*, 911-940.

Matz, M. V., Fradkov, A. F., Labas, Y. A., Savitsky, A. P. , Zaraisky, A. G., Markelov, M. L., & A, Lukyanov S. (1999). Fluorescent proteins from nonbioluminescent Anthozoa species. *Nature Biotech, 17*, 969-973.

McAnulty, M. .J., Yen, J. Y., Freedman, B. G., & Senger, R. S. (2012). Genome-scale modeling using flux ratio constraints to enable metabolic engineering of clostridial metabolism in silico. *BMC Systems Biology, 6*, 42.

Melton, D. (1985) Injected anti-sense RNAs specifically block messenger RNA translation in vivo. *Proc Natl Acad Sci, 82*, 144-148.

Mendoza-Vargas, A., Olvera, L., Olvera, M., Grande, R., Vega-Alvarado, L., Taboada, B., Jimenez-Jacinto,V., Salgado, H., Juárez, K., Contreras-Moreira, B., Huerta, A. M., Collado-Vides, J., & Morett, E. (2009). Genome-wide identification of transcription start sites, promoters and transcription factor binding sites in *E. coli*. *PLoS ONE*, *4*, e7526.

Milligan, J. F., Matteucci, M. D., & Martin, J. C. (1993). Current concepts in antisense drug design. *J Med Chem, 36*, 1923-1937.

Milner, N., Mir, K. U., & Southern, E. M. (1997). Selecting effective antisense reagents on combinatorial oligonucleotide arrays. *Nat Biotechnol, 15*, 537-541.

Minshull, J., & Hunt, T. (1986). The use of single-stranded DNA and RNase H to promote quantitative 'hybrid arrest of translation' of mRNA/DNA hybrids in reticulocyte lysate cell-free translations. *Nucleic Acids Res, 14*, 6433-6451.

Mohsen, A. M., Khader, A. T., Ramachandram, D. & Ghallab, A. (2010). Predicting the minimum free energy RNA Secondary Structures using Harmony Search Algorithm. *Int. J. Biol. Life Sci*, *6*, 157-163.

Monia, B. P., Johnston, J. F., Geiger, T., Muller, M., & Fabbro, D. (1996). Antitumor activity of a phosphorothioate antisense oligo-deoxynucleotide targeted against C-raf kinase. *Nat Med, 2*, 668- 675.

Morvan, F., Rayner, B., & Imbach, J. L. (1991). Alpha-oligonucleotides: a unique class of modified chimeric nucleic acids. *Anticancer Drug Des, 6* (521-529).

Munroe, S., & Dong, X. (1992). Heterogeneous nuclear ribonucleoprotein A1 catalyzes RNA.RNA annealing. *Proc Natl Acad Sci., 89*, 895-899.

Murphy, P.,& Knee, R. (1994). Identification and characterization of an antisense RNA transcript (gfg) from the human basic fibroblast growth factor gene. *Mol Endocrinol, 8*, 852-859.

Nagel, K. M., Holstad, S. G., & Isenberg, K. E. (1993). Oligonucleotide pharmacotherapy: an antigene strategy. *Pharmacotherapy, 13*, 177-188.

Nakayama, S., Kosaka, T., Hirakawa, H., Matsuura, K., Yoshino, S., & Furukawa, K. (2008). Metabolic engineering for solvent productivity by downregulation of the hydrogenase gene cluster hupCBA in *Clostridium saccharoperbutylacetonicum* strain N1-4. *Appl Microbiol Biotechnol, 78*, 483-493.

Nedbal, W., Frey, M., Willemann, B., Zentgraf, H., & Sczakiel, G. (1997). Mechanistic insights into p53-promoted RNA-RNA annealing. *J Mol Biol, 266*, 677-687.

Nellen, W., & Lichtenstein, C. (1993). What makes an mRNA anti-sense-itive? *Trends Biochem Sci, 18*, 419-423.

Novick, R. P., Iordanescu, S., Projan, S. J., Kornblum, J., & Edelman, I. (1989). pT181 plasmid replication is regulated by a countertranscript driven transcriptional attenuator. *Cell, 59*, 395-404.

Overhoff, M., Alken, M., Far, R. K., Lemaitre, M., Lebleu, B., Sczakiel, G., & Robbins, I. (2005). Local RNA target structure influences siRNA efficacy: A systematic global analysis. *J Mol Biol, 348*, 871-881.

Pace, N. R., Thomas, B. C., & Woese, C. R. (1999). *Probing RNA structure, function, and history by comparative analysis*. NY: Cold Spring Harbor Laboratory Press.

Patzel, V., Steidl, U., Kronenwett, R., Haas, R., & Sczakiel, G. (1999). A theoretical approach to select effective antisense oligodeoxyribonucleotides at high statistical probability. *Nucleic Acids Res, 27,* 4328-4334.

Persson, C., Wagner, E. G. H., & Nordström, K. (1988). Control of replication of plasmid R1: kinetics of in vitro interaction between the antisense RNA, CopA, and its target, CopT. *EMBO J, 7,* 3279-3288.

Petersen, M., & Wengel, J. (2003). LNA: a versatile tool for therapeutics and genomics. *Trends in Biotechnology, 21,* 74-81.

Pontius, B. (1993). Close encounters: why unstructured, polymeric domains can increase rates of specific macromolecular association. *Trends Biochem Sci, 18,* 181-186.

Prang, N., Wolf, H., & Schwarzmann, F. (1995). Epstein-Barr virus lytic replication is controlled by posttrancriptional negative regulation of BZLF1. *J Virol, 69,* 2644-2648.

Rocheleau, C. E., Downs, W. D., Lin, R., Wittmann, C., Bei, Y., Cha, Y., Ali, M., Priess, J. R., & Mello, C. C. (1997). Wnt Signaling and an APC-Related Gene Specify Endoderm in Early *C. elegans* Embryos. *Cell, 90* (4), 707-716.

SantaLucia, J. Jr. (1998). A unified view of polymer, dumbbell, and oligonucleotide DNA nearestneighbor thermodynamics. *Proc. Natl. Acad. Sci. USA, 95,* 1460-1465.

SantaLucia, J. Jr., & Hicks, D. (2004). The thermodynamics of DNA structural motifs. *Annu Rev Bioph Biom Struct, 33,* 415-440.

Sazani, P., & Kole, R. (2003). Therapeutic potential of antisense oligonucleotides as modulators of alternative splicing. *J Clin Invest, 112,* 481-486.

Schubert, S., Grunweller, A., Erdmann, V.A., & Kurreck, J. (2005). Local RNA target structure influences siRNA efficacy: Systematic analysis of intentionally designed binding regions. *J Mol Biol, 348,* 883-893.

Sczakiel, G. (1997). The design of antisense RNA. *Antisense Nucleic Acid Drug Dev, 7*, 439-444.

Seitz, O. (1999). Chemically Modified Antisense Oligonucleotides - Recent Improvements of RNA Binding and Ribonuclease H Recruitment. *Angew Chem, 38*, 3466-3469.

Serra, M. J., & Turner, D.H. (1995). Predicting thermodynamic properties of RNA. *Methods Enzymol, 259*, 242-261.

Shapiro, B. A., & Wu, J. C. (1997). Predicting RNA H-type pseudoknots with the massively parallel genetic algorithm. *Comput Appl Biosci, 13*, 459-471.

Sharma, C. M., Hoffmann, S., Darfeuille, F., Reignier, J., Findeiss, S., Sittka, A., Chabas, S., Reiche, K., Hackermüller, J., Reinhardt, R., Stadler, P. F., & Vogel, J. (2010.). The primary transcriptome of the major human pathogen *Helicobacter pylori*. *Nature, 464*, 250-255.

Shi, F., & Hoekstra, D. (2004). Effective intracellular delivery of oligonucleotides in order to make sense of antisense. *J Control Release, 97*, 189-209.

Sillers, R., Al-Hinai, M. A., & Papoutsakis, E. T. (2009). Aldehyde-Alcohol Dehydrogenase and/or Thiolase Overexpression Coupled With CoA Transferase Downregulation Lead to Higher Alcohol Titers and Selectivity in Clostridium acetobutylicum Fermentations. *Biotechnol Bioeng, 102*, 38-49.

Simoes-Wust, A. P., Hopkins-Donaldson, S., Sigrist, B., Belyanskaya, L., Stahel, R. A., & Zangemeister-Wittke, U. (2004). A functionally improved locked nucleic acid antisense oligonucleotide inhibits Bcl-2 and Bcl-xL expression and facilitates tumor cell apoptosis. *Oligonucleotides, 14*, 199-209.

Simons, R., & Kleckner, N. (1983). Translational control of IS10 transposition. . *Cell, 34*, 683-691.

Singh, S. K., Kuma, R., & Wengel, J. (1998). Synthesis of Novel Bicyclo[2.2.1] Ribonucleosides: 2'-Amino- and 2'-Thio-LNA Monomeric Nucleosides. *J Org Chem, 63*, 6078-6079.

Sipes, T. B., & Freier, S. M. (2008). Prediction of antisense oligonucleotide efficacy using aggregate motifs. *Journal of Bioinformatics and Computational Biology, 6*, 919-932.

Sproat, B. S., Lamond, A. I., Beijer, B., Neuner, P., & Ryder, U. (1989). Highly efficient chemical synthesis of 2'-O-methyloligoribonucleotides and tetrabiotinylated derivatives; novel probes that are resistant to degradation by RNA or DNA specific nucleases. *Nucleic Acids Res, 17*, 3373-3386.

Stephenson, M. L., & Zamecnik, P. C. (1978). Inhibition of Rous sarcoma viral RNA translation by a specific oligodeoxyribonucleotide. *Proc Natl Acad Sci USA, 75*, 280-284.

Stull, R. A., Taylor, L. A.,& Szoka, Jr. F. C. (1992). Predicting antisense oligonucleotide inhibitory efficacy: a computational approach using histograms and thermodynamic indices. *Nucleic Acids Res, 20*, 3501- 3508.

Stull, R. A., Zon, G., & Szoka, F. C. (1996). An in vitro messenger RNA binding assay as a tool for identifying hybridization-competent antisense oligonucleotides. *Antisense Nucleic Acid Drug Dev, 6*, 221-228.

Summerton, J. (1999). Morpholino antisense oligomers: the case for an RNase H-independent structural type. *Biochim Biophys Acta, 1489*, 141-158.

Thisted, T., Sørensen, N. S., Wagner, E. G. H., & Gerdes, K. (1994). Mechanism of post-segregational killing: Sok antisense RNA interacts with hok mRNA via its 5'-end singlestranded leader and competes with the 3'-end of hok mRNA for binding to the mok translational initiation region. *EMBO J, 13*, 1960-1968.

Tinoco, I., & Bustamante, C. (1999). How RNA folds. *J Mol Biol, 293*, 271-281.

Tinoco, Jr. I., Borer, P. N., Dengler, B., Levine, M. D., Uhlenbeck, O. C., Crothers, D. M., & Gralla, J. (1973). Improved Estimation of Secondary Structure in Ribonucleic Acids. *Nature. New. Biol, 246*, 40-41.

Tinoco, Jr. I., Uhlenbeck, O.C. & Levine, M. D. (1971). Estimation of secondary structure in ribonucleic acids. *Nature, 230*, 362-367.

Toledo-Arana, A., Dussurget, O., Nikitas, G., Sesto, N., Guet-Revillet, H., Balestrino, D., Loh, E., Gripenland, J., Tiensuu, T., Vaitkevicius, K., Barthelemy, M., Vergassola, M., Nahori, M. A., Soubigou, G., Régnault, B., Coppée, J. Y., Lecuit, M., Johansson, J., & Cossart, P. (2009). The Listeria transcriptional landscape from saprophytism to virulence. *Nature, 459*, 950-956.

Tomizawa, J. I. (1984). Control of ColE1 plasmid replication: the process of binding of RNAI to the primer transcript. *Cell, 38*, 861-870.

Tomizawa, J., Itoh, T., Selzer, G., & Som, T. (1981). Inhibition of ColE1 RNA primer formation by a plasmid-specified small RNA. *Proc Natl Acad Sci, 78*, 1421-1425.

Tummala, S. B., Welker, N. E., & Papoutsakis, E. T. (2003a). Design of antisense RNA constructs for downregulation of the acetone formation pathway of *Clostridium acetobutylicum*. *J Bacteriol, 185*, 1923-1934.

Tummala, S. B., Junne, S. G., & Papoutsakis, E. T. (2003b). Antisense RNA down-regulation of coenzyme A transferase combined with alcohol-aldehydedehydrogenase overexpression leads to predominantly alcohologenic *Clostridium acetobutylicum* fermentations. *J Bacteriol, 185*, 3644-3653.

D H Turner, N Sugimoto, and S M Freier. (1988). RNA Structure Prediction. *Annu Rev Biophys Biophys Chem*. *17*: 167-192.

Vickers, T. A., Wyatt, J. R., & Freier, S. M. (2000). Effects of RNA secondary structure on cellular antisense activity. *Nucleic Acids Res, 28*, 1341-1347.

Wagner, E. G. H., & Flärdh, K. (2002). Antisense RNAs everywhere? *TIG, 18*, 223-226.

Wagner, R. W. (1994). Gene inhibition using antisense oligodeoxynucleotides. *Nature, 372*, 333-335.

Westerhout, E. M., Ooms, M., Vink, M., Das, A. T., & Berkhout, B. (2005). HIV-1 can escape from RNA interference by evolving an alternative structure in its RNA genome. *Nucleic Acids Res, 33*, 796-804.

Wheeler, T. M., Leger, A. J., Pandey,S. K., MacLeod, A. R., Nakamori, M., Cheng, S. H., Wentworth, B. M., & Bennett, C. F., & Thornton, C. A. (2012). Targeting nuclear RNA for in vivo correction of myotonic dystrophy. *Nature, 487*, 111-117.

Wiese, K. C., Deschenes, A. A., & Hendriks, A. G. (2008). RnaPredict-An Evolutionary Algorithm for RNA Secondary Structure Prediction. *Trans Comput Biol Bioinform, 5*, 25-41.

Wu, L., Bayle, J., Elenbaas, B., Pavletich, N., & Levine, A. (1995). Alternatively spliced forms in the carboxy-terminal domain of the p53 protein regulate its ability to promote annealing of complementary single strands of nucleic acids. *Mol Cell Biol, 15*, 497-504.

Wyatt, J. R., Vickers, T. A., Roberson, J. L., Buckheit, R. W., Klimkait, T., DeBaets, E., Davis, P. W., Rayner, B., Imbach, J. L., & Ecker, D. J. (1994). Combinatorially selected guanosine-quartet structure is a potent inhibitor of human immunodeficiency virus envelope-mediated cell fusion. *Proc Nat Acad Sci USA, 91*, 1356-1360.

Zadeh, J. N., Steenberg, C. D., Bois, J. S., Wolfe, B .R., Khan, A. R., Pierce, M. B., Dirks, R. M., Pierce, N. A. (2011). NUPACK: analysis and design of nucleic acid systems. *J Comput Chem, 32*, 170-173.

Zamecnik, P. C., & Stephenson, M. L. (1978). Inhibition of Rous sarcoma virus replication and cell transformation by a specific oligodeoxynucleotide. *Proc Natl Acad Sci USA, 75*, 280-284.

Zeiler, B. N., & Simons, R. W. (1997). *Antisense RNA structure and function. In RNA Structure and Function*. NY: Cold Spring Harbor Laboratory Press.

Zellweger, T., Miyake, H., Cooper, S., Chi, K., Conklin, B. S., Monia, B. P., & Gleave, M. E. (2001). Antitumor activity of antisense clusterin oligonucleotides is improved in vitro and in vivo by incorporation of 2'-O-(2-methoxy)ethyl chemistry. *J Pharmacol Exp Ther., 298*, 934-940.

Chapter 3: MATERIAL AND METHODS

3.1. STRAINS

Two strains of *Escherichia coli* were used. *E. coli* Top10 strain (*F- mcrA Δ*(*mrr-hsdRMS-mcrBC*) *φ80lacZΔM15 ΔlacX74 recA1 araD139 Δ*(*ara-leu*) *7697 galU galK rpsL* (*StrR*) *endA1 nupG λ-*) (Invitrogen: Grand Island, NY) was used as the host for cloning and replicating recombinant plasmids. The *E. coli 10beta* (*araD139* Δ(*ara-leu*)7697 fhuA lacX74 galK (*ϕ80* Δ(*lacZ*) *M15*) *mcrA galU recA1 endA1 nupG rpsL* (*StrR*) Δ(*mrr-hsdRMS-mcrBC*)) strain (New England Biolabs: Ipswich, MA) was used for the expression of heterologous genes.

3.2. PLASMIDS

The plasmid *pUC19-pro-term-LacZ* was used as the backbone for all plasmid construction and gene expression. The common *pUC19* plasmid (Invitrogen: Grand Island, NY) was modified to have additional promoter (*plac* promoter) and terminator (*rho independent terminator*). The construction of this plasmid was already performed. This construct enables the insertion of both the fluorescent gene and the antisense gene in the same plasmid (Figure.3.1).

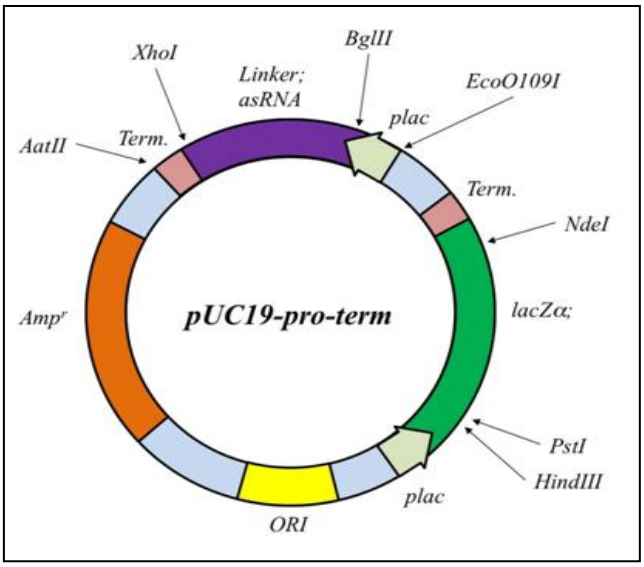

Figure.3.1. Diagram of the *pUC19-pro-term* plasmid.

Other plasmids containing different fluorescent genes were used. These plasmids are: (i) pAmCyan plasmid (Clontech: Montain View, CA) for Cyan fluorescent protein (CFP) cloning, (ii) pZsYellow (Clontech: Montain View, CA) used to amplify Yellow fluorescent protein (YFP) gene and (iii) Green fluorescent protein (GFP) plasmid.

3.3. REAGENTS

Liquid Luria Bertani (LB) medium and LB agar plates were used to culture *E. coli* cells. The liquid media was prepared according to the following protocol: 5 g yeast extract, 10 g tryptone and 10 g NaCl were dissolved in 950 mL deionized water. Once the pH was adjusted to 7.0 with sodium hydroxide (1M), the total volume was brought to 1 L with deionized water. The vessel was autoclaved at 121°C for 25 min. After cooling to about 55°C, antibiotic (Ampicilin with a final concentration of 100 µg/mL) or chemical indictors (X-gal and IPTG) were added in proper concentrations. For solid media, the same ingredients were mixed with 15 g agar and the same procedure was followed. 20 mL of liquid medium was placed into each plate, the medium solidified at room temperature, and the plates were sealed with parafilm, and both liquid media and plates were stored +4°C.

Super Optimal broth with added glucose (SOC) medium was used for the transformation protocol (2% tryptone, 0.5% yeast extract, 10 mM NaCl, 2.5 mM KCl, 10 mM $MgCl_2$, 10 mM $MgSO_4$, 20 mM glucose). Vials of SOC media are provided with competent cells.

3.4. GENETIC MANIPULATIONS

The extraction of plasmids from *E. coli* was carried out after harvest, using a Hurricane Miniprep Kit (Biotech: Oxford, OH) according to the manufacturer's protocol. PCR products were purified using a PCR purification kit (QIAGEN: Valencia, CA) according to manufacturer's protocol. The cloning was performed using two methods: (i) Infusion cloning kit (Clontech: Montain View, CA) according to the manufacturer's protocol and (ii) ligation with T4 DNA ligase provided from New England Biolabs (Ipswich, MA). Plasmids were gel

band purified by Gel extraction kit (QIAGEN: Valencia, CA). All experimental procedures were performed according to standard protocol and any change in the standard procedure is mentioned.

3.4.1. PCR amplification of fluorescent protein genes

Fluorescent protein genes were PCR amplified with the designed primers (Table.3.1) using the plasmids from Clontech (Montain View, CA) as templates. The following PCR reaction components were employed: (i) 5 µL 10x thermo buffer, (ii) 2.5 µL forward and reverse primers (1.0 ng/mL), (iii) 1 µL template DNA (plasmid at 10 pg-10 ng/mL), (iv) 1 µL stock dNTP mixture, (v) 1 µL VentR polymerase, (vi) 37 µL molecular biology grade water (total volume was 50 µL). The PCR program used is described as follows: (i) denaturing at 94°C for 5 min, (ii) annealing at a specified temperature for 1 min, and (iii) elongation at 72°C for 1.5 min (30 cycles). A final extension step at 72°C for 3 min was applied. The PCR products were visualized by 2% agarose gel and were recovered by PCR purification for cloning (QIAGEN: Valencia, CA).

Table.3.1. PCR primers designed for the amplification of fluorescent proteins genes. The underlined sequence refers to the restriction sites added to the primer.

Primer name	Target	Sequence	Restriction site
GFP_clone_left	*GFP* gene	ATTA***CTGCAG***ATGGTGAGCA AGGGCGA	*PstI*
GFP_clone_right	*GFP* gene	GTTG***CATATG***TTACTTGTAC AGCTCGTCCATGC	*NdeI*
AmCyan_left_PstI	*CFP* gene	CCATTA***CTGCAG***GATGGCTC T TCAAACAAGTTT	*PstI*
AmCyan_right_NarI	*CFP* gene	CCATTA***GGCGCC***TCAGAAAG GGACAACAGAGG	*NarI*
ZSYellow_left_PstI	*YFP* gene	CCATTA***CTGCAG***ATGGCTCA TTCAAAGCACGG	*PstI*
ZSYellow_left_PstI (2)	*YFP* gene	CCATTA***CTGCAG***GATGGCTC ATTCAAAGCACGG	*PstI*
ZsYellow_right_NarI	*YFP* gene	CCATTA***GGCGCC***TCAGGCCA AGGCAGAAGGGA	*NarI*

3.4.2. Construction of the pUC19-pro-term-fluorescent protein plasmid

3.4.2.1. Extraction of pU19-pro-term

An overnight culture (5 mL) at 37°C of *E. coli* cells transformed with *pUC19-pro-term* was centrifuged and the pellet was recovered. The plasmid extraction was performed using Hurricane Miniprep kit: (i) re-suspend the pelleted cells in 250 µL of solution A by pipetting, (ii) add 250 µL of buffer B with gentle mixing (iii) add 325 µL of buffer C and mix by inverting the tube, (iii) centrifuge the tube for 10 min at 10,000 rpm at room temperature, (iv) transfer the supernatant carefully to the DNA Binding Column Unit and centrifuge for 1 min at 16,904 x g at room temperature, (v) discard the liquid from the collection tube and add 750 µL of 70% ethanol, (vi) Centrifuge the unit at 16,904 x g for 1 min at room temperature, (vii) transfer the DNA binding column to a new 1.5 mL collection tube and add 50 µL of pre-heated sterile water to the center of the DNA binding column and let it stand at room temperature for 1 minute, and finally (viii) elute the plasmid in a new tube by centrifuging the unit for 1 minute at 16,904 x g at room temperature.

3.4.2.2. Digestion of pU19-pro-term

The result of extraction was verified by gel electrophoresis. And then the extracted plasmid was digested with two restriction enzymes specific to each fluorescent protein (Table.3.2). The same procedure was undertaken to digest the fluorescent gene with its specific restriction enzymes. The digestion reaction contains (i) 20 µL of *pUC19-pro-term* for plasmid digestion (or PCR product for fluorescent gene digestion), (ii) 6 µL 10XBuffer 4, (iii) 6 µL 10X BSA, (iv) 1 µL *PstI*, (v) 1 µL of the *NarI* or *NdeI* depending on the fluorescent protein, and (vi) 26 µL deionized water (total volume was 60 µL). The digestion was incubated 2 hrs at 37°C.

Table.3.2. Restriction enzymes for each fluorescent protein

Fluorescent proteins	**Restriction enzymes**
Cyan fluorescent protein (CFP) Yellow fluorescent protein (YFP)	*PstI + NarI*
Green fluorescent protein (GFP)	*PstI + NdeI*

3.4.2.3. Purification and ligation of pU19-pro-term with the fluorescent gene

The digested plasmid was visualized and recovered by gel-purification. In fact, the DNA fragment was excised from the agarose gel and supplemented with buffer QG at the ratio 1:3, and incubated at 50°C until the gel slice is completely dissolved. An equivalent of gel volume of isopropanol is added to the tube and the mix is placed in a QIAquick spin column. The sample is centrifuged for 1 min at 16,904 x g. Buffers are then discarded and 750 µL of PE buffer is added to the column. After centrifugation and elimination of the liquid, 50 µL of molecular biology grade water are placed in the center of column to dissolve the plasmid in. The recovered linearized plasmid was then ready for ligation. The linearized plasmid and digested DNA fragment were mixed in a ratio of 1:6. The ligation reaction was realized by T4 DNA ligase and incubated overnight at room temperature.

3.4.3. Chemical transformation of pUC19-pro-term-fluorescent protein plasmid into E. coli Top10 cells

The chemical transformation of *E. coli Top10* cells was performed as following: (i) add 0.5 µL of ligation solution into one 50 µL vial of chemically competent cells, (ii) incubate 30 min on ice, (iii) heat shock the mixed culture at 42°C for 30 seconds, (iii) incubate on ice again for 2 min (iv) then, add 1 mL of SOC medium, (v) incubate the culture in the shaker at 37°C for 1 hour, finally (vi) spread 50 µL of the culture on solid LB supplemented with X-gal and IPTG. Since the digestion occurs in multiple cloning site of *pUC19-pro-term*, it removes a part of *LacZ* gene enabling a blue and white screening of colonies.

3.4.4. Construction of pUC19-pro-term-fluorescent protein-asRNA

3.4.4.1. Amplification of asRNA genes

The fluorescent gene sequence served as backbone for the design of asRNA fragment. Different regions of the gene were randomly selected and primers (Table.3.3) were specifically designed to amplify these regions and insert them in the *pUC19-pro-term* plasmid by Infusion cloning method. The resulted DNA fragments have different sizes and each fragment bind to a specific region on the mRNA. The fluorescent protein genes were used as templates for PCR amplification of the different DNA fragments. The PCR reaction reagents were the same as those described above (Chapter 3: Part 3.4.1). The PCR programs used are base on a touch-down PCR program. This PCR allows the annealing temperature to be reduced by a defined value. In this program, the temperature increment was -1°C (Figure.3.2). The annealing temperatures and repetition of cycles employed in this procedure were chosen accordingly to all primers annealing temperatures for each fluorescent protein.

	PCR Step	Temperature	Time
1	Denaturation	94° C	5 min
2	Denaturation	94° C	2 min
3	Annealing	?	1 min
	Temperature increment	-1° C	
4	Elongation	72° C	90 sec
5	Number of cycles	Go to 2	Repeat ?
6	Denaturation	94° C	2 min
7	Annealing	?	1 min
8	Elongation	72° C	90 sec
9	Number of cycles	Go to 6	Repeat ?
10	Final elongation	72° C	7 min
11	Cooling and storage	Hold -4° C	
	End	end	

Figure.3.2. Touch-down PCR program.

Table.3.3. PCR primers designed for the amplification of antisense DNA fragments for all fluorescent proteins genes. The digestion sites are in italic and underlined.

	Primer name	Target	Sequence	Restriction site
Antisense GFP	asGFP_A left	*asGFP* genes	TTCAACTTTA*CTCGAG*TCA AGACCCGCCACAACATC	*XhoI*
	asGFP_A right	*asGFP* genes	GTGTGGAATT*AGATCT*TGG GGTCTTTGCTCAGGGCG	*BglII*
	asGFP_2 left	*asGFP* genes	TTCAACTTTA*CTCGAG*TGG CCCACCCTCGTG	*XhoI*
	asGFP_3 left	*asGFP* genes	TTCAACTTTA*CTCGAG* AG CAGCACGACTTCTTCAAG	*XhoI*
	asGFP_4 left	*asGFP* genes	TTCAACTTTA*CTCGAG*TGA AGTTCGAGGGCGACA	*XhoI*
	asGFP_4 right	*asGFP* genes	GTGTGGAATT*AGATCT*TGT GCCCCAGGATGTTG	*BglII*
	asGFP_5 left	*asGFP* genes	TTCAACTTTA*CTCGAG*CTA TATCACCGCCGACAAGC	*XhoI*
	asGFP_5 right	*asGFP* genes	GTGTGGAATT*AGATCT*GAA CTCCAGCAGGACCATGT	*BglII*
	asGFP_L left	*asGFP* genes	TTCAACTTTA*CTCGAG*ACG ACGGCAACTACAAGACC	*XhoI*
Antisense CFP	asCFP_left1	*asCFP* genes	TTCAACTTTA*CTCGAG*ACC TACCATATGGATGGCTGT	*XhoI*
	asCFP_right1	*asCFP* genes	GTGTGGAATT*AGATCT*CCG TTGGCCATGGTG	*BglII*
	asCFP_left2	*asCFP* genes	TTCAACTTTA*CTCGAG*GGG CCCCTTGCATTCTC	*XhoI*
	asCFP_right2	*asCFP* genes	GTGTGGAATT*AGATCT*CGC AGTAAAGCATCGATTTC	*BglII*
	asCFP_left3	*asCFP* genes	TTCAACTTTA*CTCGAG*ATG CCCGACTATTTCAAACAA	*XhoI*
	asCFP_right3	*asCFP* genes	GTGTGGAATT*AGATCT*ATG GGTCCCAACCAGTTGTC	*BglII*
	asCFP_left4	*asCFP* genes	TTCAACTTTA*CTCGAG*AAA ATGACTGTCTGCGATGG	*XhoI*
	asCFP_right4	*asCFP* genes	GTGTGGAATT*AGATCT*CTT TGTCAAGGTCGGTCCTC	*BglII*
	asCFP_left5	*asCFP* genes	TTCAACTTTA*CTCGAG*GTG TTCAGCTGACGGAGCA	*XhoI*
	asCFP_right5	*asCFP* genes	GTGTGGAATT*AGATCT*TCA GAAAGGGACAACAGAGG	*BglII*

Antisense YFP	asYFP_left1	*asYFP* genes	TTCAACTTTA*CTCGAG*AGG CATTGGATATCCGTTCA	*XhoI*
	asYFP_right1	*asYFP* genes	GTGTGGAATT*AGATCT*GTCT TCGGAAAATGGCAATG	*BglII*
	asYFP_left2	*asYFP* genes	TTCAACTTTA*CTCGAG*CGG AGACAGGATTTTCACTG	*XhoI*
	asYFP_right2	*asYFP* genes	GTGTGGAATT*AGATCT*GAA AAGACCTGCCCCATGTA	*BglII*
	asYFP_left3	*asYFP* genes	TTCAACTTTA*CTCGAG*CTGC TGATGGACCTGTGATG	*XhoI*
	asYFP_right3	*asYFP* genes	GTGTGGAATT*AGATCT*CATG GAGACATCCCCTTTCA	*BglII*
	asYFP_left4	*asYFP* genes	TTCAACTTTA*CTCGAG*GGA TGGTGGGCGTTACC	*XhoI*
	asYFP_right4	*asYFP* genes	GTGTGGAATT*AGATCT*GCA GAAGGGAATGCAATAGC	*BglII*

3.4.4.2. Purification of asRNA genes

After amplification, all antisense DNA fragments were PCR verified by 2% agarose gel and then purified with the purification kit (QIAGEN: Valencia, CA). The PCR reaction was supplemented with buffer PB at the ratio 1:5. The sample was discarded into a spin column and then centrifuged 1 min at 16,904 x g. After eliminating the liquid, 750 µL of buffer PE is added and the column is centrifuged again. The DNA fragments are recuperated with 50 µL of buffer EB.

3.4.4.3. Extraction and digestion of puc19-pro-term-fluorescent protein

Colonies transformed with *pUC19-pro-term-fluorescent protein* vector were harvested and the plasmid was extracted according to the protocol stated previously (Chapter 3: Part 3.4.2.1). The plasmid was then digested with *BglII* and *XhoI* following the same steps as mentioned before using the appropriate buffer (Chapter 3: Part 3.4.2.2) and the reaction was incubated overnight. The linearized plasmid was verified by gel electrophoresis and purified.

3.4.4.4. Infusion cloning method

The antisense fragments were cloned into the linearized vector containing the corresponding fluorescent gene, using InFusion cloning (Clontech: Montain View, CA) according to the manufacturer's protocols. The InFusion cloning approach is different from the conventional ligase approach ("sticky-end" cloning). In fact, the antisense DNA fragments share 16 bases of homology with the ends of the linearized vector. This sequence homology is added to the insert through the PCR primers. This method was proven to enhance cloning efficiency considerably and enabled all PCR fragments to be cloned simultaneously and located on a single plate. This led to a combinatorial design for evaluating *asRNA* genes.

AsDNA fragments were purified and each fragment concentration was determined by Nanodrop machine. Then, they were mixed appropriately to have the same fraction in the mix (combinatorial approach). The concentration of *pUC19-pro-term-fluorescent protein* plasmid was adjusted accordingly to the resulted mixture concentration. The InFusion cloning was performed according to the following procedure: (i) 2 µL mixtures of vector and insert both with the concentration of 10 pg-10 ng/mL were added to the reaction with the molar ratio of 1:6 (vector: insert), (ii) 1 µL 5X InFusion HD enzyme premix buffer was added, (iii) the total volume was adjusted to 5 µL with molecular biology grade water, (iv) the reaction was incubated at 50°C for 15 min, (v) the reaction was then placed on ice for 30 min for chemical transformation into *E. coli 10beta* competent cells (Clontech: Montain View, CA). The chemical transformation steps were as mentioned above (Chapter 3: Part 3.4.3).

3.5. FLUORESCENT PROTEIN EXPRESSION LEVEL DETERMINATION

Positive colonies on each plate were randomly selected and sub-cultured into 24-well plate with the final concentration of IPTG 0.8 mM and ampicillin 100 µg/mL. The culture was incubated in a plate reader at 25°C (Studier, 2005) with slow shaking. OD_{600} and fluorescence readings were determined every 30 min or 1 hour. The excitation and emission

wavelengths for each fluorescent protein are summarized in Table.3.4. The plate reader (Synergy™ HT) has a computer interface controlled by BioTek's Gen5™ software which enables the user to fix all the parameters and outputs the growth and fluorescence curves.

Table.3.4. Fluorescent proteins excitation and emission wavelengths.

Fluorescent proteins	Exitation (nm)	Emission (nm)	References
CFP	458	489	Clontech Protocol No. PT3404-1 Version No. PR37085 (Montain View, CA)
YFP	494	538	Labas et al., (2002)
GFP	480	515	http://www.microscopyu.com/articles/livecellimaging/fpintro.htmL

The expression level was determined as the difference between the peak and the bottom of the fluorescence intensities. The fluctuation in the expression level was interpreted as an effect of the antisense DNA fragment inserted into the colony. The suspected colonies were selected and the insertion of *asRNA* gene was verified by PCR using primers (Table.3.5) designed for the *plac* promoter (left) and the *lacZ* terminator (right).

Table.3.5. PCR primers designed for the verification of antisense DNA fragments inserted into *pUC19-pro-term-fluorescent protein-Antisense*. The restriction sites are in italic and underlined.

Primer name	Part Amplified	Sequence	Restriction site
pLacZ_left	*plac* promoter of *pUC19*	AATGC*AGGTCCT*GTTGGCCG ATTCATTA	*EcoO109I*
lacZ_term3_right	*lacZ* terminator of *pUC19*	ATTAGA*GACGTC*AATTACCT GATGGACTGG	*AatII*

3.6. DETERMINATION OF FREE ENERGY AND BINDING PERCENTAGE

The determination of the thermodynamic parameters: (i) minimum free energy and (ii) binding percentage of asRNA and mRNA complexes were determined with NUPACK software.

3.7. SOFTWARE

The thermodynamic analysis of asRNA and mRNA complexes was implemented by NUPACK software offered from http://www.nupack.org. The primers were designed using Primer3Plus software (http://www.bioinformatics.nl/cgi-bin/primer3plus/primer3plus.cgi). The fluorescence and growth curves were provided from BioTek's Gen5™ software with the plate reader.

3.8. REFRENCES

Labas, Y. A., Gurskaya,N. G., Yanushevich, Y. G., Fradkov, A. F., Lukyanov, K. A., Lukyanov, S. A., & Matz, M. V. (2002). Diversity and evolution of the green fluorescent protein family. *PNAS, 99*, 4256-4261.

Studier, F. W. (2005). Protein production by auto-induction in high-density shaking cultures. *Protein Expr Purif, 41*, 207-234.

Chapter 4: RESULTS AND DISCUSSION

AsRNA fragments are known to down regulate gene expression. The process is accomplished by the binding of asRNA to the target mRNA resulting in the reduction of the protein expression. This is the simplest scheme. However, many parameters are involved in this mechanism including RNA secondary structure, binding percentage, minimum free energy, and cellular concentration among several others. In this study, the purpose is to find a relationship between the expression level and the different thermodynamic parameters influencing asRNA efficiency. Therefore, fluorescent protein genes were used as reporters to improve our understanding of asRNA efficacy and mechanisms. This section is dedicated to the results found for the different fluorescent protein used: (i) Cyan fluorescent protein (CFP), (ii) the Green fluorescent protein (GFP) and (iii) the Yellow fluorescent protein (YFP) respectively.

4.1. CYAN FLUORESCENT PROTEIN

4.1.1. Construction of pUC19-pro-term-CFP

The *pUC19-pro-term* plasmid (Figure.3.1) was digested with *PstI and NarI* and the *LacZ* gene was removed as described previously (Chapter 3: Part 3.4.2.2). The cyan fluorescent protein (*CFP*) gene was PCR amplified (Table.3.1) and then digested with the same restriction enzymes. After the ligation and transformation in *E. coli 10beta* cells, several “white” colonies were randomly chosen and PCR amplified (Table.3.1) to check the transformation. Selected PCR results showing a successful transformation are shown in Figure.4.1. The positive colonies are indicated in lanes 1, 2 and 6. These transformants have approximately the same gene size (690 bp). To confirm the results, the colonies (including colony tested in lane 5) were cultured overnight at 37°C and then the fluorescence with excitation filter at 458

nm and emission filter at 489 nm (Table.3.4) was measured. The colony having the highest expression level was chosen for the next experiments.

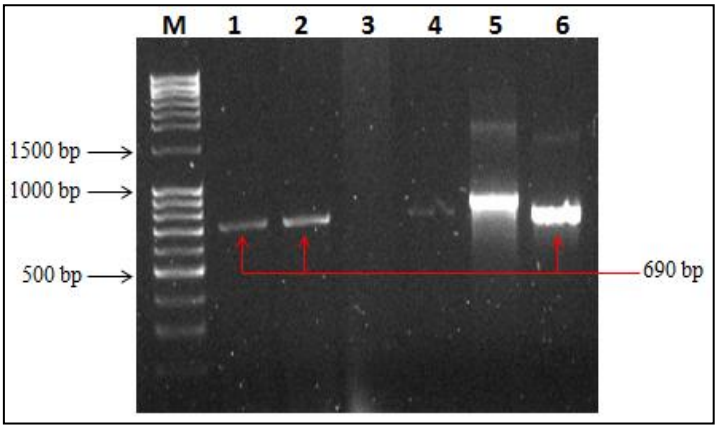

Figure.4.1. Gel electrophoresis of colony PCR to determine transformed colonies with *pUC19-pro-term-CFP*.

4.1.2. Amplification of antisense CFP gene fragment

With the designed primers (Table.3.3), 15 different antisense DNA fragments combinations were obtained. The antisense CFP DNA fragments (asCFP) were separately PCR amplified and visualized by gel electrophoresis. Figure.4.2 shows the PCR results of 15 selected asCFP DNA fragments and their sizes and sequences are shown in Table.4.1.

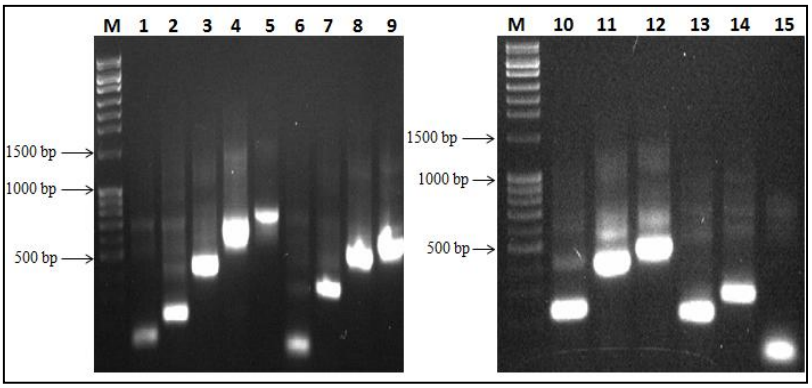

Figure.4.2. PCR amplification of 15 asCFP DNA fragments with a mid-range ladder. The following sample IDs are shown: Lane 1: antisense 1_1; lane 2: antisense 1_2; lane 3: antisense 1_3; lane 4: antisense 1_4; lane 5: antisense 1_5; lane 6: antisense 2_2; lane 7: antisense 2_3; lane 8: antisense 2_4; lane 9: antisense 2_5; lane 10: antisense 3_3; lane 11: antisense 3_4; lane 12: antisense 3_5; lane 13: antisense 4_4; lane 14: antisense 4_5 and lane 15: antisense 5_5.

Table.4.1. Antisense CFP sizes.

Antisense Name	Fragments size (bp)	Antisense sequence
1_1	116	uggaugguauaccuaccgacacaguuacccguaaugaaauggcaguuuccacuuccguc gcccuucgguaugcuuccccugcgucuggagcugaaaauuucaguggguaccgguugcc
1_2	186	uggaugguauaccuaccgacacaguuacccguaaugaaauggcaguuuccacuuccguc gcccuucgguaugcuuccccugcgucuggagcugaaaauuucaguggguaccgguugcca cccggggaacguaagaggaaacuguaugauagaugucacaaguacauaccuuuagcuac gaaaugacgc
1_3	400	uggaugguauaccuaccgacacaguuacccguaaugaaauggcaguuuccacuuccguc gcccuucgguaugcuuccccugcgucuggagcugaaaauuucaguggguaccgguugcca cccggggaacguaagaggaaacuguaugauagaugucacaaguacauaccuuuagcuac gaaaugacgcauaggauggucauacgggcugauaaaguuuguucguaaaggacugccu uacaguauacuuuccugaaaauggauacuucuaccuccucaacgaugucggucaacccu uuauucggaauuuccguugacgaaacucguguuuaggugcaaaguaccucacuugaaa ggacgacuaccuggacacuaccgcuucuacuguugaccaacccuggguagaaaacucuu uuacugacagacgcuaccuuauaacuucccacuacaguggcgcaaggaguacgacguuc cuccaccguuaaugucuacgguuaaggugugaagaauguucuguuuuuuuggccacug cuacgguggguuugguacgccaccuuguagcguaacgcuccuggcuggaacuguuuc
1_5	648	uggaugguauaccuaccgacacaguuacccguaaugaaauggcaguuuccacuuccguc gcccuucgguaugcuuccccugcgucuggagcugaaaauuucaguggguaccgguugcca cccggggaacguaagaggaaacuguaugauagaugucacaaguacauaccuuuagcuac gaaaugacgcauaggauggucauacgggcugauaaaguuuguucguaaaggacugccu uacaguauacuuuccugaaaauggauacuucuaccuccucaacgaugucggucaacccu uuauucggaauuuccguugacgaaacucguguuuaggugcaaaguaccucacuugaaa ggacgacuaccuggacacuaccgcuucuacuguugaccaacccuggguagaaaacucuu uuacugacagacgcuaccuuauaacuucccacuacaguggcgcaaggaguacgacguuc cuccaccguuaaugucuacgguuaaggugugaagaauguucuguuuuuuuggccacug cuacgguggguuugguacgccaccuuguagcguaacgcuccuggcuggaacuguuucca ccguugucacaagucgacugccucgugcgacaacguguauauuggagacaacagggaaa gacu
2_2	69	cccggggaacguaagaggaaacuguaugauagaugucacaaguacauaccuuuagcuac gaaaugacgc
2_3	283	cccggggaacguaagaggaaacuguaugauagaugucacaaguacauaccuuuagcuac gaaaugacgcauaggauggucauacgggcugauaaaguuuguucguaaaggacugccu uacaguauacuuuccugaaaauggauacuucuaccuccucaacgaugucggucaacccu uuauucggaauuuccguugacgaaacucguguuuaggugcaaaguaccucacuugaaa ggacgacuaccuggacacuaccgcuucuacuguugaccaacccuggggua
2_4	466	cccggggaacguaagaggaaacuguaugauagaugucacaaguacauaccuuuagcuac gaaaugacgcauaggauggucauacgggcugauaaaguuuguucguaaaggacugccu uacaguauacuuuccugaaaauggauacuucuaccuccucaacgaugucggucaacccu uuauucggaauuuccguugacgaaacucguguuuaggugcaaaguaccucacuugaaa

		ggacgacuaccuggacacuaccgcuucuacuguugaccaacccuggguagaaaacucuu uuacugacagacgcuaccuuauaacuucccacuacaguggcgcaaggaguacgacguuc cuccaccguuaaugucuacgguuaaggugugaagaauguucuguuuuuuuggccacug cuacggugguuugguacgccaccuuguagcguaacgcuccuggcuggaacuguuuc
2_5	531	cccggggaacguaagaggaaacuguaugauagaugucacaaguacauaccuuuagcuac gaaaugacgcauaggauggucauacgggcugauaaaguuuguucguaaaggacugccu uacaguauacuuuccugaaaauggauacuucuaccuccucaacgaugucggucaacccu uuauucggaauuuccguugacgaaacucguguuuaggugcaaaguaccucacuugaaa ggacgacuaccuggacacuaccgcuucuacuguugaccaacccuggguagaaaacucuu uuacugacagacgcuaccuuauaacuucccacuacaguggcgcaaggaguacgacguuc cuccaccguuaaugucuacgguuaaggugugaagaauguucuguuuuuuuggccacug cuacggugguuugguacgccaccuuguagcguaacgcuccuggcuggaacuguuucca ccguugucacaagucgacugccucgugcgacaacguguauauuggagacaacagggaaa gacu
3_3	202	uacgggcugauaaaguuuguucguaaaggacugccuuacaguauacuuuccugaaaau ggauacuucuaccuccucaacgaugucggucaacccuuuauucggaauuuccguugacg aaacucguguuuaggugcaaaguaccucacuugaaaggacgacuaccuggacacuaccg cuucuacuguugaccaacccuggguagaaaacucuuuuacugacagacgcuaccuuaua acuucccacuacaguggcgcaaggaguacgacguuccuccaccguuaaugucuacgguu aaggugugaagaauguucuguuuuuuuggccacugcuacggugguuugguacgccacc uuguagcguaacgcuccuggcuggaacuguuuc
3_4	385	uacgggcugauaaaguuuguucguaaaggacugccuuacaguauacuuuccugaaaau ggauacuucuaccuccucaacgaugucggucaacccuuuauucggaauuuccguugacg aaacucguguuuaggugcaaaguaccucacuugaaaggacgacuaccuggacacuaccg cuucuacuguugaccaacccuggguagaaaacucuuuuacugacagacgcuaccuuaua acuucccacuacaguggcgcaaggaguacgacguuccuccaccguuaaugucuacgguu aaggugugaagaauguucuguuuuuuuggccacugcuacggugguuugguacgccacc uuguagcguaacgcuccuggcuggaacuguuuccaccguugucacaagucgacugccu cgugcgacaacguguauauuggagacaacagggaaagacu
3_5	450	
4_4	175	uuuuacugacagacgcuaccuuauaacuucccacuacaguggcgcaaggaguacgacgu uccuccaccguuaaugucuacgguuaaggugugaagaauguucuguuuuuuuggccac ugcuacggugguuugguacgccaccuuguagcguaacgcuccuggcuggaacuguuuc
4_5	240	uuuuacugacagacgcuaccuuauaacuucccacuacaguggcgcaaggaguacgacgu uccuccaccguuaaugucuacgguuaaggugugaagaauguucuguuuuuuuggccac ugcuacggugguuugguacgccaccuuguagcguaacgcuccuggcuggaacuguuuc caccguugucacaagucgacugccucgugcgacaacguguauauuggagacaacaggga aagacu
5_5	56	cacaagucgacugccucgugcgacaacguguauauuggagacaacagggaaagacu

These antisense fragments were designed to bind to different regions in the mRNA (Figure.4.3). In fact, according to the region of hybridization, the effectiveness of asRNA and the mechanism of action can be different. It has been reported that some antisense RNA can

reduce protein expression when targeted to any region of mRNA (Dias and Stein, 2002); these are the Rnase-H dependent oligonucleotides. In contrast, the steric blocker antisenses are efficient only when targeted to 5' or AUG initiation codon region (Dean et al., 1994). Since the mechanism of action of the antisense fragments used is not well elucidated, different region of the gene were targeted.

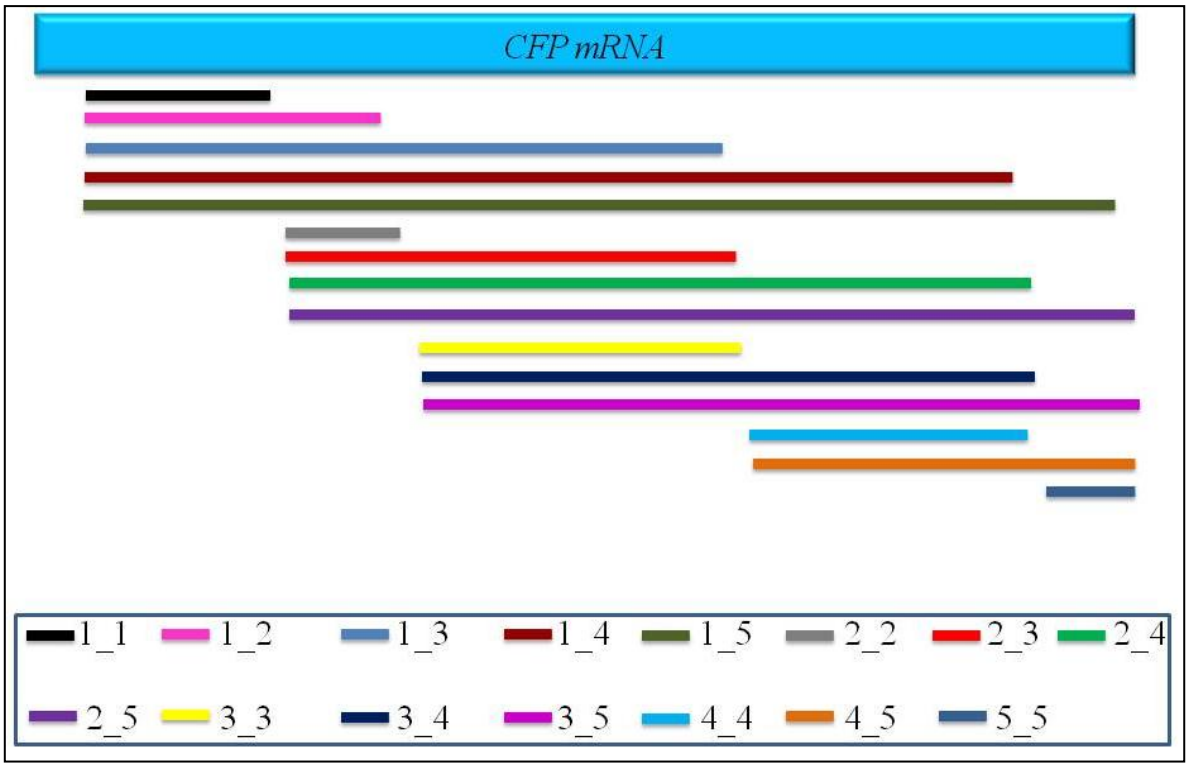

Figure.4.3. Localization of the binding of the different asCFP fragments in the mRNA of *CFP* gene (Scale: 1 cm corresponds to 30 bp).

4.1.3. Construction of pUC19-pro-term-CFP-asCFP

The construction of *pUC19-pro-term-CFP-asCFP* was performed by InFusion cloning methods, as described in Chapter 3 Part 3.4.4.4. Each of the 15 antisense DNA fragments was cloned separately into *pUC19-pro-term-CFP* already digested by *XhoI* and *BglII*. The InFusion cloning method yielded high efficiency. Each antisense fragment was individually cloned resulting in 15 different plates with colonies containing a specific and known antisense DNA fragment. Therefore, the screening of antisense fragments was just employed as a

verification tool. The combinatorial approach of cloning all fragments simultaneously was not used in this case.

4.1.4. Quantitative analysis of CFP expression level

The *E. coli* 10beta colonies with *pUC19-pro-term-CFP-asCFP* plasmids were sub-cultured in a single plate of a 24-well and their fluorescence intensities were measured with the growth (optical density at 600 nm) in the plate reader incubator at 25°C for 48 hours. The plate reader allows to measure fluorescence and OD_{600} as a function of time and outputs the results via BioTek's Gen5™ software (Chapter 3: Part 3.5). The fluorescence was determined at the cyan color wavelength, namely 458 nm for excitation and 489 nm for emission (Table.3.4). For each of the different antisense fragments, biological replicates were cultured in the well plate for more accuracy. The results of fluorescence for several different colonies and antisense RNA genes are listed in Table.4.2 with some thermodynamic factors.

Table.4.2. Determination of CFP expression level and thermodynamic parameters.

Antisense fragments	**Antisense fragment size (bp)**	**Expression level compared to the control**	**Free energy (kcal/mol)**	**Binding percentage (%)**
Control	N/A	1	N/A	N/A
1_1	116	0.22	-310.83	96
1_2	186	0.67	-328.71	99
1_3	400	0.33	-406.34	100
1_4	583	0.24	-472.22	100
1_5	648	0.25	-501.56	100
2_2	69	0.61	-281.21	31
2_3	283	0.57	N/A	N/A
2_4	466	0.28	-422.91	13
2_5	531	0.16	-453.09	99.21
3_3	202	0.29	-323.73	0.43
3_4	385	0.25	-395.58	9.4
3_5	450	N/A	-425.14	99
4_4	175	N/A	-327.54	2.2
4_5	240	N/A	-358.42	99
5_5	56	N/A	-279.93	31

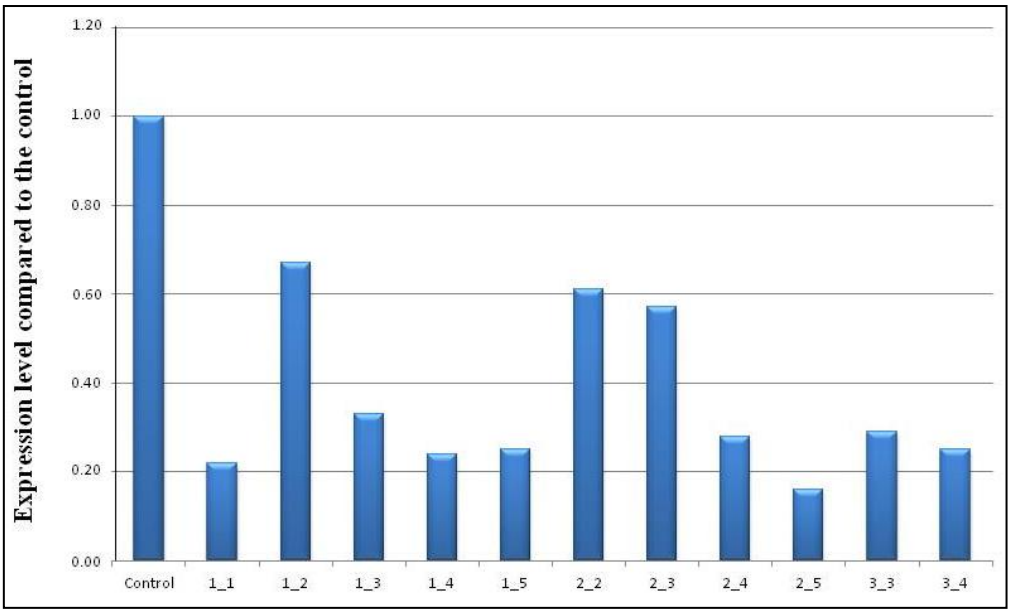

Figure.4.4. *CFP* gene expression level in the presence of specified antisense CFP fragments.

According to data provided from Table.4.2 and Figure.4.4, a dramatic decrease was observed in the expression level of CFP in the presence of antisense fragments. In fact, the control colony (does not contain an antisense fragment) over-expressed the target protein, but with the presence of antisense RNA fragments the measured fluorescence diminished efficiently. The minimum free energy (MFE) and binding percentages were calculated with NUPACK software at 25°C and the relationships between the expression level and the MFE were plotted and are given in Figure.4.5.

To correlate the binding region of antisense fragments and the expression levels, both Figure.4.3 and Figure.4.4 are of interest. The first observation is that the lowest expression levels (16% to 25%) are observed for the antisense that bind either near the AUG region (asCFP 1_1) and the end of CFP mRNA (asCFP: 1_4; 1_5; 2_4; 2_5 and 3_4). The asRNA fragments that hybridize in between have also reduced the expression level but the reduction did not exceed 50% compared to the control. These results imply that the beginning and the end of *CFP* gene contain a "favorable region" for hybridization that trigger the antisense down-regulation machinery. The analysis of minimum free energy for those particular

antisense fragments (Table.4.2) shows a low energy required for the formation of asRNA-mRNA complex, which facilitates the hybridization. This remark is mainly for asCFPs that binds to the end of *CFP* mRNA.

The relationship between the expression level and the MFE is represented in Figure 4.5. Relatively low correlations were found when the expression level is plotted against the natural log of minimum free energy (ln(-MFE)). A coefficient of determination (R^2) of 0.377 was obtained. Although somewhat poor linear correlations were observed between the ln(-MFE) and the expression level, a somewhat linear trends were observed. For lower (more negative) values of MFE, a more linear relationship was observed. In fact, the lower the free energy of binding, the more stable the asRNA-mRNA structure (Layton and Bundschuh, 2005). In this case, the expression level of the CFP decreased as the minimum free energy of the mRNA-asRNA complex decreased. Therefore, at weak MFE the complex (asRNA-mRNA) is possibly more stable and induces the lowest expression levels for the CFP gene. The asCFP-CFP mRNA complexes having the lowest MFE of binding have decreased the expression levels to 16-25% compared to the control (100%). These antisense (asCFP: 1_3; 1_4; 1_5; 2_4; 2_5 and 3_4) bind to the region at the ends of CFP mRNA. These results are in agreements with the analysis of the localization of the binding of the different asCFP fragments in the mRNA of *CFP* gene (Chapter 4: part 4.1.4) and suggest that there is a "favorable region" for antisense hybridization that stimulates the antisense down-regulation machinery.

However, when the free energy of binding is higher, the deviation becomes larger and the linearity was not conserved. The higher free energy values indicate the formation of a more unstable asRNA-mRNA complex. These antisense fragments did not decrease the expression level significantly. Although, and at higher MFE values (-310), the antisense fragment 1_1

reduced the fluorescence level considerably (0.22). This antisense binds near to AUG initiation codon suggesting the blockade of the elongation steps.

Nevertheless, the weak coefficient of determination suggests more factors are required to convincingly link the expression level of the fluorescent protein with the thermodynamics of mRNA-asRNA binding. Besides, the weak coefficients imply the intervention of other forces mainly at high levels of the MFE. These are discussed in detail in the following sections.

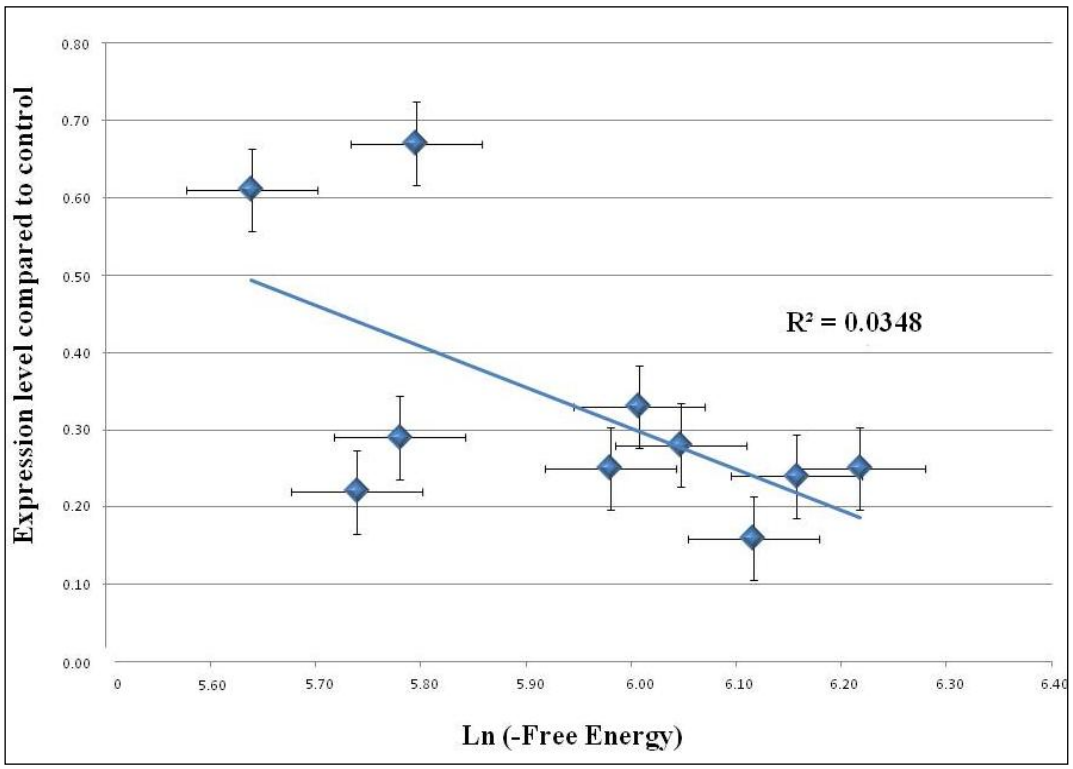

Figure.4.5. Relationships between the observed expression level of CFP in the presence of an asCFP fragment (relative to the control) as a function of minimum free energy : ln(-MFE).

4.1.5. Verification of antisense CFP fragments

In order to confirm the plate reader results, each colony showing a decrease in its expression level was verified by colony PCR method. The primers used were *pLacZ_left* and *lacZ_term_right* primers (Table.3.5). Thus, the PCR products included the *plac* promoter, the antisense RNA gene, and the *lacZ* terminator. These are shown in Chapter 3 Figure 3.1. Since the promoter and terminator had both a combined size of 450 bp, this size was added to the

antisense RNA fragment size. The PCR products were analyzed by gel electrophoresis and are shown in Figure.4.6.

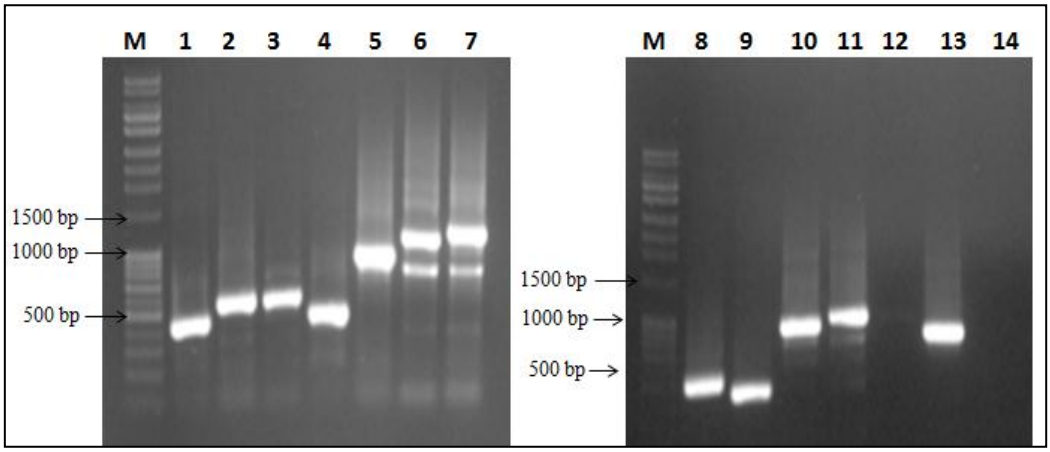

Figure.4.6. PCR verification of asCFP DNA fragments. The different lanes show the different colonies screened. Lane 1 is the control with a band of 450 bp.

4.1.6. Hybridization of CFP antisense RNA fragments with mRNA

NUPACK software enabled the visualization of binding between CFP mRNA with the different asCFP RNA fragments. The figures below show some examples of the pairing. These data are independent of concentration and of all other ordered complexes in solution (Zadeh et al., 2011). The equilibrium profile is shown by the color pallet ranging from blue, yellow to red to refer to equilibrium probability (from 0 to 1).

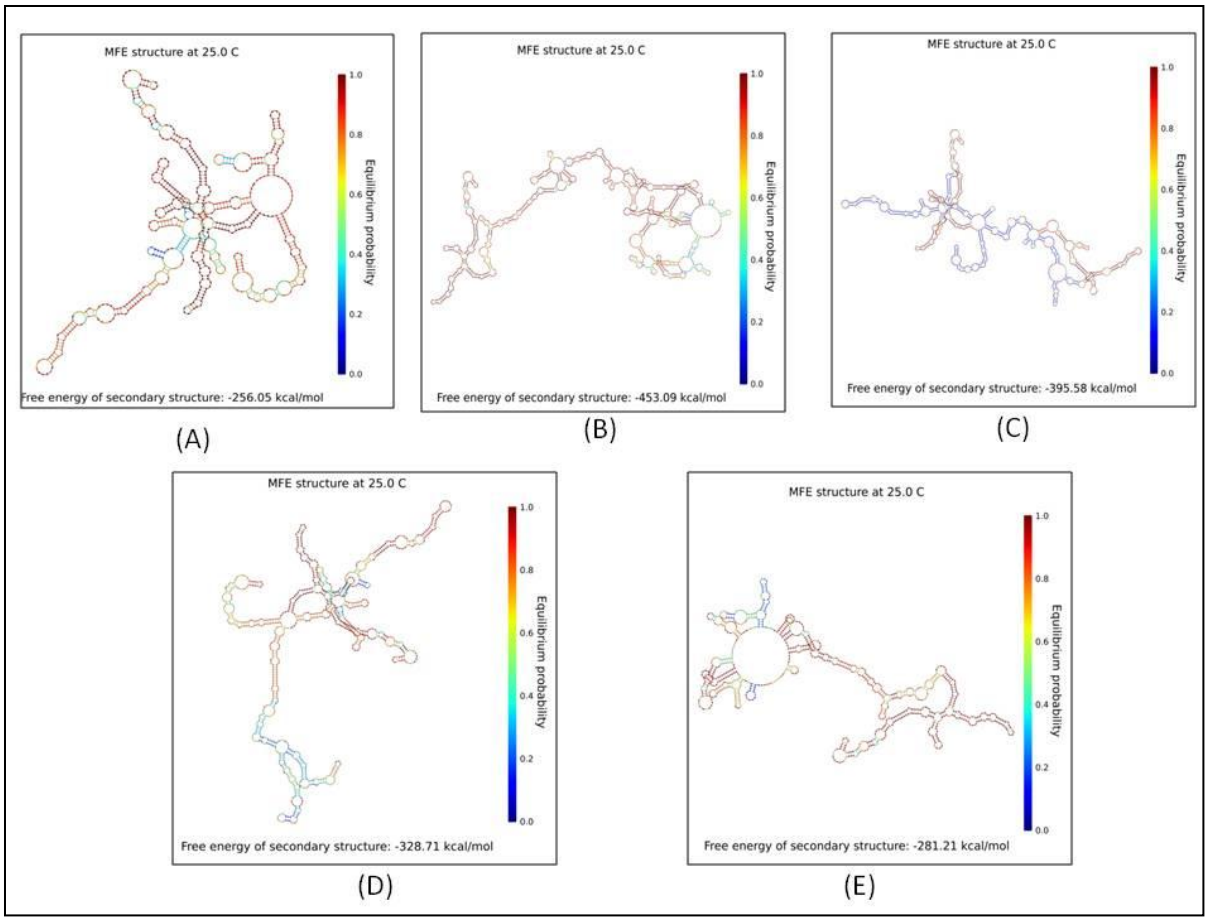

Figure.4.7. The secondary structure of CFP mRNA and the asCFP hybridization with CFP mRNA complex predicted by NUPACK software ((A): CFP mRNA; (B) antisense 2_5; (C): antisense 3_4; (D): antisense 1_2 and (E): antisense 2_2).

At equilibrium, the formation of CFP mRNA requires -256.05 kcal/mol. The structure is stable, this is shown by the omnipresence of the red color and the absence of dark blue (Figure.4.7 (A)). In general, the binding with asRNA requires less energy; however it introduces more instability to the structure (Figure.4.7 B, C, D and E). The complex mRNA-asCFP 2_5, which has the highest reduction level, presents a stable binding with a low minimum free energy of hybridization (Figure.4.7 (B)). This implies that not only the location of asRNA binding is important but also the stability of the complex for an effective reduction. The asCFP 1_2 and 2_2 reduction level was about 30%, the pairing scheme show many instability region that may be the origin of the low efficiency (Figure.4.7 D and E). However,

the asCFP 3_4, which reduced the expression by 75%, when it binds with CFP mRNA shows many dark blue regions referring to low equilibrium domains (Figure.4.7 (C)). The conclusion is that the reduction level could be related to both asRNA binding location and secondary structure of the asRNA-mRNA complex.

4.2. GREEN FLUORESCENT PROTEIN

4.2.1. Amplification of antisense GFP gene fragment

The construction of the *pUC19-pro-term-GFP* plasmid (Figure.4.8) was already performed in previous research in the Senger Lab.

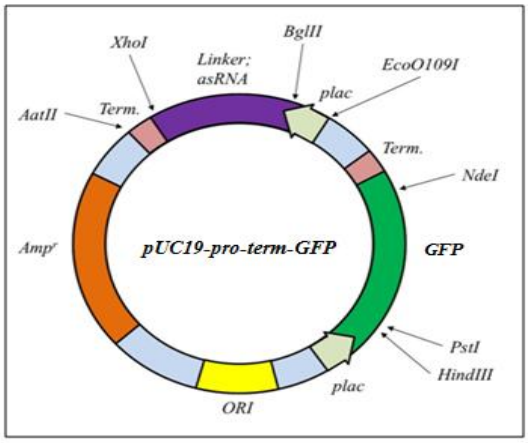

Figure.4.8. Diagram of the *pUC19-pro-term-GFP* plasmid.

Eight antisense GFP (asGFP) DNA fragments (Table.4.3) were PCR amplified separately and visualized by gel electrophoresis. Each fragment was designed to have sixteen base pairs in common with the *pUC19-pro-term-GFP* plasmid sequence. These overhangs were added to the primer sequences (Table.3.3) to enable the Infusion cloning technique. The PCR result is shown in Figure.4.9.

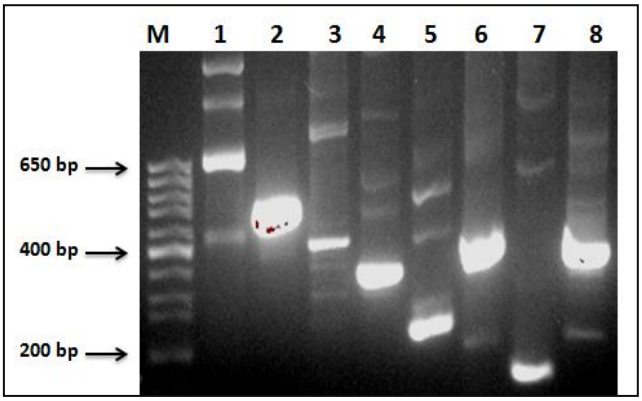

Figure.4.9. PCR amplification of 8 asGFP DNA fragments. The following sample IDs are shown: Lane 1: antisense 1_A; Lane 2: antisense 2_A; Lane 3: antisense 3_A; Lane 4: antisense 4_A; Lane 5: antisense 5_A; Lane 6: antisense L_A; Lane 7: antisense A_4 and Lane 8: antisense A_5.

Table.4.3. Antisense GFP sequences.

AsGFP	Size (bp)	AsGFP sequence
1_A	634	cacucguucccgcuccucgacaaguggccccaccacggguaggaccagcucgaccugccgcu gcauuugccgguguucaagucgcacaggccgcucccgcucccgcuacgguggaugccguuc gacugggacuucaaguagacgugguggccguucgacgggcacgggaccgggugggagcac ugguggaacuggaugccgcacgucacgaagcgggcgaugggcugguguacuucgucgug cugaagaaguucaggcgguacgggcuuccgaugcagguccucgcgugguagaagaaguucc ugcugccguugauguucugggcgcggcuccacuucaagcucccgcugugggaccacuuggc guagcucgacuucccguagcugaaguuccuccugccguuguaggaccccguguucgaccuc auguugauguugucgguguuccagauauaguggcggcuguucgucuucuugccguaguuc cacuugaaguucugggcgguguuguagcuccugccgucgcacgucgagcggcuggugaug gucgucuuguggggguagccgcugccggggcacgacgacgggcuguuggugauggacucg ugggucaggcgggacucguuucuggggu
2_A	466	accgggugggagcacugguggaacuggaugccgcacgucacgaagcgggcgaugggcug guguacuucgucgugcugaagaaguucaggcgguacgggcuuccgaugcagguccucgcg ugguagaagaaguuccugcugccguugauguucugggcgcggcuccacuucaagcucccgc ugugggaccacuuggcguagcucgacuucccguagcugaaguuccuccugccguuguagga ccccguguucgaccucauguugauguugucgguguuccagauauaguggcggcuguucgu cuucuugccguaguuccacuugaaguucugggcgguguuguagcuccugccgucgcacgu cgagcggcuggugauggucgucuuguggggguagccgcugccggggcacgacgacgggcu guuggugauggacucgugggucaggcgggacucguuucuggggu
3_A	399	ucgucgugcugaagaaguucaggcgguacgggcuuccgaugcagguccucgcgugguaga agaaguuccugcugccguugauguucugggcgcggcuccacuucaagcucccgcuguggga ccacuuggcguagcucgacuucccguagcugaaguuccuccugccguuguaggaccccgug uucgaccucauguugauguugucgguguuccagauauaguggcggcuguucgucuucuug ccguaguuccacuugaaguucugggcgguguuguagcuccugccgucgcacgucgagcgg cuggugauggucgucuuguggggguagccgcugccggggcacgacgacgggcuguuggug auggacucgugggucaggcgggacucguuucuggggu
4_A	300	acuucaagcucccgcugugggaccacuuggcguagcucgacuucccguagcugaaguuccu ccugccguuguaggaccccguguucgaccucauguugauguugucgguguuccagauaua guggcggcuguucgucuucuugccguaguuccacuugaaguucugggcgguguuguagcu ccugccgucgcacgucgagcggcuggugauggucgucuuguggggguagccgcugccggg gcacgacgacgggcuguuggugauggacucgugggucaggcgggacucguuucuggggu
5_A	185	gauauaguggcggcuguucgucuucuugccguaguuccacuugaaguucugggcgguguu guagcuccugccgucgcacgucgagcggcuggugauggucgucuuguggggguagccgcu gccggggcacgacgacgggcuguuggugauggacucgugggucaggcgggacucguuucu gggggu
L_A	330	ugcugccguugauguucugggcgcggcuccacuucaagcucccgcugugggaccacuuggc guagcucgacuucccguagcugaaguuccuccugccguuguaggaccccguguucgaccuc auguugauguugucgguguuccagauauaguggcggcuguucgucuucuugccguaguuc cacuugaaguucugggcgguguuguagcuccugccgucgcacgucgagcggcuggugaug gucgucuuguggggguagccgcugccggggcacgacgacgggcuguuggugauggacucg ugggucaggcgggacucguuucuggggu
A_4	112	guuguaggaccccguguucgaccucauguugauguugucgguguuccagauauaguggcg gcuguucgucuucuugccguaguuccacuugaaguucugggcgguguuguag
A_5	176	aguucugggcgguguuguagcuccugccgucgcacgucgagcggcuggugauggucgucu uguggggguagccgcugccggggcacgacgacgggcuguuggugauggacucguggguca ggcgggacucguuucugggguugcucuucgcgcuaguguaccaggacgaccucaag

4.2.2. Results of pUC19-pro-term-GFP-asGFP construction

The obtained eight asGFP DNA fragments were purified separately and were mixed appropriately to have the same fraction in the mix. The concentration of *pUC19-pro-term-GFP* plasmid was adjusted accordingly to the mix concentration. The resulted mixture of asGFP fragments and *pUC19-pro-term-GFP* plasmid were then ready for the ligation step. The ligation was performed based on the InFusion cloning method (Chapter 3: Part 3.4.4.4) and the reaction product was transformed into *E. coli 10beta* competent cells with the heat-shock technique. Hundreds of positive colonies transformed with *pUC19-pro-term-GFP-asGFP* were obtained per plate (Chapter 3: Part 3.4.3). This enabled an entire library of *asGFP* fragments to be cloned at the same time. However, since the cloning was simultaneous for each asGFP fragment, individual colonies must be screened to determine the identity of each asGFP fragment present in each colony. This procedure is described below.

4.2.3. Determination of GFP expression level

After the transformation of *E. coli 10beta* colonies with *pUC19-pro-term-GFP-asGFP,* colonies were randomly selected from LB solid plate and were sub-cultured in the same 24-well plate. The results obtained after 48 hours revealed some differences in the observed expression level of *GFP* gene in the presence of antisense fragments. GFP expression levels were analyzed along with culture growth at 25°C in real time using the plate reader and the fluorescent wavelengths for excitation and emission of 480 nm and 515 nm (Table.3.4), respectively.

4.2.4. Identification of asGFP fragments

The identification of antisense RNA genes was determined by PCR methods. The reaction was performed using *pLacZ_left* and *lacZ_term_right* primers (Table.3.5). As mentioned previously (Chapter 4: Part 4.1.5) the PCR product have 450 bp added to its original size, these base pairs represents both promoter and terminator combined sizes (Figure.4.8).

Selected examples of antisense RNA fragment identification are shown in Figure.4.10. It is noted that some colonies have two plasmids. This is observed by two bands in the electrophoresis gel.

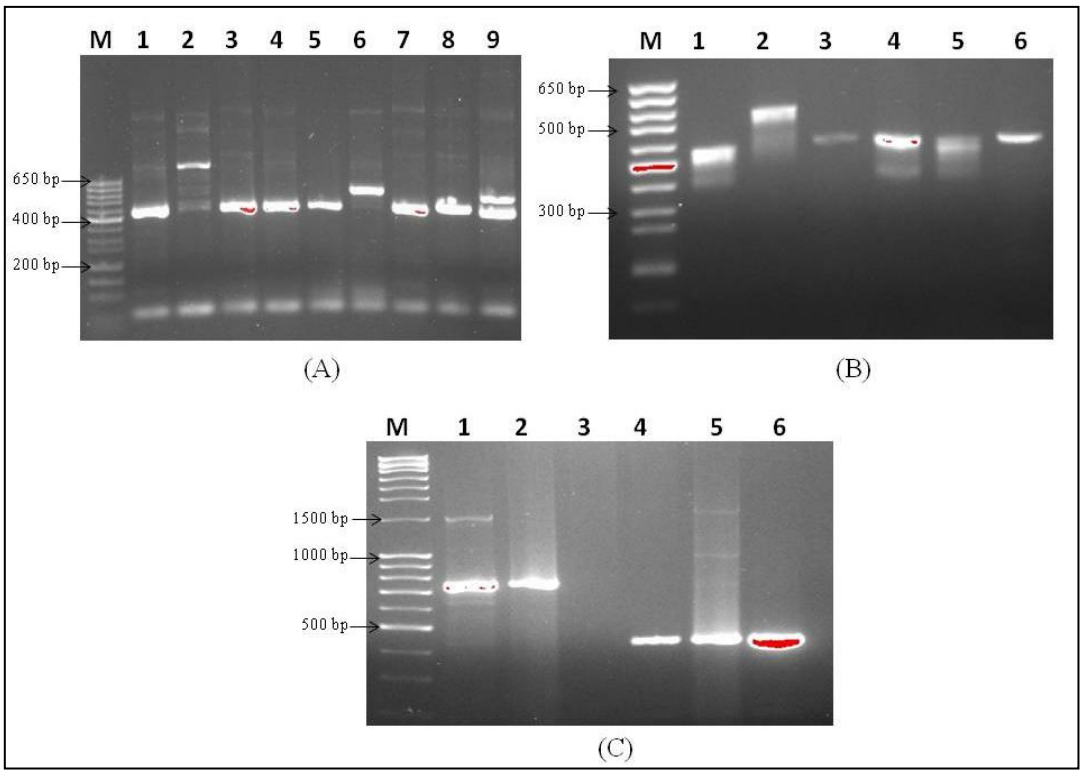

Figure.4.10. Identification of asGFP DNA fragments by PCR method. The insertion results of pro-asGFP-term in *E. coli* 10beta are shown in Lane 2 (A); Lane 6 (A); Lane 2 (B); Lane 1 (C) and Lane 2 (C).

4.2.5. Analysis of GFP expression level

The expression levels of GFP are listed in Table.4.4 along with other important thermodynamic indicators, including the binding percentage and the minimum free energy. Those thermodynamic parameters were determined by the NUPACK software at 25°C.

Table.4.4. Determination of GFP expression level for different antisense DNA fragments and thermodynamic parameters.

Antisense fragments	Antisense fragment size (bp)	Expression level compared to the control	Free energy (kcal/mol)	Binding percentage (%)
Control	-	1	N/A	N/A
2_A	466	0.87	-532.97	100
3_A	399	N/A	N/A	N/A
4_A	300	1.23	-443.83	100
5_A	185	1.2	-398.91	100
L_A	330	1.34	-463.76	100
A_4	112	0.86	-354.51	100
A_5	176	0.77	-404.52	100

The expression level of *GFP* gene in the presence of different antisense fragments compared to the control (with no antisense RNA fragment) is plotted in Figure.4.11. Depending on the antisense RNA fragment inserted, different expression levels were observed. Some antisense fragments effectively reduced the expression level of the fluorescent protein such as antisense fragment A_5, which reduced the expression by 23%. Other antisense produced little change or led to an increase in the expression of the GFP. This is the case for antisense fragments 4_A and 5_A.

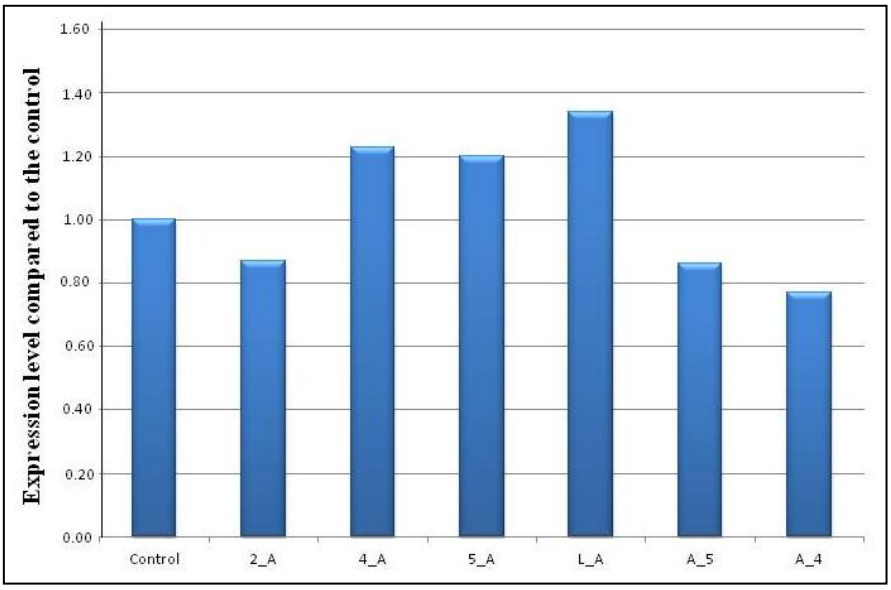

Figure.4.11. The GFP expression level in the presence of specified asGFP fragments.

The diversity of the asGFP fragments tested was not only in the sequence but also in the location of the binding of the antisense with the mRNA (Figure.4.12). The multiplicity of antisense fragments and hybridization region provides more data for the thermodynamic modeling. The analysis of both targeted regions and expression level indicates that asGFP A_4 and A_5 fragments which bind to almost the same region of GFP mRNA have the best reduction of the expression level among the other antisense fragments. asGFP 2_A also reduced the expression level by 13% and it binds in the middle region of the mRNA. These antisense fragments (2_A; A_4 and A_5) share the common region of 67 bp. This may suggest that this region promotes antisense binding and the inactivation mechanism. However, the remaining asGFPs have increased the expression of the *GFP* gene. Cases of positive antisense control such as by alteration of mRNA structure to facilitate translation initiation or to protect against ribonucleolytic attack are probable (Wagner and Simons, 1994).

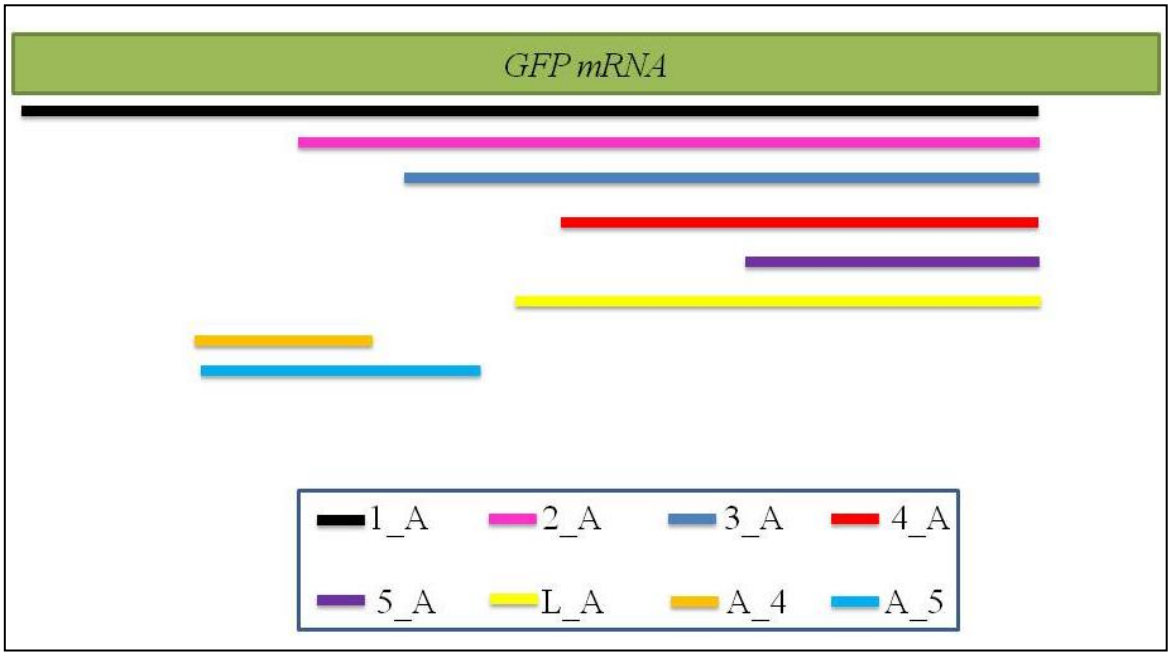

Figure.4.12. Localization of the binding of the different asGFP fragments in the mRNA of *GFP* gene (Scale: each 30 bp are represented by 1 cm).

The relationship between the minimum free energy and the expression level, relative to the control, is plotted in Figure 4.13. The analysis of correlation coefficient (0.034) indicates

that there is a very weak relationship between the expression level and MFE. This correlation suggests that the free energy of asRNA-mRNA binding is not implicated in the expression of the *GFP* gene. It is noted that these results are in disagreement with previous results obtained by the Senger Lab; however, these results lead to the following observation. Not only is the minimum free energy of the asRNA-mRNA binding important, but the location of these interactions may also play a big role in knocking-down mRNA translation or increasing mRNA translation, possibly through increased mRNA stability. In fact, antisense fragments designed for *GFP* gene induced an increase of the expression level. It can be considered as a particular case, and more antisense fragments should be tested to analyze the data appropriately

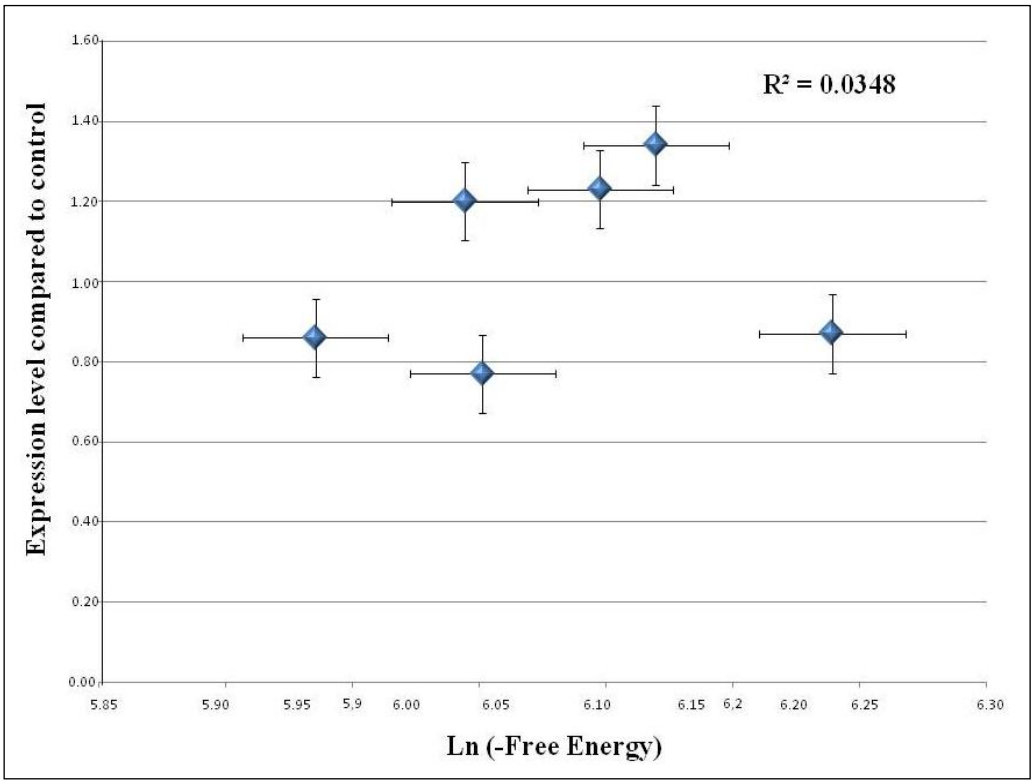

Figure.4.13. Relationships between the observed expression level of GFP in the presence of an asGFP fragment (relative to the control) as a function of the minimum free energy: ln (-MFE).

4.2.6. Hybridization of antisense RNA fragments with mRNA

Examples of complexes formed between asGFP and GFP mRNA generated by NUPACK software are shown in Figure.4.14. These diagrams represent the pairing of GFP mRNA with the asGFP molecules. The equilibrium of these complexes are shown by a color code.

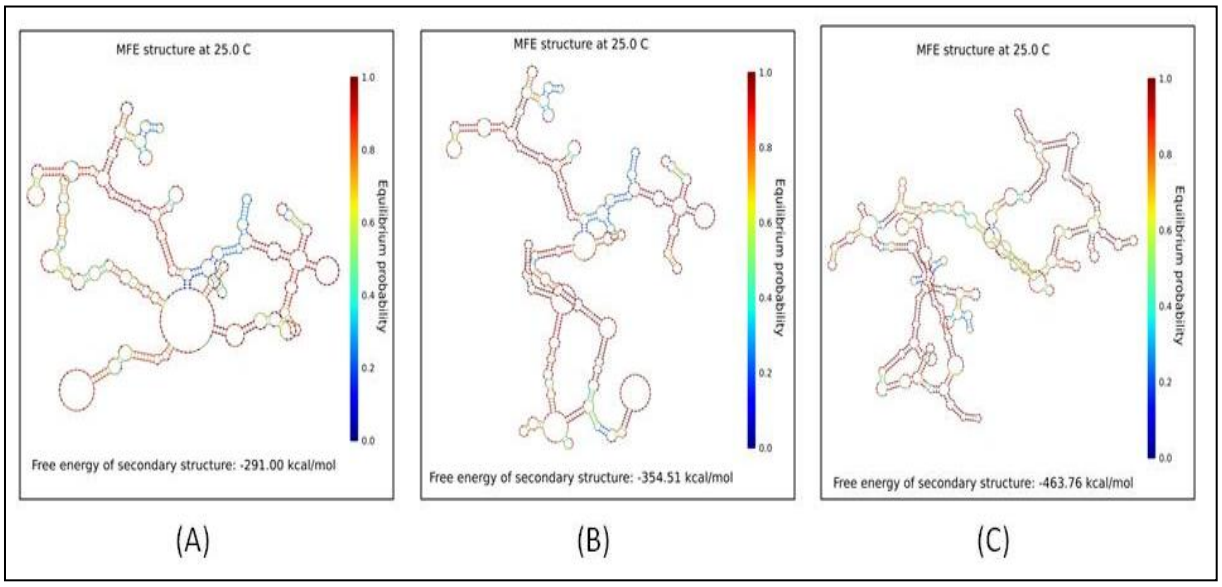

Figure.4.14. The secondary structure of the GFP mRNA (A) and the asGFP with GFP mRNA complex computed by NUPACK software (B: asGFP A_4; C: asGFP L_A).

At equilibrium, the secondary structure adapted by GFP mRNA requires -219 kal/mol (Figure.4.14 (A)). However, lower energy is required to form the complex asRNA-mRNA (Figure.4.14 B and C). The binding with asGFP lowers the equilibrium probability for certain regions. For the complex mRNA-asGFP A_4 (reduction), the equilibrium of the secondary structure is maintained (Figure.4.14 (B)). Meanwhile for the pairing of mRNA-asGFP L_A (positive control), the structure is more unstable (Figure.4.14 (C)). In this case, more fragments should be analyzed to come with a more accurate conclusion to relate the efficacy of antisense with the secondary structure.

4.3. YELLOW FLUORESCENT PROTEIN

4.3.1. Construction of pUC19-pro-term-YFP

The yellow fluorescent protein (*YFP*) gene was PCR amplified and digested with *PstI* and *NarI*. The plasmid *pUC19-pro-term* (Figure.3.1) was also linearized with the same restriction enzymes. Then the digestion products were linked with T4 DNA ligase and incubated overnight at room temperature (Figure.4.15). The ligation product was transformed into *E. coli 10beta* competent cells (Chapter 3: Part 3.4.3). The culture was plated in LB_{amp} Petri dish supplemented with Xgal/IPTG enabling blue and white screening of the positive colonies.

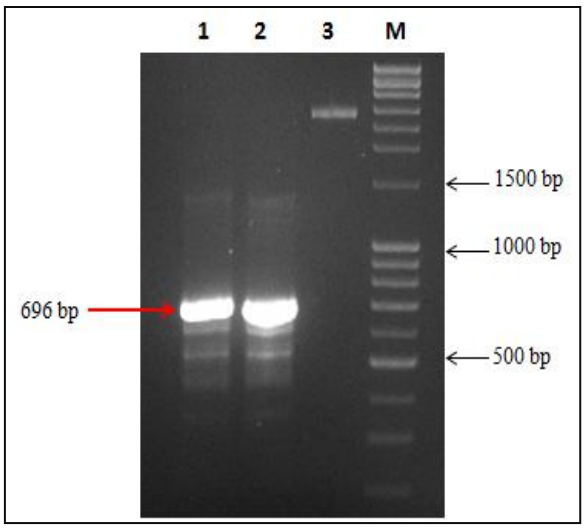

Figure.4.15. Gel electrophoresis of *YFP* gene (Lane 1), digested *YFP* gene with *PstI* and *NarI* (Lane 2) and digested *pUC19-pro-term PstI* and *NarI* (Lane 3).

The "white" colonies obtained after cloning were verified by PCR for the presence of the *YFP* gene insert (696 bp). Figure.4.16 shows some positive colonies that have inserted the recombined plasmid *pUC19-pro-term-YFP*.

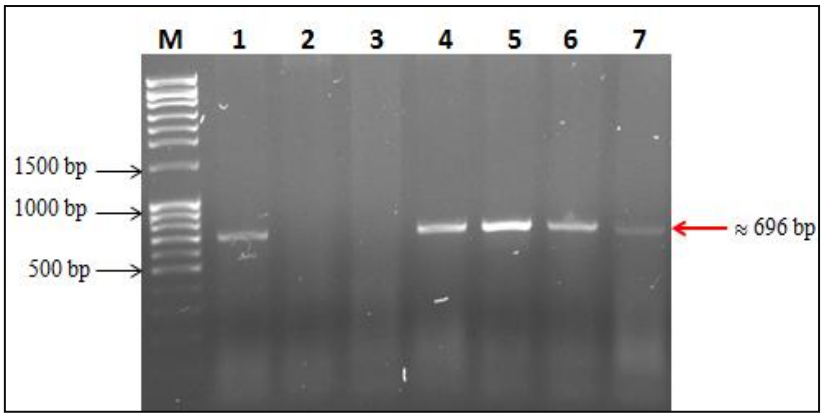

Figure.4.16. PCR identification of positive colonies having *pUC19-pro-term-YFP* plasmid. M is a mid-range ladder. The lanes 1 to 7 are for the different colonies tested.

4.3.2. Construction of pUC19-pro-term-YFP-asYFP

To generate antisense YFP (asYFP) fragment, gradient PCR method was employed (Chapter 3: Figure.3.2). This method enabled the amplification of eight different asYFP fragments (Table.4.5). The generated fragments were analyzed by gel electrophoresis and are shown in Figure.4.17.

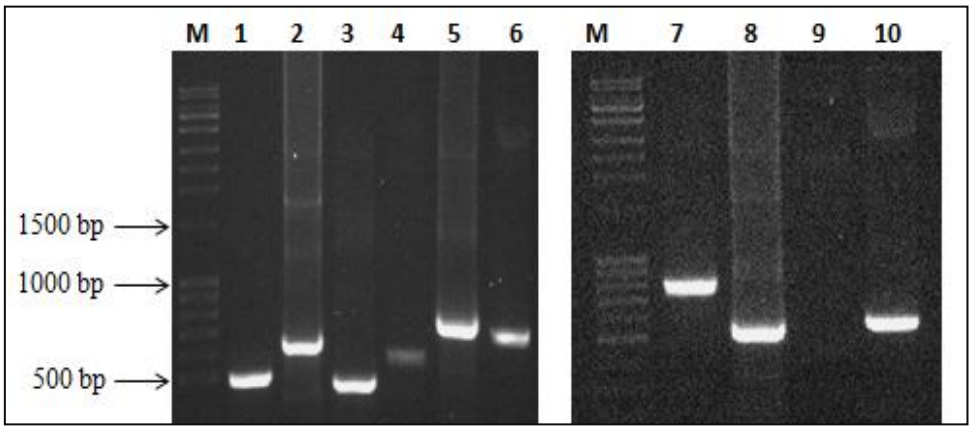

Figure.4.17. PCR amplification of asYFP DNA fragments with a mid-range ladder. The following sample IDs are shown:Lane 1: antisense 1_1; lane 2: antisense 1_2; lane 3: antisense 1_3; lane 4: antisense 1_4; lane 5: antisense 2_2; lane 6: antisense 2_3; lane 7: antisense 2_4; lane 8: antisense 3_3; lane 9: antisense 3_4; and lane 10: antisense 4_4.

Table.4.5. Antisense YFP sizes.

Antisense Name	Fragment size (bp)	Fragment size with overhangs (bp)
1_1	82	114
1_2	197	229
1_3	406	438
1_4	591	623
2_2	92	124
2_3	301	333
2_4	486	518
3_3	107	139
3_4	292	324
4_4	171	203

Eight PCR amplified asYFP fragments were transformed separately in *pUC19-pro-term-YFP* plasmid with the InFusion technique. The recombined vectors, *pUC19-pro-term-YFP-asYFP*, were transformed in *E. coli 10beta* competent cells.

4.3.3. Expression level of YFP under the control of different antisense fragments

Randomly selected colonies transformed with different asYFP fragments were cultured for 48 hrs in the same 24 well plate. The growth was at 25°C and fluorescence measured at 494 nm for excitation and 538 nm for emission wavelengths. The variations of growth and fluorescent signal are shown by figures.4.18 and 4.19.

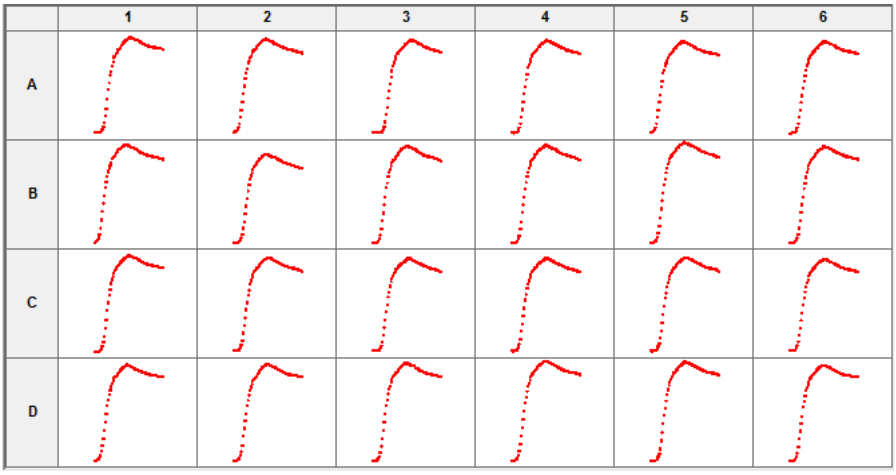

Figure.4.18. Growth curves of the control (*pUC19-pro-term-YFP*) and colonies having different antisense fragments (Well A1 contains the control; the remaining wells have colonies with antisense fragments).

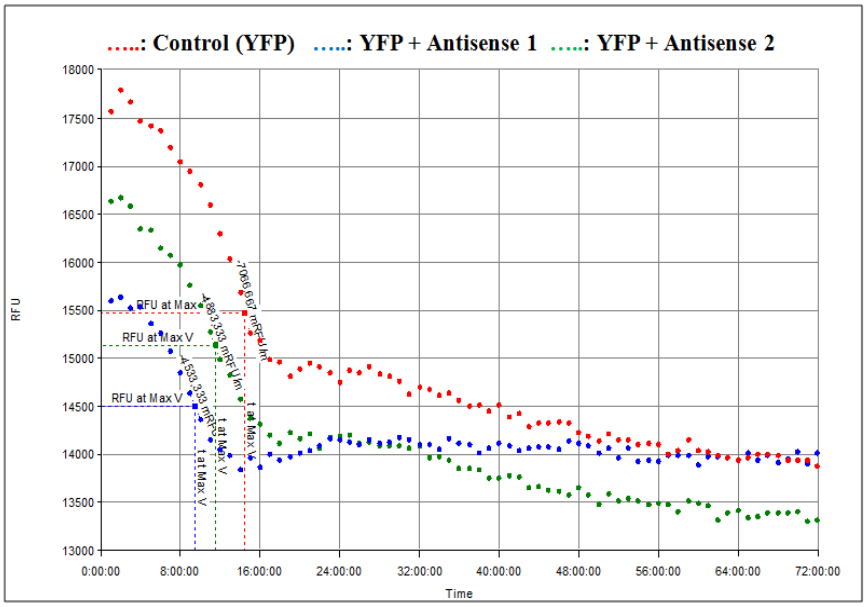

Figure.4.19. Comparison of fluorescence level between the control and random colonies having antisense fragments.

Since the expression of fluorescent proteins gene is growth associated, the generated plot should have the shape of an exponential growth curve. Surprisingly, the YFP fluorescence curves have a different form. In fact, the expression level seems to decline with respect to time even for the control colony. Although, the growth is "normal" and curves have the conventional exponential tendency. Several colonies were selected from the plate reader to verify the presence of the plasmids *pUC19-pro-term-YFP* and *pUC19-pro-term-YFP-asYFP* for the control and the other colonies respectively. The verification method was the colony PCR using *pLacZ_left* and *lacZ_term_right* primers (Table.3.5).

As stated previously, the PCR products have an extra 450 bp, therefore the control colony had a fragment of 450bp since it did not have an antisense fragment. All the results are indicated in Figure.4.20.

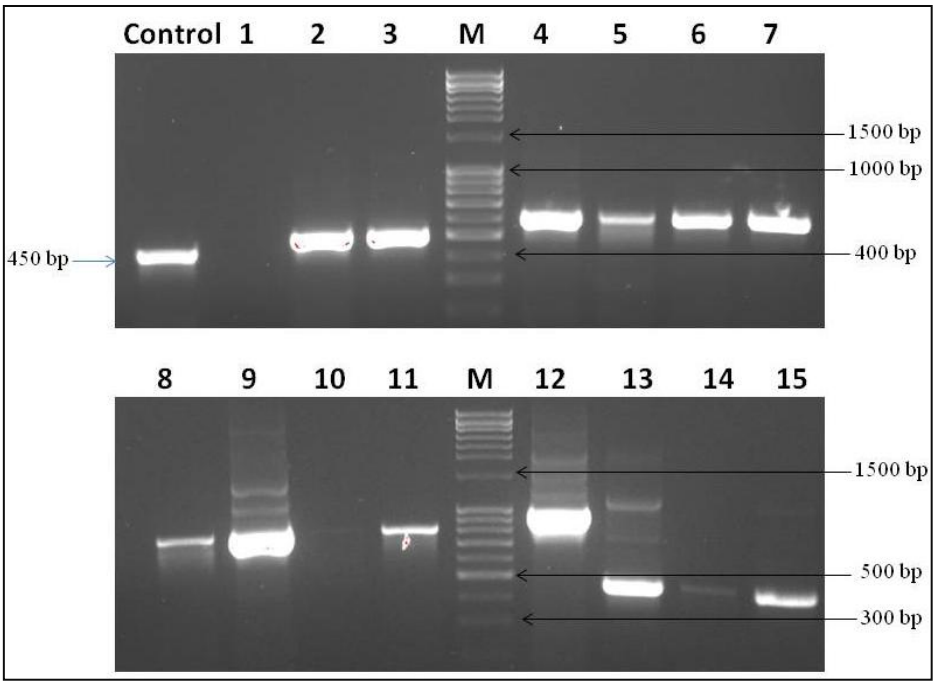

Figure.4.20. Gel electrophoresis of different colonies to verify the presence *pUC19-pro-term-YFP* for the control and *pUC19-pro-term-YFP-asYFP* for the other colonies.

Gel electrophoresis output shown by Figure.4.20 confirms the presence of *pUC19-pro-term-YFP* plasmid in the control colony and also the presence of some antisense fragments in colonies transformed with *pUC19-pro-term-YFP-asYFP*. Those observations cannot explain the uncommon fluorescence profile obtained with the *YFP* gene. This pattern can be the result of different parameters. The first factor that was verified was the plate reader setting and more precisely the wavelengths. The protocol provided with YFP plasmid indicates that the excitation is at 494 nm and the emission is at 538 nm. For that, a screening of the emission and excitation wavelengths was performed. In fact, the excitation was fixed at 450 nm and a scan for the optimal wavelength (between 300 and 700 nm) for emission was obtained. The controls were (i) water, (ii) LB medium, (iii) LB medium with IPTG and (iv) LB with *E. coli 10beta* cells (Figure.4.21 (A)). The first observation was that the optimal emission wavelength was 540 nm which was not so far from 538 nm used previously. The emission curves show that LB media without cells had a fluorescent signal (Figure.4.21 A and B) and that the

fluorescence emitted from LB was about half of the fluorescence emitted by YFP in RFU (Figure.4.21 B). This was due to the presence of Yeast extract which contains some aromatic amino acids among other complex compounds. This problem can be overcome by using minimal media M9; it contains only oligonucleotides and glucose. The fluorescence was also observed for *E. coli* cells without plasmids. This can be explained by the growth of cells and secretion of proteins in the media. All these extra signals interfere with the readings of YFP fluorescent signal.

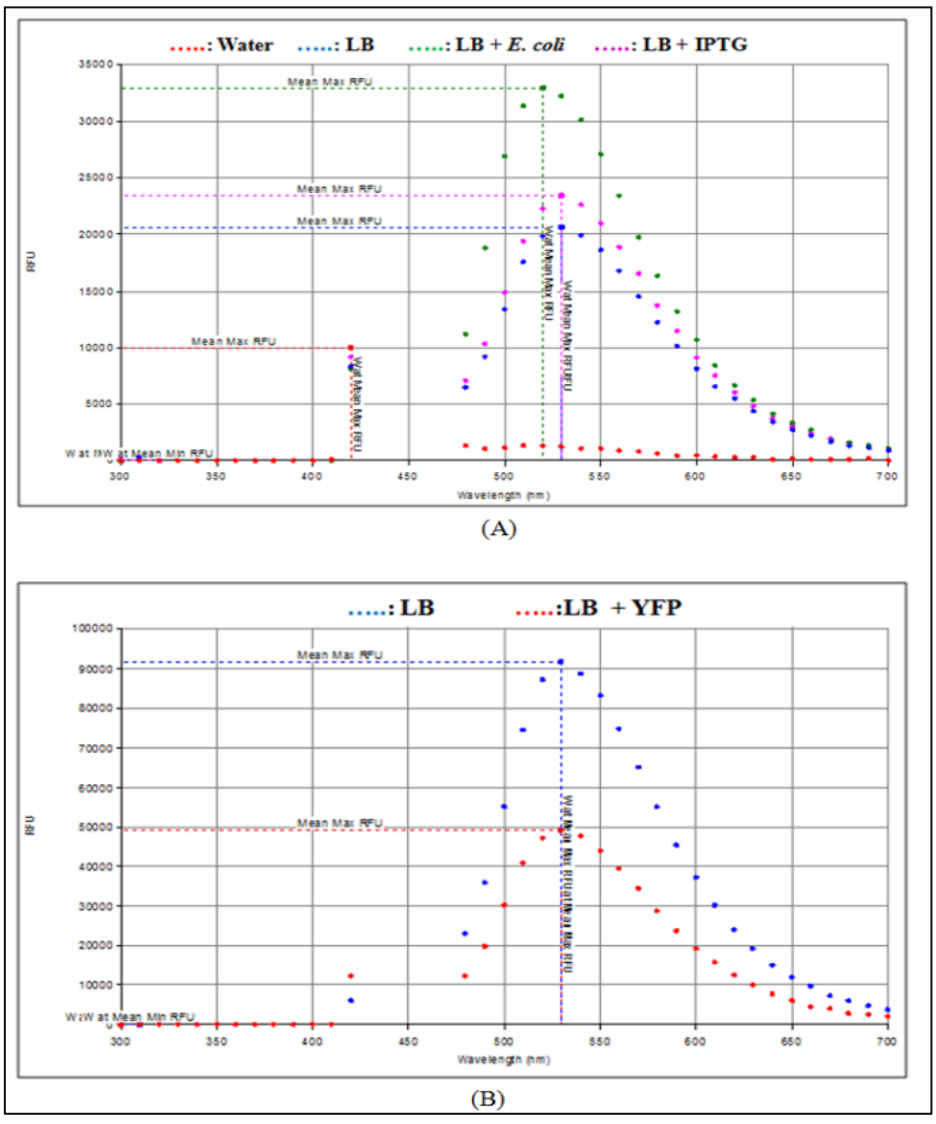

Figure.4.21. Emission spectrum for YFP protein; the excitation is fixed at 450 nm.

The optimal excitation wavelengths were determined by fixing the emission at 540 nm and screening the excitation spectrum for a range of 300 to 700 nm (Figure.4.22). Two optima values for excitation were found at 360 nm and 450 nm.

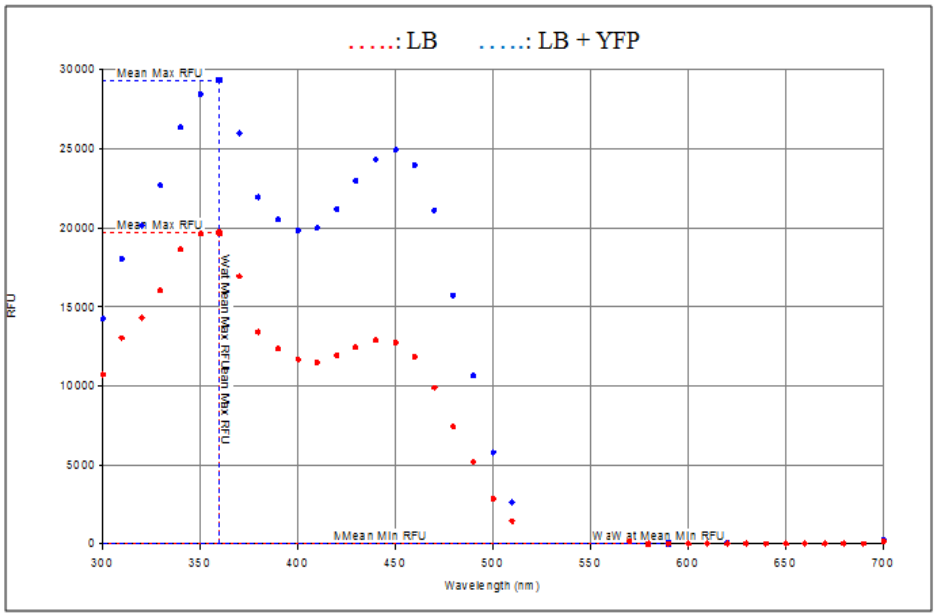

Figure.4.22. Excitation spectrum for YFP protein with LB media as a control. The emission is fixed at 540 nm.

The screening of wavelengths for emission and excitation gave almost the same values used for the first experiments. Therefore, deeper analyses related to DNA sequences were undertaken to check if the *YFP* gene was "out of frame" in the constructed plasmid.

4.3.4. Analysis of DNA sequences

The analysis of sequences of both *pUC19* plasmid and the *YFP* gene indicated that the protein produced was a fusion protein LacZ-YFP as illustrated in Figure.4.23. In fact, digestion of the plasmid *pUC19-pro-term* with *NarI* and *PstI* will cut only a part of *LacZ* gene. The *YFP* gene will bind to the remaining regions resulting in the production of a fusion protein. Therefore, the sequence of *YFP* should be in frame with the *LacZ* gene to obtain the desired expression.

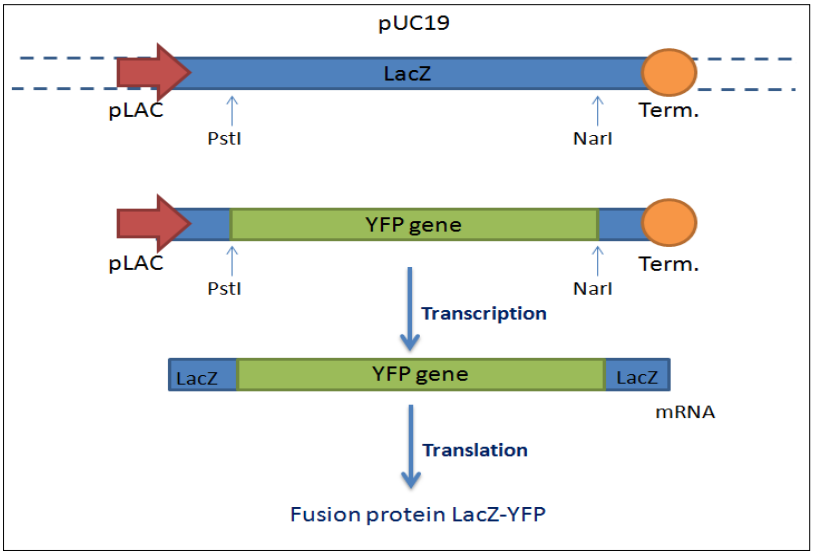

Figure.4.23. Scheme of fusion between *pUC19* plasmid and *YFP* gene.

The fusion protein had shifted in the reading frame (Figure.4.24). These results explain the decrease in the expression levels of YFP. The suggested solution was to design new primers (Table.3.1) to adjust the frame shift in the sequence.

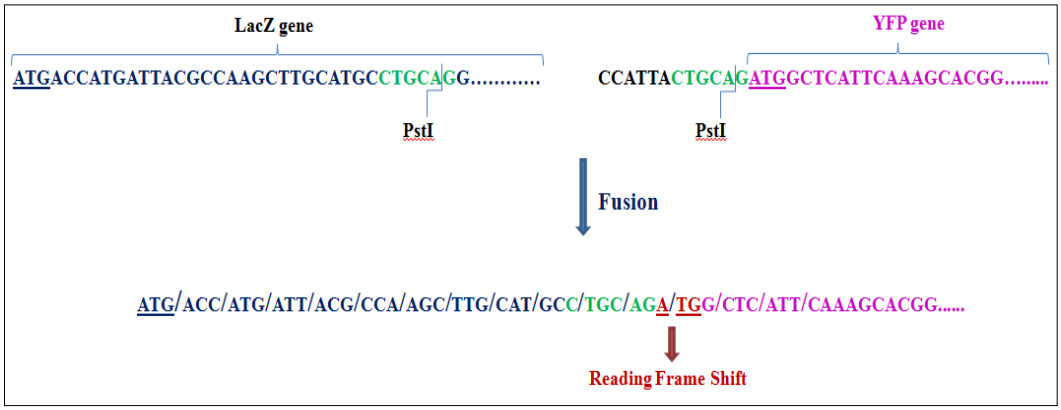

Figure.4.24. Frame shifting in *YFP* gene after fusion with *LacZ* gene.

4.3.5. Quantitative analysis of YFP expression level

With the new sets of primers, the *YFP* gene was re-amplified and inserted "in-frame" with the *LacZ* gene to produce a functional fusion. The result of transformation in *E. coli 10beta* cells are shown in Figure.4.25. Three positive colonies were selected.

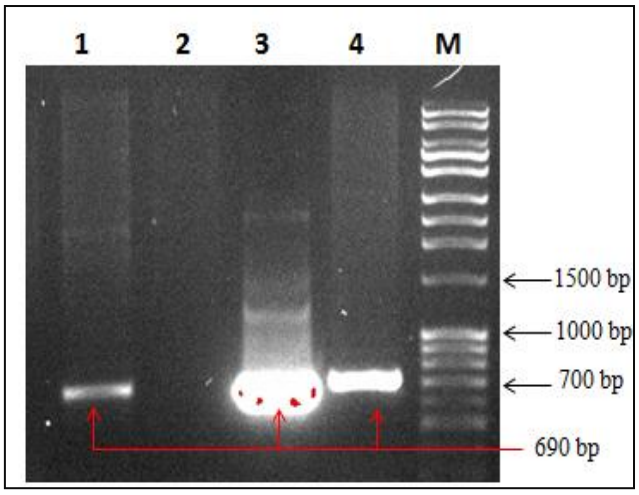

Figure.4.25. PCR identification of positive colonies having *pUC19-pro-term-YFP* plasmid. M is a mid-range ladder. Lanes 1 to 4 are for the different colonies tested.

The expression levels of the three positive colonies of YFP were analyzed. Different controls were used (i) LB media, (ii) *E. coli 10beta* cells without plasmid and (iii) *E. coli 10beta* transformed with common *pUC19* plasmid.

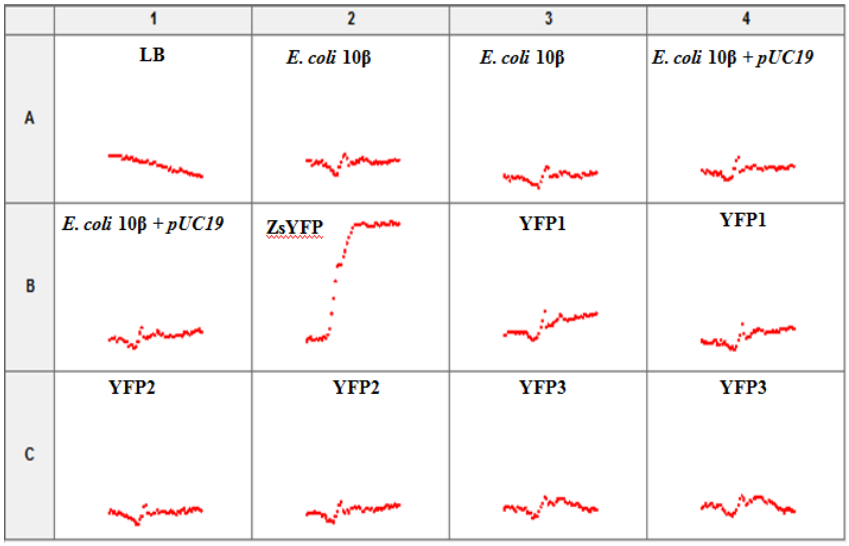

Figure.4.26. Plate reader results for colonies having *pUC19-pro-term-YFP* plasmid compared to LB media, *E. coli 10beta* cells, *E. coli* 10beta cells transformed with *pUC19* and *ZsYFP*.

The first observation was that the *YFP* gene was expressed along with the growth of cells and had an exponential behavior. The comparison of the fluorescent signal emitted from

pUC19-pro-term-YFP, *E. coli 10beta* cells, *E. coli 10beta* cells transformed with *pUC19* and *ZsYFP* (*YFP* gene inserted into the plasmid *pUC19* provided from Clontech showed that the YFP expression level was higher than the control (growth media). In addition, non-transformed *E. coli* cells (another control) were found to emit some fluorescence; however, the signal was lower than cells expressing *YFP* gene. ZsYFP, when inserted into *E. coli 10beta*, produced much higher expression of the protein than the *pUC19-pro-term-YFP* plasmid constructed in this research. This is shown in Figure.4.27. This result suggests that this expression system still need some adjustments. This is probably a result of the fusion with the *LacZ* gene. This result can be also attributed to the pH of LB media (7.0). In fact, YFP is very sensitive to acidic pH and becomes only 50% fluorescent at pH 6.5. In addition, YFP is also sensitive to chloride ions and photo-bleaches much more quickly than the GFPs (Patterson et al., 2001).

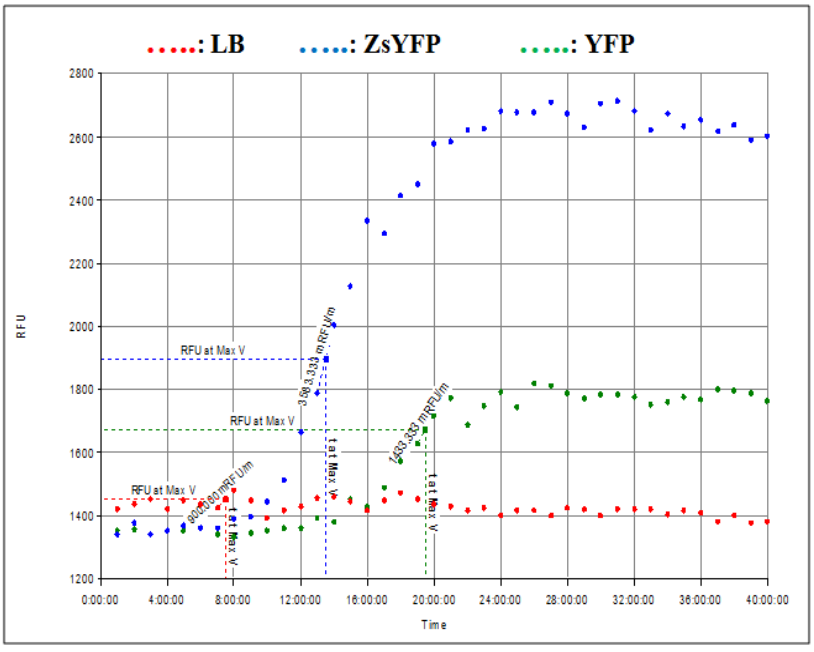

Figure.4.27. Comparison of the expression level between *pUC19-pro-term-YFP*, *ZsYFP* and LB media.

4.4. DISCUSSION

Antisense technology is a concept that is expected to revolutionize many areas of research. It provides an easy way to investigate unknown gene functions. This will supply metabolic engineering field with an additional tool to use for the manipulation of cellular functions. The most common asRNA application is the down-regulation of gene expression. This method allows the over-expression of a particular bio-product without complete knock-out of genes, offering a sophisticated means to direct metabolic pathways toward desired products.

The effectiveness of asRNA technology depends closely on the formation of asRNA-mRNA complex. Many parameters are involved in the pairing of asRNA and its target including asRNA concentration, target availability, asRNA structure, energy of hybridization, and other variables not yet defined. In this research, the focus was the design of asRNA for "fine-tuning" of genes expression. Fluorescent proteins were used to determine the expression level in the presence of different constructs of asRNA fragments. The minimum free energy and binding percentage were determined by NUPACK software. Then, a relationship between the expression level and minimum free energy was computed. Different results have been observed according to the fluorescent protein and the antisense fragment sequence.

4.4.1. Antisense design and location

The adjustments operated for the *YFP* gene enabled a successful cloning of both *CFP* and *GFP* genes. The CFP expression level was decreased by 33% to 84%, compared to the control. The asCFP fragments were targeted to different regions in mRNA. It was noticed that the effectiveness of asRNA and the mechanism of action depend on the binding region. In fact, depending on the localization of hybridization the mechanism can be by blocking translation machinery or by activating Rnase-H enzyme. Some fragments that hybridize to a common region (at the AUG end of the gene) were more efficient at reducing the observed

expression of CFP. Others were efficient when targeted to the 5' region. These results can suggest that there are some "favorable regions" more accessible to the asRNA. These regions should be exploited for the down-regulation process and which need more investigations.

However, the down-regulation of *GFP* gene did not exceed 30% for the different constructs used. The analysis of both targeted regions and expression level indicates that asGFPs that have in common a region of 67 bp (position 171-238) have inhibited the translation of GFP mRNA more efficiently compared to the other antisense fragments. This result is in agreement with the findings for the CFP. There are probably some regions which promote antisense binding and favorite the down-regulation. Though, some of the antisense fragments improved the expression level of GFP suggesting a possible positive antisense control.

Since some regions in the mRNA might be implicated in the antisense hybridization and reduction of expression, these regions should be investigated. In fact, protein synthesis requires a series of catalytic and regulatory elements including ribosomal recognition of the mRNA ribosome binding site (RBS) (Shine, J. & Dalgarno, 1974, Yusupova et al., 2001) and the start codon (Wikstrom et al., 1992). The 5'UTRs regions, which contain RBS, keep mRNAs from degradation and protect them from cleavage. (Hambraeus et al., 2002). Annealing of the asRNA to the RBS of the mRNAs not only inhibits ribosome binding but also produces a target for mRNA cleavage by RNase III (Blomberg et al., 1990; Case et al., 1990). Several cases of RBS blocking by natural asRNA have been reported in bacteria (Wagner and Simons, 1994). This property was exploited by Bonoli et al. (2006) to demonstrate the effectiveness of antisense-based gene silencing in *Saccharomyces cerevisiae*. In addition, novel regulatory RNA elements acting as riboswitches have been developed using asRNA techniques to provide a more valuable means of controlling gene expression. (Isaacs et al., 2004). These examples provide a promising method for designing new antisense

fragments targeted either to the 5'UTR or RBS region. Other important regions can be targeted including the conserved polyadenylation signal, the primer binding site (PBS), the major splicing donor (SD) or the major packaging signal (Psi), and AUG (in Eukaryotes). Those elements led to a highly efficient inhibition of HIV-1 gene expression and virus production in cell culture (Reyes-Darias et al., 2012).

4.4.2. Thermodynamic calculations

The exploitation of the minimum free energy as a function of the observed expression level of CFP revealed weak correlations. Although a poor correlation was obtained, linear trends were observed at low values of free energy of binding and low expression levels. In fact, the stability of the complex formed by the asRNA-mRNA is closely related to the free energy. This complex is more stable at low energy values and the more stable the complex is, the more efficient is the asRNA to trigger the knock-down mechanisms. Therefore, it can be concluded that the antisense fragments which hybridize to the CFP mRNA with lower energy are more efficient at reducing the fluorescence level of the protein. These fragments are the same fragments that have been shown in the previous section to share a common region of 175 bp that is suspected to promote the binding of the antisense and induce the decrease of the expression.

Meanwhile, at high values of minimum free energy, the linearity is no longer observed and the expression level is not correlated to this thermodynamic parameter. The complex asRNA-mRNA is unstable at high energy of binding; hence, the antisense acting machinery was not induced efficiently and therefore the reduction of the expression was not significant (only 33% of fluorescence was lost). However, the antisense fragment 1_1, which binds near the AUG initiation codon, has reduced the fluorescence level by 78% and it has a high energy of hybridization. This suggests that not only the minimum free energy is involved in the

variation of the expression level but there are other parameters and forces implicated in this mechanism. These parameters should be determined and investigated.

As for the GFP, the relationship between the minimum free energy and the expression level, relative to the control, indicate that there is a very weak relationship. These results are in disagreement with previous results obtained by the Senger Lab. In fact, not only is the free energy of the mRNA and asRNA binding is essential, but the location of these interactions may also play an important role in knocking-down mRNA translation. Nevertheless, the weak correlation implies more factors are required to correlate the expression level of the fluorescent protein with the thermodynamics of asRNA-mRNA complex formation. More data points are required to get more information about the behavior of the antisense fragments inside cells and to enable fitting the thermodynamic model. Other fluorescent proteins should be investigated for more accuracy.

4.5. REFRENCES

Blomberg, P., Wagner, E.G., & Nordström, K. (1990). Control of replication of plasmid R1: The duplex between the antisense RNA, CopA, and its target, CopT, is processed specifically *in vivo* and *in vitro* by RNase III. *EMBO J, 9*, 2331-2340.

Bonoli, M., Graziola, M., Poggi, V., & Hochkoeppler, A. (2006). RNA complementary to the 5' UTR of mRNA triggers effective silencing in *Saccharomyces cerevisiae*. *Biochem Biophys Res Commun, 339*, 1224-1231.

Case, C.C., Simons, E.L., & Simons, R.W. (1990). The IS10 transposase mRNA is destabilized during antisense RNA control. *EMBO J, 9*, 1259-1266.

Dean, N. M., McKay, R., Condon, T. P., & Bennett, C. F. (1994). Inhibition of protein kinase C- expression in human A549 cells by antisense oligonucleotides inhibits induction of intercellular adhesion molecule 1 (ICAM-1) mRNA by phorbol esters. *J Biol Chem, 26*, 16416-16424.

Dias, N., & Stein, C. A. (2002). Antisense Oligonucleotides: Basic Concepts and Mechanisms. *Mol Cancer Ther, 1*, 347-355.

Hambraeus, G., Karhumaa, K.,& Rutberg, B. (2002). A 5' stem-loop and ribosome binding but not translation are important for the stability of Bacillus subtilis aprE leader mRNA. *Microbiol, 148*, 1795-1803.

Isaacs, F. J., Dwyer, D. J., Ding, C., Pervouchine, D. D., Cantor, C. R., & Collins, J. (2004). Engineered riboregulators enable post-transcriptional control of gene expression. *J Nat Biotechnol, 22*(841-847).

Layton, D. M., & Bundschuh, R. (2005). A statistical analysis of rna folding algorithms through thermodynamic parameter perturbation. *Nucleic Acids Res, 33*,. 519-524.

Patterson, G., Day, R. N., & Piston, D. (2001). Fluorescent protein spectra. *J Cell Sci, 114*, 837-838.

Reyes-Darias, J. A., Sánchez-Luque, F. J., & Berzal-Herranz, A. (2012). HIV RNA dimerisation interference by antisense oligonucleotides targeted to the 5' UTR structural elements. *Virus Res, 1*, 63-71.

Shine, J., & Dalgarno, L. (1974). The 3'-terminal sequence of Escherichia coli 16S ribosomal RNA: complementarity to nonsense triplets and ribosome binding sites. *Proc Natl Acad Sci, 71* 1342-1346.

Wagner, E. G. H.,& Simons, R. W. (1994). Antisense RNA control in bacteria, phages, and plasmids. *Annu Rev Microbiol, 48*, 713-742.

Wikström, P. M., Lind, L. K., Berg, D. E., & Björk, G. R. (1992). Importance of mRNA folding and start codon accessibility in the expression of genes in a ribosomal protein operon of Escherichia coli. *J Mol Biol, 4*, 949-966.

Yusupova, G. Z., Yusupov, M. M.,Cate, J. H. D.,& Noller, H. F. (2001). The path of messenger RNA through the ribosome. *Cell, 106*, 233-241.

Chapter 5: CONCLUSION AND RECOMMENDATIONS

5.1. CONCLUSION

Antisense strategies were employed as a means for the down-regulation of fluorescent protein expression. Three fluorescent proteins (i) CFP, (ii) GFP and (iii) YFP were studied and their expression levels were determined in the presence of different antisense fragments. Then, the minimum free energy and binding percentage were calculated by NUPACK software. These systems allowed the investigation of the quantitative relationships between the target gene expression level and designed asRNA sequence. Generally, there is a weak correlation between the expression level and minimum free energy; however, linear trends were observed at low (highly negative) free energy values and low fluorescence levels (high degree of gene expression knock-down) for the *CFP* gene. In fact, the minimum free energy of hybridization is involved in the expression level of the target gene. The stability of the complex asRNA-mRNA is maintained at lower free energies. Therefore, the lower the energy, the more stable is the asRNA-mRNA complex, and greater reduction of the expression is obtained. The stability of the asRNA-mRNA complex would favor the knock-down mechanisms. Nevertheless, the low correlation at higher free energy values pointed to the existence of other parameters implicated in the design of antisense fragments. This study also revealed that target accessibility is a crucial parameter for the design of antisense fragments. There are specific regions in the gene that are more accessible to asRNA and promote the down-regulation mechanism. These regions include the AUG start codon region and should be further investigated. This leads to targeting new regions in the mRNA, mainly the ribosome binding site (RBS). The ribosome is known to confer to the mRNA the protection of degradation by nucleases. Consequently, targeting this region or 5'UTR would destabilize the mRNA and make it more susceptible to degradation and reducing thus the protein expression

level. These adjustments enlarge the domain of work and may introduce more accuracy to a thermodynamic model. Expanding this model to other genes is also of interest. The development of such a model, that is applicable to all genes, will enable the down-regulation of any protein. More insights are for the implementation of these “fine-tuned” asRNA strategies in cellular pathways to engineer metabolic shifts to increase synthesis of desired end-products without resorting to gene knock-out. The most attractive and modern application is to re-route cellular metabolism to the production and the improvement of biofuel and chemical commodities yields and the establishment of renewable, economically friendly energy sources.

Further attempts will be directed to the development of a program to create new asRNA fragments that can reduce gene expression of a target protein by any degree desired. This would be accomplished after the validation of a thermodynamic model.

5.2. RECOMMENDATIONS

More fluorescent proteins should be investigated to gather more data for more accuracy. In addition, more thermodynamic parameters should be joined to the minimum free energy to elucidate the relation between the expression level and the thermodynamic aspects. A complex mathematical model will be developed and should be tested for precision for other protein (not only fluorescent proteins). To make a more accurate design, preliminary researches are needed to have information about (i) the target mRNA secondary structure, (ii) the stability of the complex asRNA-mRNA secondary structure studied via the minimum free energy analysis and (iii) the exactitude of the open reading frame of the fluorescent gene after the insertion in *pUC19-pro-term* plasmid.